

# SANDIA REPORT

SAND2022-12615

Printed September 2022



Sandia  
National  
Laboratories

## Performance Evaluation of a Prototype Moving Packed-Bed Particle/sCO<sub>2</sub> Heat Exchanger

Kevin J. Albrecht, Hendrik F. Laubscher, Christopher P. Bowen, Clifford K. Ho

Prepared by  
Sandia National Laboratories  
Albuquerque, New Mexico 87185  
Livermore, California 94550

Issued by Sandia National Laboratories, operated for the United States Department of Energy by National Technology & Engineering Solutions of Sandia, LLC.

**NOTICE:** This report was prepared as an account of work sponsored by an agency of the United States Government. Neither the United States Government, nor any agency thereof, nor any of their employees, nor any of their contractors, subcontractors, or their employees, make any warranty, express or implied, or assume any legal liability or responsibility for the accuracy, completeness, or usefulness of any information, apparatus, product, or process disclosed, or represent that its use would not infringe privately owned rights. Reference herein to any specific commercial product, process, or service by trade name, trademark, manufacturer, or otherwise, does not necessarily constitute or imply its endorsement, recommendation, or favoring by the United States Government, any agency thereof, or any of their contractors or subcontractors. The views and opinions expressed herein do not necessarily state or reflect those of the United States Government, any agency thereof, or any of their contractors.

Printed in the United States of America. This report has been reproduced directly from the best available copy.

Available to DOE and DOE contractors from

U.S. Department of Energy  
Office of Scientific and Technical Information  
P.O. Box 62  
Oak Ridge, TN 37831

Telephone: (865) 576-8401  
Facsimile: (865) 576-5728  
E-Mail: reports@osti.gov  
Online ordering: <http://www.osti.gov/scitech>

Available to the public from

U.S. Department of Commerce  
National Technical Information Service  
5301 Shawnee Road  
Alexandria, VA 22312

Telephone: (800) 553-6847  
Facsimile: (703) 605-6900  
E-Mail: orders@ntis.gov  
Online order: <https://classic.ntis.gov/help/order-methods>



# Performance Evaluation of a Prototype Moving Packed-Bed Particle/sCO<sub>2</sub> Heat Exchanger

Kevin J. Albrecht  
Concentrating Solar Technologies  
Sandia National Laboratories  
P.O. Box 5800  
Albuquerque, NM 87185-9999  
kalbrec@sandia.gov

Hendrik F. Laubscher  
Concentrating Solar Technologies  
Sandia National Laboratories  
P.O. Box 5800  
Albuquerque, NM 87185-9999  
hlaubsc@sandia.gov

Christopher P. Bowen  
Concentrating Solar Technologies  
Sandia National Laboratories  
P.O. Box 5800  
Albuquerque, NM 87185-9999  
cpbowen@sandia.gov

Clifford K. Ho  
Concentrating Solar Technologies  
Sandia National Laboratories  
P.O. Box 5800  
Albuquerque, NM 87185-9999  
ckho@sandia.gov

## ABSTRACT

Particle heat exchangers are a critical enabling technology for next generation concentrating solar power (CSP) plants that use supercritical carbon dioxide ( $s\text{CO}_2$ ) as a working fluid. This report covers the design, manufacturing and testing of a prototype particle-to- $s\text{CO}_2$  heat exchanger targeting thermal performance levels required to meet commercial scale cost targets. In addition, the the design and assembly of integrated particle and  $s\text{CO}_2$  flow loops for heat exchanger performance testing are detailed. The prototype heat exchanger was tested to particle inlet temperatures of 500 °C at 17 MPa which resulted in overall heat transfer coefficients of approximately 300 W/m<sup>2</sup>-K at the design point and cases using high approach temperature with peak values as high as 400 W/m<sup>2</sup>-K.

## **ACKNOWLEDGMENT**

The authors would like to acknowledge the contributions of Vacuum Processing Engineering (VPE) and Solex Thermal Science for the collaborative effort on the design and manufacturing of the 20-kW<sub>t</sub> prototype heat exchanger developed in this project. The authors would also like to acknowledge the contributions of Matthew Carlson, Robert Crandell, Roger Buck, Daniel Ray, and Lam Banh who contributed significant technical know-how and effort in the assembly of the test system. This work was funded in part or whole by the U.S. Department of Energy Solar Energy Technologies Office under Award Numbers 34211 and 34152.



## CONTENTS

1. Introduction .....	9
1.1. Particle-Based Concentrating Solar Power .....	9
1.2. Particle/sCO <sub>2</sub> Heat Exchanger Prior Work .....	9
2. Test Facility Development .....	10
2.1. Design Requirements .....	11
2.2. Process Flow Diagram .....	12
2.3. Process Flow Modeling .....	13
2.4. Piping and Instrumentation Diagrams .....	13
2.5. Particle Loop Component Thermal and Mechanical Design .....	16
2.5.1. Electric Particle Heater .....	16
2.5.2. Particle Screw Lift .....	18
2.5.3. Particle Weigh Hopper .....	20
2.6. System Integration and Operation .....	20
2.6.1. Component Connections and Thermal Expansion .....	21
2.6.2. Supervisory Control and Data Acquisition .....	21
3. Heat Exchanger Design Modeling .....	22
3.1. Heat Exchanger Model Development .....	22
3.1.1. sCO <sub>2</sub> Microchannel Flow and Heat Transfer .....	23
3.1.2. Particle Flow and Heat Transport .....	24
3.1.3. Heat Exchanger Thermal Performance .....	25
3.2. Prototype Heat Exchanger Design .....	26
3.3. Heat Exchanger Heat Loss Analysis .....	26
4. Heat Exchanger Performance Testing .....	27
4.1. Prototype Heat Exchanger Manufacturing .....	27
4.2. Heat Exchanger Testing Procedure .....	28
4.3. Heat Exchanger Performance Measurements .....	30
5. Conclusion .....	33
5.1. Lessons Learned .....	33
5.1.1. Particle and sCO <sub>2</sub> Flow Loops .....	33
5.1.2. Particle/sCO <sub>2</sub> Heat Exchanger .....	34
References .....	35
Appendix A. HProject Milestones .....	38
Appendix B. Heat Exchanger General Arrangement Drawings .....	40
Appendix C. Particle Flow Loop Drawings .....	43

## LIST OF FIGURES

Figure 1-1. Specific heat exchanger cost as a function of overall heat transfer coefficient and cost per surface area .....	11
Figure 2-1. Process flow diagram of the integrated particle and sCO <sub>2</sub> flow loops .....	14
Figure 2-2. Piping and instrumentation diagram (P&ID) of the integrated particle and sCO <sub>2</sub> flow loops for heat exchanger testing .....	15
Figure 2-3. Illustration of the integrated particle and sCO <sub>2</sub> flow loops for heat exchanger testing .....	16
Figure 2-4. Illustration of the 60 kW <sub>t</sub> particle heater assembly and exploded view identifying the approach to sealing and supporting the heater elements .....	17
Figure 2-5. Image of the assembled 60 kW <sub>t</sub> particle heater prior to installation in the heat exchanger test stand .....	18
Figure 2-6. Illustration of the screw lift and exploded view identifying the components and manufacturing detail .....	19
Figure 2-7. Photos of the screw lift assembly and low-temperature commissioning setup .....	20
Figure 2-8. Illustration of the particle weigh hopper assembly and exploded view identifying the components .....	21
Figure 3-1. Illustration of the 1 MW <sub>t</sub> G3P3 heat exchanger concept and subscale 20 kW <sub>t</sub> version .....	23
Figure 3-2. Pressure drop in the 20 kW <sub>t</sub> subscale heat exchanger from CFD analysis of the microchannel network .....	24
Figure 3-3. Flow uniformity in the 20 kW <sub>t</sub> subscale heat exchanger from CFD analysis of the microchannel network .....	25
Figure 3-4. Illustration of the 20 kW <sub>t</sub> heat exchanger design with instrumentation .....	26
Figure 3-5. Temperature and heat flux contour plots of the 20 kW <sub>t</sub> heat exchanger surrounded with 4-inch of Superwool .....	27
Figure 4-1. Photos of the 20 kW <sub>t</sub> heat exchanger core after manufacturing at VPE and prior to testing at Sandia .....	28
Figure 4-2. Photo of the 20 kW <sub>t</sub> heat exchanger installed in the test facility at Sandia without insulation .....	29
Figure 4-3. Experimental measurements of the 20 kW <sub>t</sub> heat exchanger overall heat transfer coefficient as a function of the particle inlet temperature .....	31
Figure 4-4. Experimental measurements of the 20 kW <sub>t</sub> heat exchanger pressure drop as a function of operating temperature at the design point flow rate (0.1 kg/s) and 50% above (0.15 kg/s) and below (0.05 kg/s) the design point flow rate .....	32

## LIST OF TABLES

Table 2-1. Design Requirements for Prototype Heat Exchanger Testing (20 kW <sub>t</sub> Scale) .....	12
Table 2-2. Design Requirements for Particle Screw Lift .....	19
Table 2-3. National Instruments supervisory control and data acquisition system hardware ..	22

## 1. INTRODUCTION

Concentrating solar power (CSP) is a renewable energy generation technology that can provide large-scale and long-duration energy storage to increase the penetration of other renewables on the electric grid [1]. Energy captured in the solar receiver can be stored in an intermediate vessel as thermal energy prior to being dispatched to a heat engine to produce electrical energy. However, the cost of electrical energy produced by CSP is typically higher than that of photovoltaic panels, which directly convert sunlight into electrical energy. Thus, the enabling role of CSP through large-scale thermal energy storage is anticipated to become a driving force for adoption of the technology once renewable are installed at a level where curtailment begins to occur. Cost reduction for CSP systems is also being pursued under the DOE Gen3 program [2] which is focused on increasing the operating temperature of the thermal equipment to improve energy conversion efficiency thereby reducing the cost of electricity. To allow for such an increase in operating temperature, an alternative heat transfer and energy storage material is required to replace the current nitrate salts. One of the three options for a replacement material being considered for next-generation CSP plants is solid particles [3].

### 1.1. Particle-Based Concentrating Solar Power

The use of solid particles as a heat transfer and energy storage media is a promising concept for next-generation CSP systems which has received considerable effort in research and development over the past decade. Although the idea and benefits of a directly irradiated particulate heat transfer fluid was originally documented in a Sandia report from the 1980's [4], progress toward the commercialization of particle CSP technology has gained significant traction under the recent Gen3 program. The high-temperature stability and benign nature of ceramic particles allows for increased temperature operation such that CSP plants can be coupled to supercritical CO<sub>2</sub> (sCO<sub>2</sub>) power cycles. The sCO<sub>2</sub> power cycle allows for thermal-to-electric conversion efficiencies exceeding 50% in certain configurations and heat rejection that is more suitable for dry-cooled applications [5]. However, heat exchanger designs for particle CSP have yet to meet performance and cost targets [6, 7] and are one of the critical components that must be proven prior to commercial realization of a particle-based CSP plant. This report discusses the development of a test facility and subscale testing of a prototype particle/sCO<sub>2</sub> heat exchanger for a next generation CSP plant.

### 1.2. Particle/sCO<sub>2</sub> Heat Exchanger Prior Work

Sandia National Laboratory initiated the development of particle/sCO<sub>2</sub> heat exchangers for the application of CSP in a project that began in 2015. This project considered several different options for particle heat exchanger technology including moving packed-bed heat exchangers in both shell-and-plate and shell-and-tube configurations as well as fluidized bed concepts. Through a systematic down selection process, the leading candidate was chosen to be a moving packed-bed design [8]. However, the benefits of a moving packed-bed design were only anticipated to be marginal compared to fluidized bed configurations.

Following the down select process Sandia procured a 100 kW<sub>t</sub> moving packed bed shell-and-plate heat exchanger that was anticipated to have a heat transfer coefficient of 150 W/m<sup>2</sup>-K and be capable of producing sCO<sub>2</sub> at temperatures above 700 °C. However, the experimental data collected for the heat exchanger indicated overall heat transfer coefficients between 50-70 W/m<sup>2</sup>-K [7]. The lessons learned from the project indicated particle flow non-uniformity, sCO<sub>2</sub> flow non-uniformity, and high sCO<sub>2</sub> pressure drop were the primary reasons why the heat exchanger performance was less than anticipated. The project also identified reducing heat exchanger plate spacing to enhance the particle side heat transfer coefficient and moving to a single bank pure counter-flow heat exchanger as the most important features to pursue in a future design which valued high overall heat transfer coefficients and low pressure drop [9].

The German Aerospace Center (DLR) has similarly been developing heat exchanger technology for the application of particle CSP. Baumann and Zunft reported on a design that used a staggered array of horizontally oriented tubes for containing the power cycle working fluid and a moving packed bed of particles contacting the outer surface. A prototype electrically heated test occurred in 2014 that used thermal oil as the working fluid for evaluating heat transfer coefficients up 400 °C [10]. The intermediate temperature experimental results measured overall heat transfer coefficients up to 250 W/m<sup>2</sup>-K with a negative correlation to heat exchanger effectiveness.

Finally, KSU has been developing heat exchanger technology for particle CSP, but focused on air as a power cycle working fluid for use in hybridized gas turbine engines [11]. KSU evaluated heat exchanger performance in a prototype unit up to 35 kW<sub>t</sub> using exhaust heat from a small gas turbine and measured overall heat transfer coefficients up to 30 W/m<sup>2</sup>-K [12].

To date, there are no known demonstrations of particle/sCO<sub>2</sub> heat exchangers that have achieved overall heat transfer coefficients above 100 W/m<sup>2</sup>-K. Current DOE cost targets for primary power cycle heat exchangers are \$150/kW<sub>t</sub> for the 2020 LCOE target of \$0.06/kW<sub>e</sub> and some analysis [13] suggest that a cost target of \$100/kW<sub>t</sub> should be used for the 2030 LCOE target of \$0.05/kW<sub>e</sub>. Current technoeconomic considerations for manufacturing diffusion bonded plates of microchannel heat exchangers place the cost of nickel alloy surface area between \$5000-10000/m<sup>2</sup>. This suggests that an all nickel particle/sCO<sub>2</sub> heat exchanger must demonstrate overall heat transfer coefficient above 600 W/m<sup>2</sup>-K even to meet the 2020 cost targets with liberal estimates for heat transfer surface area cost (Figure 1-1). Therefore, significant progress in particle/sCO<sub>2</sub> heat exchanger performance is required to progress particle CSP to commercialization.

## 2. TEST FACILITY DEVELOPMENT

Evaluating the performance of a prototype particle/sCO<sub>2</sub> heat exchanger requires the development of dedicated flow loops for both the particle and sCO<sub>2</sub> fluids. The flow loops will ideally be able to operate indefinitely and hold heat exchanger boundary temperatures constant such that steady-state operation is achieved. The operation should also be flexible enough that the heat exchanger performance can be evaluated over the entire range of operating conditions such that the sensitivity of the performance to flow rate, temperature, and particle type can be determined.

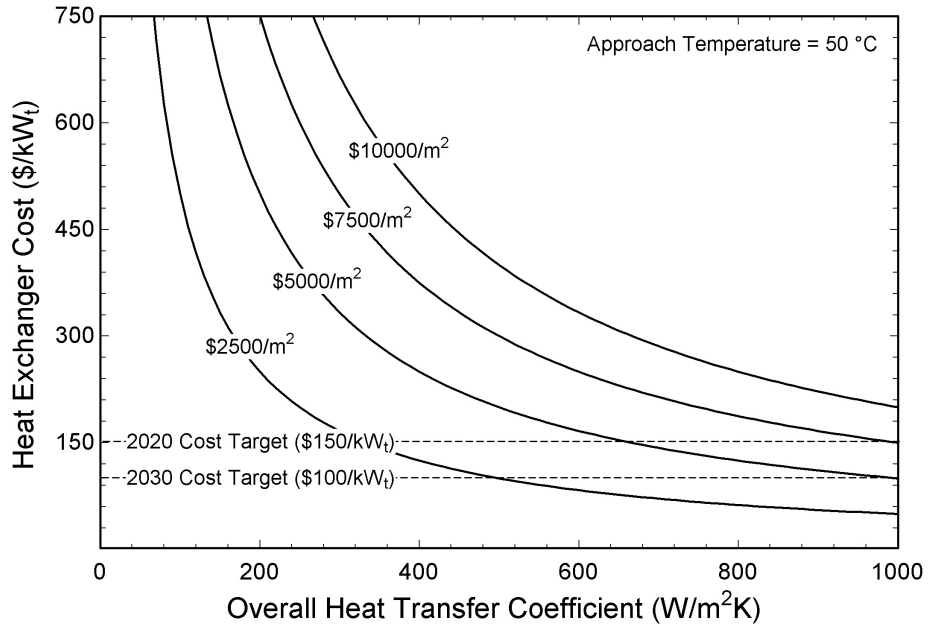


**Figure 1-1 Specific heat exchanger cost as a function of overall heat transfer coefficient and cost per surface area**

Historically, the complexity and expense of developing such a facility has been a limitation resulting in experiments that are less than ideal for evaluating heat exchanger performance. Many of these experiments seek to avoid flow loops through operating in a batch mode or using a fluid other than  $s\text{CO}_2$  as the coolant. Others have tried to evaluate heat exchanger performance by using electrical heating of a surface [14] to approximate a heat flux boundary condition which overlooks the challenges of accommodating a high pressure fluid and can suffer from large measurement uncertainty. Approaches other than building and testing heat exchanger prototypes are all deficient to some extent where features that are important to evaluate for a given heat exchanger design are neglected. The following sections detail the design and analysis of integrated  $s\text{CO}_2$  and particle flow loops for evaluating subscale prototype heat exchanger thermal performance.

## 2.1. Design Requirements

The test system design requirements for a  $20 \text{ kW}_t$  scale heat exchanger are provided in Table 2-1. These numbers were established based on a combination of equipment ratings that are available from past projects and ratings for off-the-shelf equipment. In addition, the manufacturing cost and lead time for heat exchanger prototype constructed from stainless-steel are substantially lower. Therefore, the system is capable of quickly turning around results and ideally iteratively developing a design with small scale and low cost prototypes prior to constructing MW scale equipment from high nickel alloys.

**Table 2-1 Design Requirements for Prototype Heat Exchanger Testing (20 kW<sub>t</sub> Scale)**

Metric	Value	Units
Thermal Duty	20.0	kW
Design Temperature	550	°C
Design Pressure (MAWP)	20.0	MPa
Operating Pressure	17.0	MPa
Particle Inlet Temperature	500	°C
Particle Outlet Temperature	340	°C
Particle Flow Rate	0.112	kg/s
sCO <sub>2</sub> Inlet Temperature	290	°C
sCO <sub>2</sub> Outlet Temperature	450	°C
sCO <sub>2</sub> Flow Rate	0.103	kg/s
sCO <sub>2</sub> Pressure Drop	<40	kPa

## 2.2. Process Flow Diagram

From the high-level design requirements, a process flow diagram (Figure 2-1) was developed to capture the arrangement of the system components and identify the points of control within the system. The sCO<sub>2</sub> isobaric flow loop in the process flow diagram is based on the initial work presented by Carlson et al. [15, 16], but has been refined based on the lessons learned. The electrically heated particle loop is based on the initial work presented by Albrecht et al. [7] in the same effort, but scaled down and modified to improve control and measurement accuracy.

The key changes to the sCO<sub>2</sub> flow loop were the addition of a large packaged chiller for cooling the pump recirculation flow, using an alternative valve for throttling sCO<sub>2</sub> flow, and switching to trace heat for the sCO<sub>2</sub> preheating rather than impedance heating. Significant cooling on the pump recirculation is required to reliably operate the system during the hottest months of the year. The density of the sCO<sub>2</sub> begins to fall as the temperature increases which results in dimensioned pump performance and operating conditions that can damage the pump bearings. Therefore a chilled water supply is required for maintaining the pump inlet conditions below ambient in some scenarios. The system also switched to a bonnet style valve rather than the ball valves used in the initial effort to improve the control over the sCO<sub>2</sub> flow and be capable of obtaining positive shutoff on the recirculation legs. This style of valve was not available to the previous systems due to higher flow rates and lack of a remote actuator. However, the reduced flow rate within the present system and identification of a third party supplier for valve actuators has enabled their use. Finally, trace heating of the heat exchanger inlet and outlet connections was identified as a low cost approach to sCO<sub>2</sub> inlet temperature control for the current system based on thermal duty. The combination of these modifications was shown to work well for the isobaric flow loop constructed in this project.

The particle flow loop built on the designs and lessons learned from the electrically heated ground-based testing within the past 100-kW<sub>t</sub> prototype. The key changes include conditioning the particle flow prior to temperature measurements, an in line weigh hopper for continuous particle flow rate data, and superior system integration that allows for component inspection and

maintenance. The key changes are discussed in more detail within the following sections covering the design of the particle flow loop components.

### **2.3. Process Flow Modeling**

A process flow model was developed to evaluate the mass and energy flows within the system to aid in the selection and design of hardware. The model uses steady-state thermodynamic models of the system components that are configured consistent with the system arrangement presented in the process flow diagram. Since the majority of the sCO<sub>2</sub> loop hardware was borrowed from a prior effort at Sandia, the model provided a verification that the equipment could meet the needs of the system rather than used to specify design requirements. However, the model did allow for high level design requirements for the particle loop components to be specified such as heater thermal input and particle flow rate.

### **2.4. Piping and Instrumentation Diagrams**

The piping and instrumentation diagram (P&ID) for the system is shown in Figure 2-2. The diagram is consistent with the process flow diagram presented previously, but contains information on the instrumentation and connections between the equipment. Some detail on the quantity and specific location of additional instruments that were installed on the prototype heat exchanger are not shown. However, all of the sensors for system operation and control are shown in the diagram.

Temperature measurements for the particle side of the system are made using special limits of error (SLE) type-K thermocouples. Depending on the location and mechanical loads on the instrument, either 0.0625 inch or 0.125 inch diameter probes were used to minimize the stem effect. As part of the commissioning process for the thermocouples, they were each tested in a dry-well calibrator (Additel 875-660) up to 600 °C to confirm measurement accuracy. The mass flow rate measurements of particles were made using load cells to make real time measurements of weigh hopper inventory. The weigh hopper was supported on Omega LC501 cantilever beam load cells which have a provided calibration curve. The load cell measurements were verified using known weights prior to being put in service.

Temperature measurements on the sCO<sub>2</sub> side of the system are made using class A 100Ω 4-wire RTDs. These probes allow for superior accuracy and stability in temperature measurement, but are only available as small as 0.125 inch diameter. This allows for their use in the sCO<sub>2</sub> flow where high heat transfer coefficients between the fluid and probe minimize stem effects. The flow rate measurement of the sCO<sub>2</sub> is accomplished using a Coriolis flow meter on the cold side of the system, which has been shown to be the best approach to deal with the highly variable sCO<sub>2</sub> density.

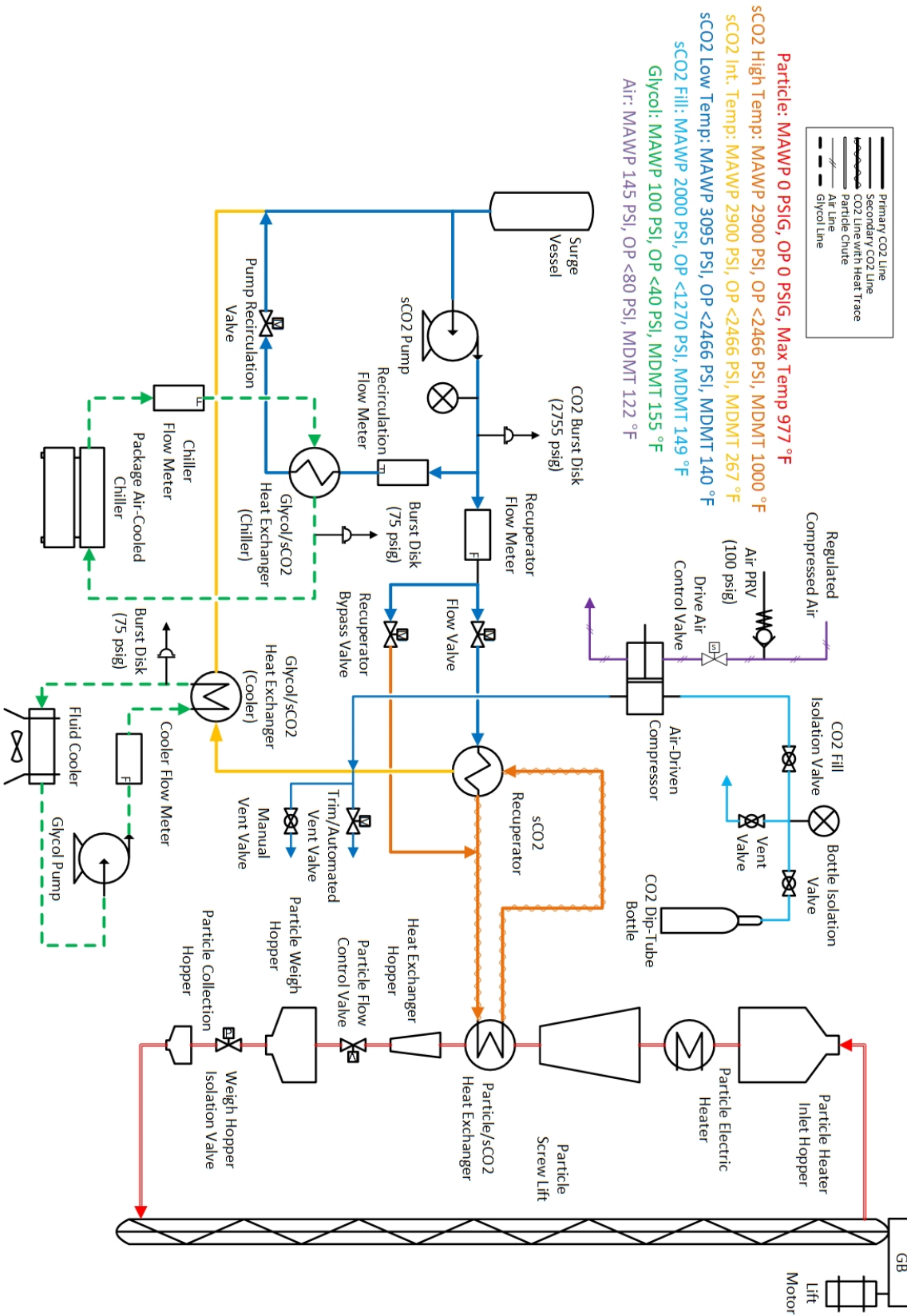


Figure 2-1 Process flow diagram of the integrated particle and sCO<sub>2</sub> flow loops

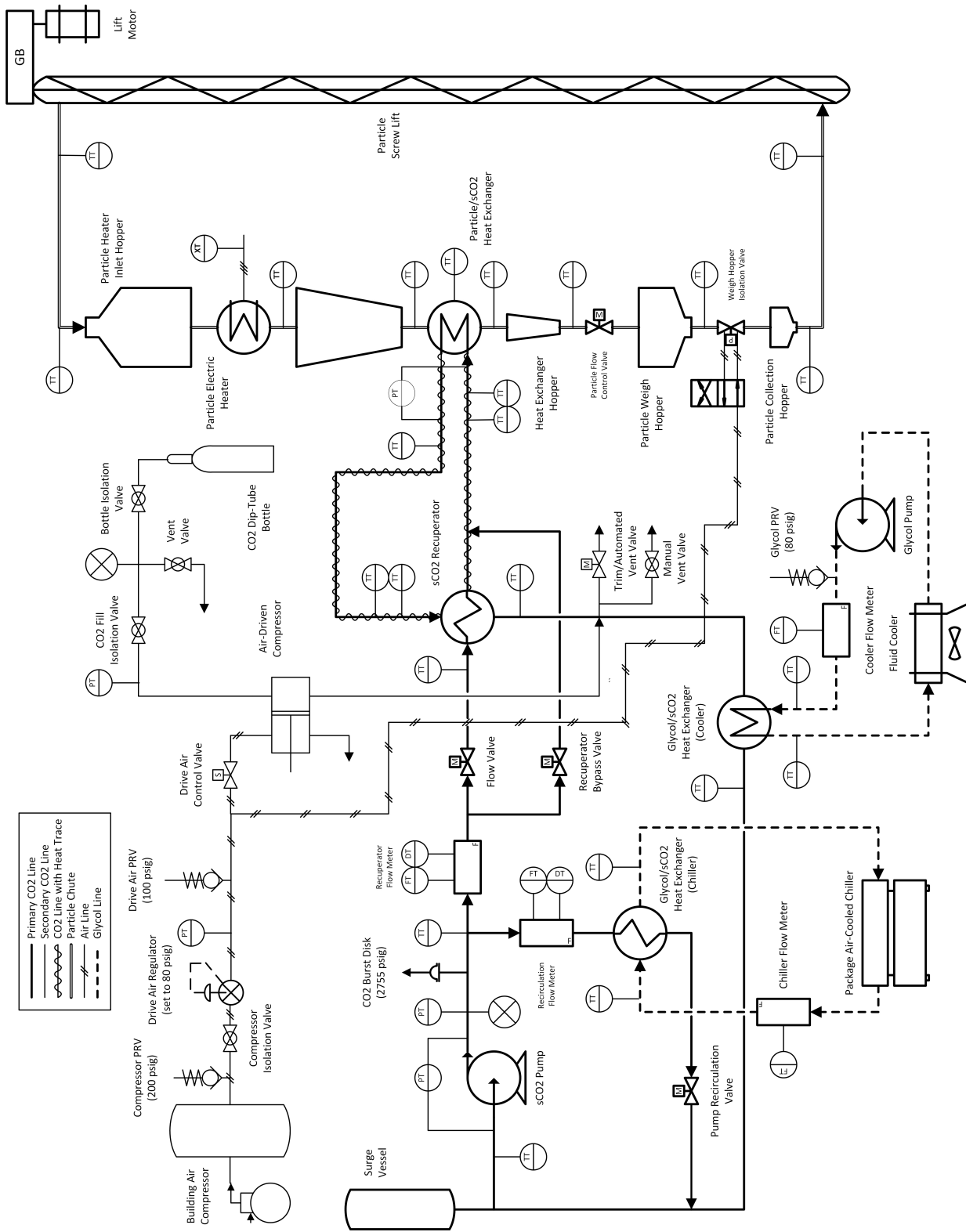
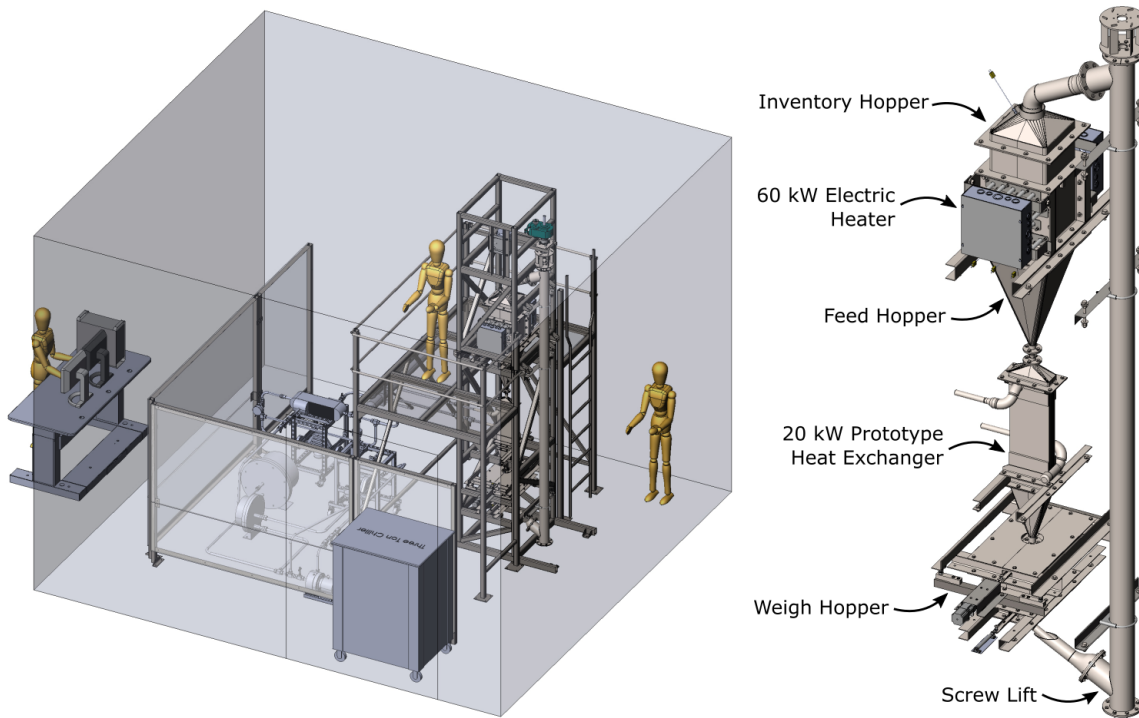


Figure 2-2 Piping and instrumentation diagram (P&ID) of the integrated particle and sCO<sub>2</sub> flow loops for heat exchanger testing



**Figure 2-3 Illustration of the integrated particle and sCO<sub>2</sub> flow loops for heat exchanger testing**

## 2.5. Particle Loop Component Thermal and Mechanical Design

The detailed thermal and mechanical designs of the particle flow loop components were generated following the completion of the process flow and piping and instrumentation diagrams. An illustration of the complete integrated system is shown in Figure 2-3 with the particle flow loop components identified. Since particle equipment vendors typically do not have components at this scale for high-temperature operation, many of the components were designed as part of this effort and either manufactured at Sandia or contracted to local fabrication shops. The following sections detail the designs of the major particle equipment and general arrangement drawings are contained in Appendix C.

### 2.5.1. **Electric Particle Heater**

The particle heater was constructed based on a design that was conceptualized and initially constructed within the SuNLaMP project [17]. The original heater design was documented in a prior report and used to perform ground-based commissioning of the 100 kW<sub>t</sub> prototype heat exchanger. However, several key changes were implemented in the current iteration to improve manufacturability and simplify any future maintenance. The design uses Watlow Firerod cartridge heaters that are arranged in a staggered configuration by penetrating through both faces of the heater. The 60 kW<sub>t</sub> design shown in Figure 2-4 consists of 42 heaters that each have a maximum

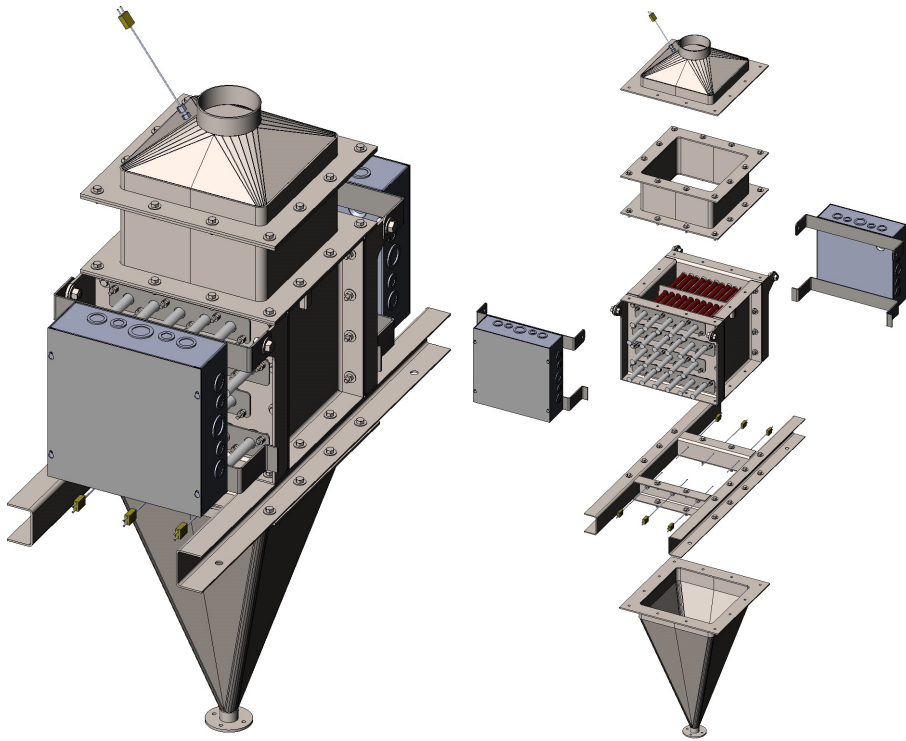


**Figure 2-4 Illustration of the 60 kW<sub>t</sub> particle heater assembly and exploded view identifying the approach to sealing and supporting the heater elements**

thermal output of 1.5 kW. The total heater power output is controlled using a phase angle fired power controller that is controlled by a PID block in the LabVIEW software. This allows for the heater outlet temperature to be held constant and accommodate any inlet temperature changes due to the thermal capacitance and heat loss from the particle conveyance equipment.

The particle heater uses a mass flow cone at the outlet to both allow for uniform flow through the electric heater and provide a thermal equilibration region prior to the heat exchanger inlet. In a prior effort the heat exchanger inlet was directly connected to the electric heater outlet which resulted in large amounts of uncertainty in heat exchanger inlet temperature measurement. Local particle temperatures near heater elements can be substantially higher than the average particle temperature leaving the heater. The mass flow cone gives the particle flow sufficient residence time and necks down the flow into a small diameter outlet where a single temperature probe can provide an accurate measurement of particle temperature entering the heat exchanger.

The heater assembly and commissioning was completed by Sandia (Figure 2-5), but the manufacturing of the stainless steel sheet metal case was contracted to a local shop in Albuquerque, NM. The electrical cartridge heater elements were procured from Watlow based on specifications for a custom length, thermal duty, and locating ring. The initial heater design used NPT connections to support heater elements in the case. However, the NPT connection was abandoned for the current iteration in favor of a locating ring, clamp connection, and ceramic gaskets due to issues with heater alignment and particle binding in the threaded connections.



**Figure 2-5 Image of the assembled 60 kW<sub>t</sub> particle heater prior to installation in the heat exchanger test stand**

### **2.5.2. Particle Screw Lift**

The particle conveyance through the system is provided using a screw lift which was constructed in-house using custom formed flighting and commonly available pipe sections. The design is detailed in Figure 2-6 which was established based on the design requirements in Table 2-2. The outer screw case is a 4-inch schedule-10 pipe and the inner shaft is a 1.5-inch schedule-10 pipe. The flighting is welded to the inner shaft twice per revolution with a bead that is one inch in length and the outer diameter of the flighting is held back from the inner diameter of the case by 1/8 inch to accommodate slight misalignment and prevent interference due to thermal expansion. The main bearing surfaces and support for the screw are contained outside of the heated region and protected through a thermal brake that takes the shape of a squirrel cage at the top of the lift. The thermal expansion of the component is accommodated by hanging the screw from the top bearing and allowing it to grow vertically downward while the case is supported from the base and allowed to grow vertically upward. At the base of the screw, there is a locating pin to ensure the screw remains centered in the case, but is not lubricated due to being immersed in particle flow and at elevated temperature. This bearing surface is considered to be a consumable item that will have to be replaced occasionally through standard maintenance.

Low-temperature commissioning of the screw lift was performed separate from the system as shown in Figure 2-7. The measured flow rate at ambient temperature operating conditions was measured to be 0.4 kg/s and the current draw by the 1.5 hp motor was well below the rating.

**Table 2-2 Design Requirements for Particle Screw Lift**

Metric	Value	Units
Mass Flow Rate	0.3	kg/s
Design Temperature	>500	°C
Particle	HSP 40/70	-
Heat Loss	<2	kW
Power Requirement	< 1.5	hp

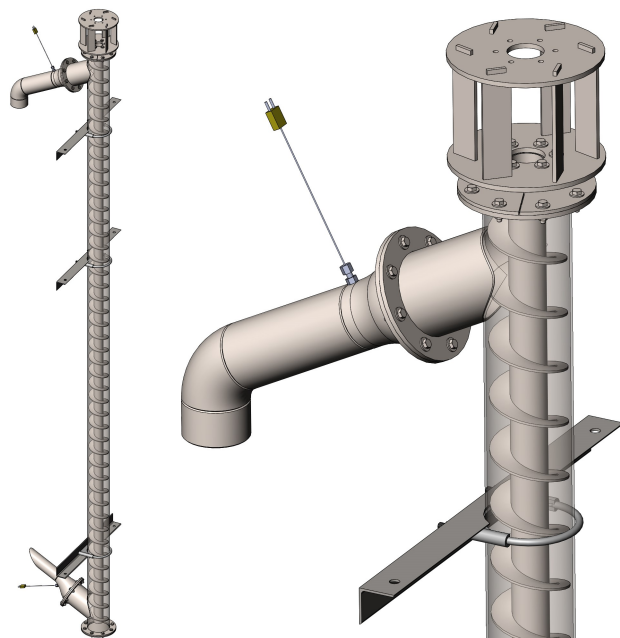


**Figure 2-6 Illustration of the screw lift and exploded view identifying the components and manufacturing detail**

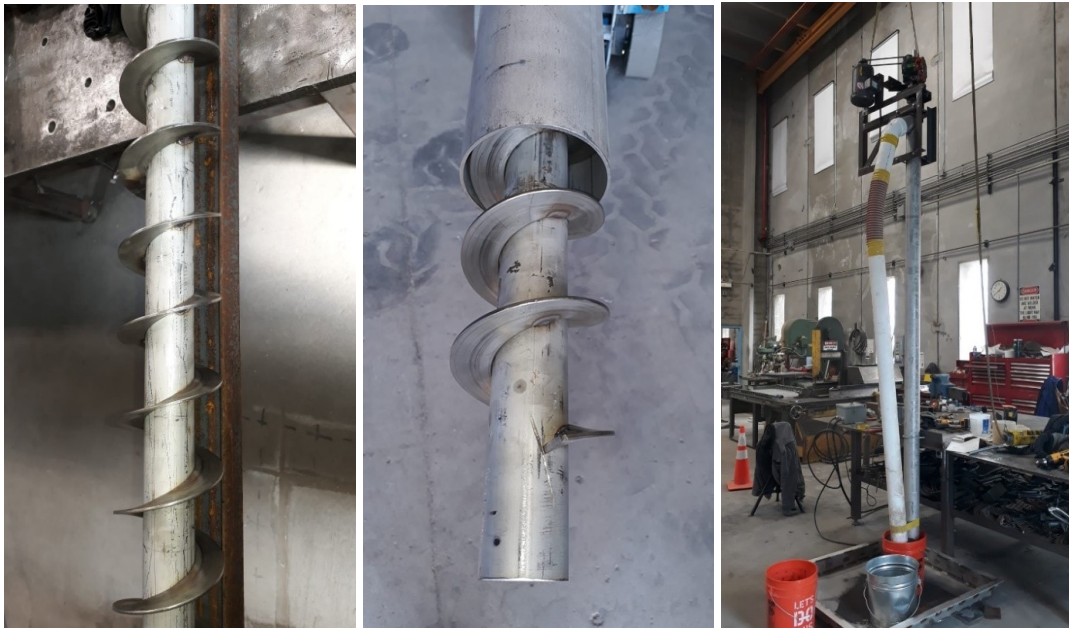


**Figure 2-7 Photos of the screw lift assembly and low-temperature commissioning setup**

### **2.5.3. Particle Weigh Hopper**

High-temperature particle mass flow rate measurements have been identified as a challenging area from past experience with the falling particle receiver development. The best approach has been identified to be in line weigh hoppers that are intermittently charged and discharged to measure mass flow rate. The weigh hopper design used in the present effort to measure particle flow rate through the heat exchanger is detailed in Figure 2-8. The design uses a pneumatically actuated slide gate with load cells that are thermally isolated from the particle volume. It is important to note that the hopper is not directly attached to the load cells, but rather skates on top such that thermal expansion of the hopper doesn't result in forces on the load cells other than hopper weight. The hopper has been sized such that it can be continuously charged as discharged to provide real time measurements of flow rate that are updated on a 30 to 60 second interval.

## **2.6. System Integration and Operation**

In addition to the detailed designs of the particle flow and sCO<sub>2</sub> flow loop components, significant effort was directed at ensuring the components would not have operational challenges when assembled into a complete system. In high-temperature experiments, the system integration and operation needs to consider the thermal expansion, component connections, allowable ramp rate, and control.

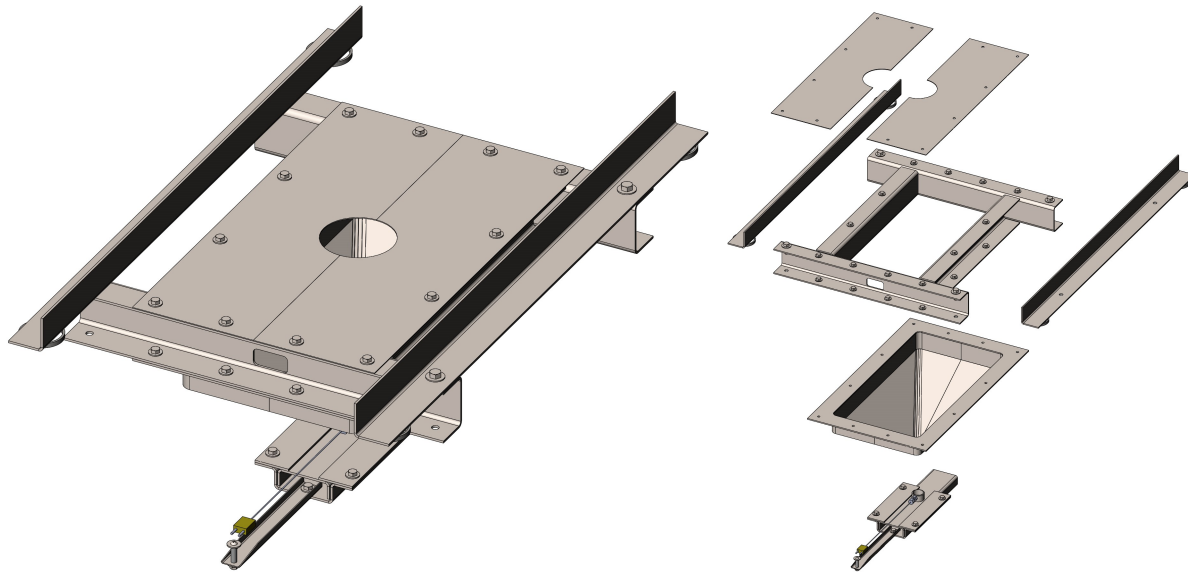


**Figure 2-8 Illustration of the particle weigh hopper assembly and exploded view identifying the components**

### **2.6.1. Component Connections and Thermal Expansion**

To address thermal expansion, calculations were performed to identify the amount of linear growth experienced by the components from the support locations. Thermal expansion on the particle components can be addressed through using tube-in-tube connections where one component is allowed to grow into another. This is only possible when using moving packed bed flow that does not require hermetic seals. In addition to linear growth, particle ducts can bend if they are preferentially heated on one side as in the case of an inclined particle chute. This is typically the result of transient operation where one duct face is suddenly exposed to high-temperature particles. A simulation of the particle duct feeding the particle heater inlet was conducted to identify if rapid heating of one face could cause interference with the heater or lift.

Thermal expansion within the sCO<sub>2</sub> loop was accommodated by using tubing elbows and expansion loops that allow for the required amount of deflection without resulting in high values of stress. In particular, the inlet and outlet tubing connecting the particle/sCO<sub>2</sub> heat exchanger to the recuperator needs to be considered due to temperature differences between the inlet and outlet. Bypass lines around thermal equipment is another area that can lead to problems since parallel length of tubing may be at different temperatures.

### **2.6.2. Supervisory Control and Data Acquisition**

The supervisory control and data acquisition system (SCADA) for the test stand uses National Instruments hardware and LabVIEW software. The system configuration is shown in Table 2-3, which uses a cRIO-9035 chassis with modules for analog control and feedback signals, and temperature measurements for RTDs and thermocouples. In addition to the NI modules, the

**Table 2-3 National Instruments supervisory control and data acquisition system hardware**

Chassis	Module	Channels	Signal
cRIO-9035	NI-9266	8	0-20 mA Output
	NI-9474	8	0,24 V Output
	NI-9208	16	$\pm$ 20 mA Input
	NI-9208	16	$\pm$ 20 mA Input
	NI-9216	8	RTDs
	NI-9216	8	RTDs
	NI-9214	16	Thermocouples
	NI-9214	16	Thermocouples

particle slide gate actuator is controlled using RS-232 for commanding and providing feedback on the position.

### **3. HEAT EXCHANGER DESIGN MODELING**

Modeling moving packed-bed particle heat exchangers has been an ongoing effort through the development of the first 100 kW<sub>t</sub> prototype and continued under the Gen3 program. The significant improvements in model fidelity that have been made through the past efforts were leveraged in the current project to evaluate the design of a 20 kW<sub>t</sub> prototype. The design was collaboratively developed between VPE, Solex, and Sandia based on the concept being considered for the Gen3 Particle Pilot Plant (G3P3).

The particle/sCO<sub>2</sub> heat exchanger concept is a shell-and-plate design that is manufactured through a combination of diffusion bonding to form microchannel plates and diffusion brazing to assemble a heat exchanger core with channels for particle flow between the plates. The sCO<sub>2</sub> is contained in microchannels within the plates which enhances heat transfer. The sCO<sub>2</sub> flow is introduced at the base of the heat exchanger and moves vertically upward through the plates in a counter-flow configuration with the downward particle flow. An illustration of the particle heat exchanger from G3P3 compared to a 20 kW<sub>t</sub> design is displayed in Figure 3-1.

#### **3.1. Heat Exchanger Model Development**

The heat exchanger model was developed inside of Sandia's high performance computing code Sierra which is a multiphysics finite element modeling tool. The code has the ability to solve mass, momentum, and energy conservation equations using various packages and transfer the thermal solution to a mechanical code for evaluating stress and strain fields in the heat exchanger material. This approach is similar to what would be encountered in Ansys, but Sierra is not license restricted in terms of nodes or parallel simulations. The modeling results described below evaluate the heat exchanger performance by first considering the isothermal flow in the sCO<sub>2</sub>

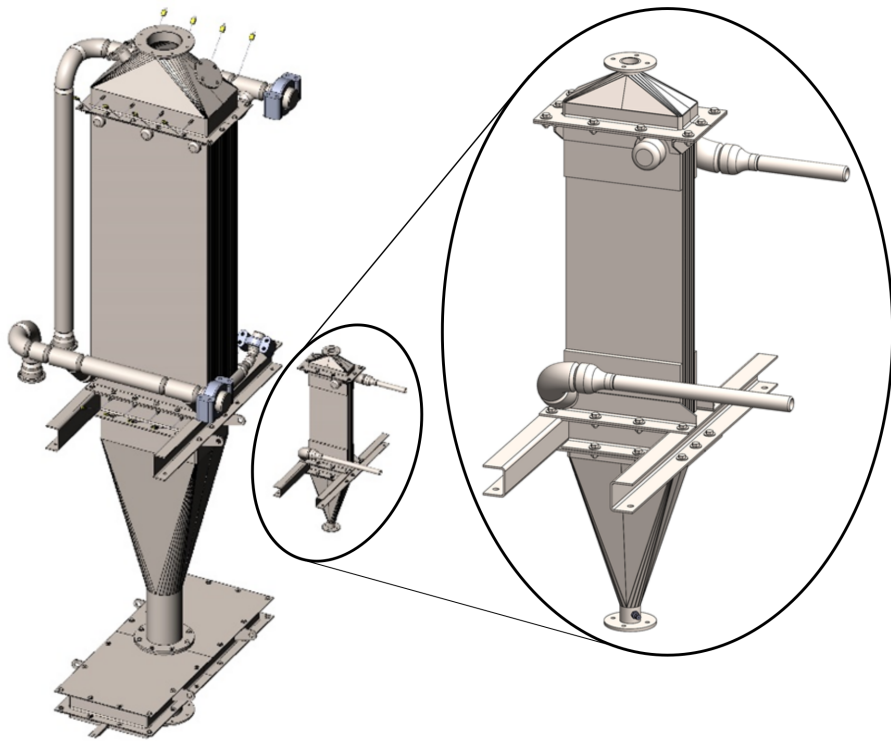


**Figure 3-1 Illustration of the 1 MW<sub>t</sub> G3P3 heat exchanger concept and subscale 20 kW<sub>t</sub> version**

channel to identify if the flow uniformity and pressure drop are acceptable. The work on the sCO<sub>2</sub> side is then expanded to include energy equations and coupled to the particle side for capturing heat transport in the moving packed bed. The following sections describe the modeling approach and results.

### **3.1.1. sCO<sub>2</sub> Microchannel Flow and Heat Transfer**

The sCO<sub>2</sub> flow within the microchannel network in the heat exchanger plate was evaluated by modeling the exact geometry of the microchannels within a single parallel plate of the heat exchanger. These simulations were conducted in the computational fluid dynamics package within Sierra called Fuego. Meshes for the microchannel network were created using Cubit and found to be grid independent for predicting pressure drop and flow non-uniformity at an element side of 0.2 mm. This resulted in mesh sizes of approximately 30M elements to represent a single microchannel plate. The model of the sCO<sub>2</sub> fluid considered a k- $\epsilon$  turbulence model and constant thermophysical properties at the operating temperature and pressure. Other turbulence models were loosely evaluated to identify sensitivity, but found to make little difference in predicting pressure drop and flow uniformity.

In order for a microchannel network to be considered acceptable for use in the prototype heat exchanger, pressure drop must be less than 40 kPa and flow non-uniformity must be less than 10%. Isothermal CFD simulations were conducted over the entire operating range of the heat

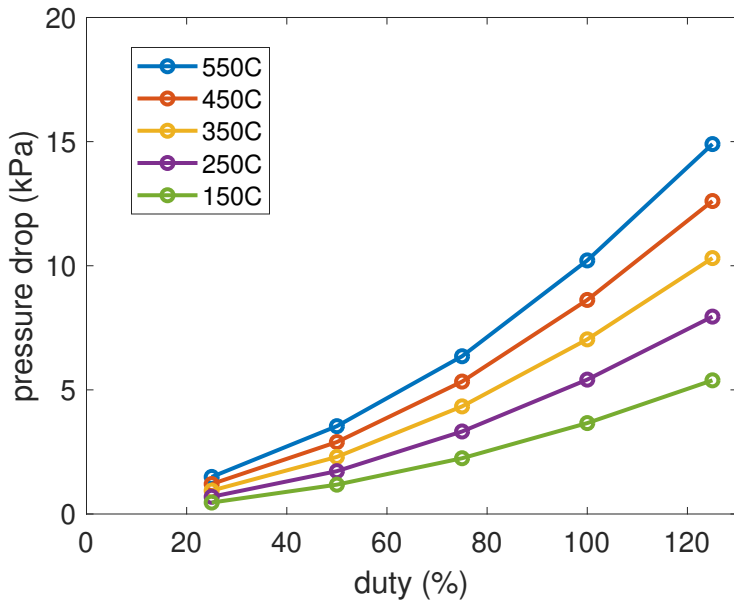


**Figure 3-2 Pressure drop in the 20 kW<sub>t</sub> subscale heat exchanger from CFD analysis of the microchannel network**

exchanger to identify if turndown or operating temperature had a significant impact on the sCO<sub>2</sub> flow uniformity.

The postprocessed values for pressure drop are displayed in Figure 3-2, which has the characteristic behavior of pressure drop increasing proportional to the square of velocity (duty). The pressure drop is shown to be well below the established 40 kPa metric based on available pump head for all operating temperatures up to 550 °C and flow rates up to 125% of the design. Pressure drop was shown to have a significant dependence on operating temperature due to the increase in viscosity and decrease in density over the range considered. However, the impact of changes in thermophysical properties of sCO<sub>2</sub> are much more significant in the lower temperature range and begin to diminish at temperatures above 400 °C.

The flow uniformity within the parallel microchannels was postprocessed from the same CFD simulations described for the pressure drop analysis. The results for the flow non-uniformity are displayed in Figure 3-3. Flow non-uniformity is shown to become slightly worse at high operating flow rates and low temperatures. However, the magnitude of the non-uniformity is always shown to remain below the 10% metric established to have a minimal impact on the thermal and mechanical performance. This result suggests that the heat exchanger can be operated over the entire space between ambient temperature and the design point without suffering from issues caused by flow non-uniformity.

### **3.1.2. Particle Flow and Heat Transport**

Overall heat transfer coefficients for the heat exchanger can be predicted through coupling the sCO<sub>2</sub> microchannel model to thermal models of the heat exchanger plate and particle domains.

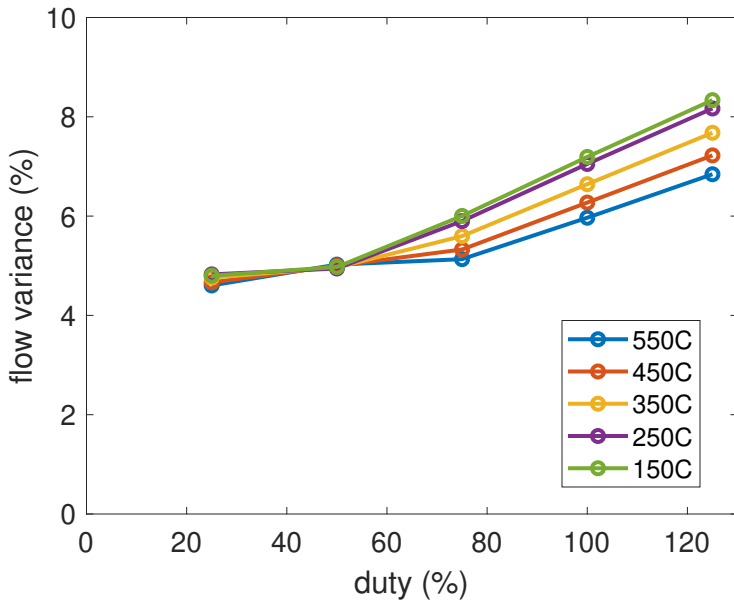


**Figure 3-3 Flow uniformity in the 20 kW<sub>t</sub> subscale heat exchanger from CFD analysis of the microchannel network**

The metallic plate domain can be simply included through a conduction equation where the internal microchannel boundary condition is coupled to the sCO<sub>2</sub> flow while the particle domain can be evaluated using an advection-diffusion equation for energy coupled to the outer surface of the plate. The challenge in modeling particle heat exchangers with continuum approximations has typically not been in solving the conservation equations, but rather obtaining thermophysical properties of the particle domain that capture realistic heat exchanger behavior. Typically, moving packed beds of particles are modeled by assuming that they move as a plug through the vertical channels and have bulk values of conductivity similar to those measured in experiments with static particles. This can be taken as a limiting case to predict heat exchanger performance, but if the conductivity differs due to particle motion or breaks down at the packed bed interface with the wall, the model will not be capable of evaluating heat exchanger performance. The initial heat exchanger modeling was performed assuming that the particle conductivity is accurately predicted by the ZBS model and the particle flow is accurately captured using an inviscid fluid approximation.

### 3.1.3. Heat Exchanger Thermal Performance

Solving the conservation equations for the coupled heat exchanger domain generates temperature field predictions as well as inlet and outlet temperature for the particle and sCO<sub>2</sub> flows. The simulation results can be postprocessed similar to the approach detailed in the experimental section to determine the overall heat transfer coefficient from a log mean temperature difference calculation assuming counter-flow arrangement. Simulating the exact heat exchanger geometry allows for potential future model validation through comparing individual point temperature measurements with locations in the simulation as well as use of the temperature field in

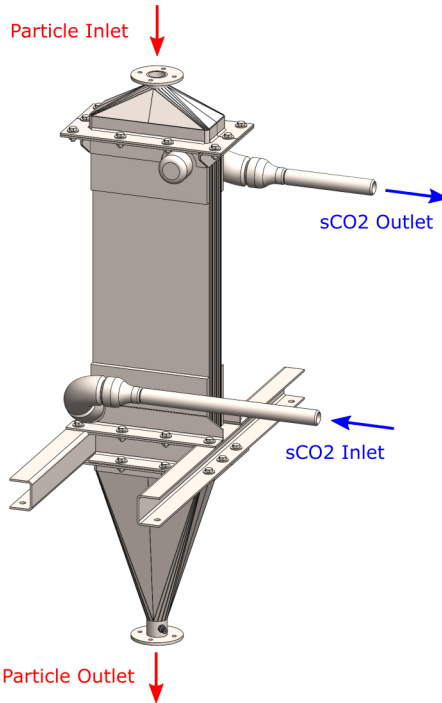


**Figure 3-4 Illustration of the 20 kW<sub>t</sub> heat exchanger design with instrumentation**

mechanical simulations. The post processed value for overall heat transfer coefficient predicted from the simulation is 449 W/m<sup>2</sup>K. Although only a single simulation result is presented for the geometry that is representative of the final design, it is important to note that the model was exercised numerous times over the iterative design process for the 20 kW<sub>t</sub> heat exchanger.

### **3.2. Prototype Heat Exchanger Design**

The prototype heat exchanger design that is based on the configuration of the G3P3 heat exchanger, but scaled down to 20 kW<sub>t</sub> is shown in Figure 3-4. The heat exchanger consists of 7 parallel plates with 3 mm particle channels, which generates 12 surfaces available for particle heat transfer that each have an effective heat transfer surface area of 0.0486 m<sup>2</sup>. The heat exchanger core has a total effective heat transfer surface area of just over 0.58 m<sup>2</sup>. Additional dimensions of the heat exchanger are provided in Appendix B.

### **3.3. Heat Exchanger Heat Loss Analysis**

The insulation design for the 20 kW<sub>t</sub> particle heat exchanger geometry must be capable of limiting heat loss such that closure of an energy balance can be achieved. Any heat that is lost from either the particle or sCO<sub>2</sub> domains between the boundary temperature measurements will contribute to measurement uncertainty. In other words, the energy balance can be used as a physical check for the data to verify the measurements even through it is not strictly required to calculate thermal performance.

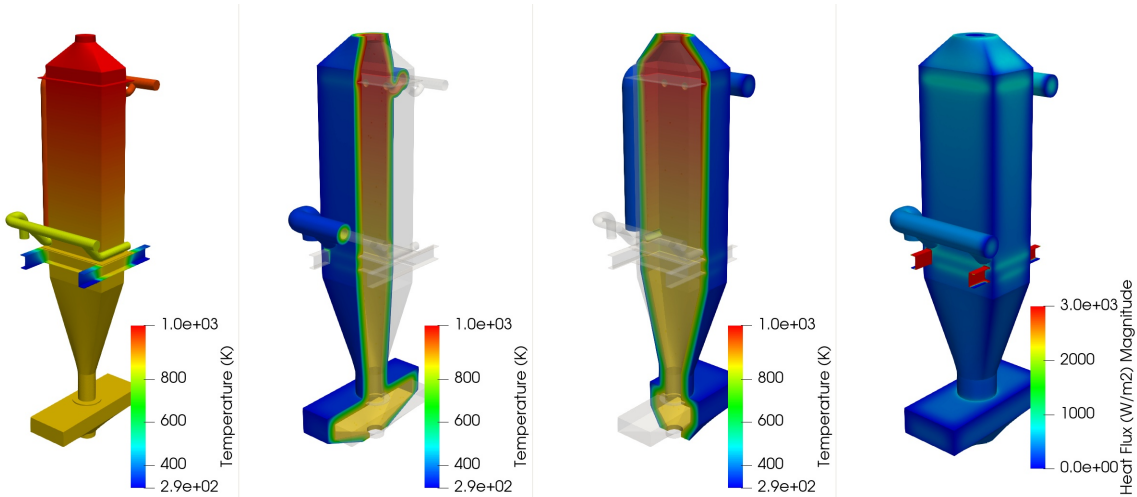


**Figure 3-5 Temperature and heat flux contour plots of the 20 kW<sub>t</sub> heat exchanger surrounded with 4-inch of Superwool**

A defeatured geometry of the 20kW<sub>t</sub> heat exchanger design was constructed and surrounded with a domain to represent layers of Superwool insulation. In addition to the heat loss through the insulation, the contact between the supporting frame and structure is captured using a constant temperature boundary condition. A parametric study was performed to assess the quantity of insulation required to limit heat loss from the 20 kW<sub>t</sub> experiment. A result for the design point simulation of the heat exchanger with 4-inch Superwool insulation is shown in Figure 3-5, which predicts a total heat loss of less than 300 W (1.5%).

## 4. HEAT EXCHANGER PERFORMANCE TESTING

The 20 kW<sub>t</sub> heat exchanger prototype that was detailed in the previous section was manufactured by Vacuum Process Engineering (VPE) for performance evaluation at Sandia using the test facility developed within this project. The following section describes the prototype heat exchanger manufacturing, testing, and performance measurements.

### 4.1. Prototype Heat Exchanger Manufacturing

The manufactured 20kW<sub>t</sub> heat exchanger core is shown in Figure 4-1 without the particle hoppers and instrumentation. These photos were taken after shipping to Sandia and prior to testing so no discoloration of the stainless-steel is observed. The heat exchanger passed both a helium leak check and hydrostatic pressure test (5400 psig) at VPE prior to shipping as part of a quality control process. Due to the proprietary nature of the port configuration and channel layout in the heat exchanger core, details beyond the these two photos in Figure 4-1 and the general dimensions in Appendix B can not be provided.



**Figure 4-1 Photos of the 20 kW<sub>t</sub> heat exchanger core after manufacturing at VPE and prior to testing at Sandia**

Following the delivery of the heat exchanger to Sandia, the core was assembled with the particle hoppers, supporting structure, and instrumentation. A photo of the heat exchanger installed in the test facility is displayed in Figure 4-2. The heat exchanger was commissioned by pressurizing incrementally with sCO<sub>2</sub> until the operating pressure was achieved while monitoring for leaks. No leaks were identified in the heat exchanger throughout the process, but two leaks in the sCO<sub>2</sub> loop were identified at instrumentation ports. The heater was commissioned through both bump testing with particle flow and holding the heat exchanger at a constant inlet temperature of 100 °C. The heat exchanger, particle flow loop, and sCO<sub>2</sub> tubing were wrapped in insulation in preparation for performance testing following the successful commissioning.

#### **4.2. Heat Exchanger Testing Procedure**

The testing procedure for measuring steady-state overall heat transfer coefficients was similarly conducted to the approach developed for the past electrically heated tests from the first 100 kW<sub>t</sub> prototype [7]. Testing of the 20 kW<sub>t</sub> subscale prototype heat exchanger occurred through starting flow of the particle and sCO<sub>2</sub> fluids at ambient temperature. The particle heat exchanger inlet temperature was slowly ramped to the desired operating temperature by controlling the electrical heat addition in the heater. Once the electric heater reached the target inlet temperature, PID control of the electric heater was enabled and the flow valves on the sCO<sub>2</sub> side were adjusted to manipulate the sCO<sub>2</sub> inlet temperature and flow rate. The temperature measurements were allowed to stabilize and remain at steady state for approximately one hour prior to moving to a new operating condition. Steady-state operating conditions for performance evaluation were identified as periods of greater than 15 minutes with less than  $\pm 1$  °C of variation at all four heat exchanger boundaries.



**Figure 4-2 Photo of the 20 kW<sub>t</sub> heat exchanger installed in the test facility at Sandia without insulation**

### 4.3. Heat Exchanger Performance Measurements

The thermal performance of the prototype heat exchanger was evaluated by measuring boundary temperatures and flow rates until steady-state operation is achieved. The overall heat transfer coefficient were calculated from the steady-state performance data according to the log mean temperature difference (LMTD) for a counter-flow configuration. The calculations are documented in the following set of equations.

$$\dot{Q}_{\text{CO}_2} = \dot{m}_{\text{CO}_2} (h_{\text{CO}_2,\text{out}} - h_{\text{CO}_2,\text{in}}) \quad (1)$$

$$\dot{Q}_s = \dot{m}_s (h_{s,\text{in}} - h_{s,\text{out}}) \quad (2)$$

$$\Delta T_{\text{lm}} = \frac{(T_{s,\text{in}} - T_{\text{CO}_2,\text{out}}) - (T_{s,\text{out}} - T_{\text{CO}_2,\text{in}})}{\ln\left(\frac{T_{s,\text{in}} - T_{\text{CO}_2,\text{out}}}{T_{s,\text{out}} - T_{\text{CO}_2,\text{in}}}\right)} \quad (3)$$

$$U_{\text{hx}} = \frac{\dot{Q}_{\text{CO}_2}}{\Delta T_{\text{lm}} A_{\text{hx}}} \quad (4)$$

The steady-state measurements of thermal performance for the 20 kW<sub>t</sub> subscale prototype are displayed in Figure 4-3. The overall heat transfer coefficient is observed to be approximately 300 W/m<sup>2</sup>K at the intermediate temperature operating conditions (400-600 °C) and displays a slight dependence on particle inlet temperature in the range of 200-400 °C. The measured values of performance were verified through evaluating closure of the heat exchanger energy balance and agreement between upstream and downstream temperature measurements. The overall heat transfer coefficients observed both above and below the trend at 300 W/m<sup>2</sup>K are the result of intentionally operating the heat exchanger at off-design flow rates. The overall heat transfer coefficient data points approaching 400 W/m<sup>2</sup>K were collected by operating the heat exchanger at particle flow rates of 0.15 kg/s. The overall heat transfer coefficient data points near 200 W/m<sup>2</sup>K were collected by operating the heat exchanger at particle flow rates of 0.05 kg/s. The measured performance for the 20 kW<sub>t</sub> subscale prototype is a large improvement over the performance of the first 100 kW<sub>t</sub> prototype developed in a prior project that had overall heat transfer coefficient values of 50-70 W/m<sup>2</sup>K and difficulty in measuring the performance due to system integration issues. The observed overall heat transfer coefficients for the 20 kW<sub>t</sub> prototype are between a factor of 4-6 times better than any other known particle to sCO<sub>2</sub> heat exchanger in existence.

Pressure drop (Figure 4-4) was measured from inlet to outlet of the heat exchanger and observed to be less than 7 kPa (0.04%) at the design point conditions which is inline with CFD modeling results and builds confidence in the pressure drop estimations for future heat exchanger prototypes. The measured pressure drop of the 20 kW<sub>t</sub> prototype was expected to be substantially lower than the 2% target of commercial scale heat exchanger designs due to a combination of the intermediate temperature sCO<sub>2</sub> properties (lower viscosity and higher density), larger channel dimensions because the allowable stress of stainless steel (105 MPa) at 550 °C is more than triple

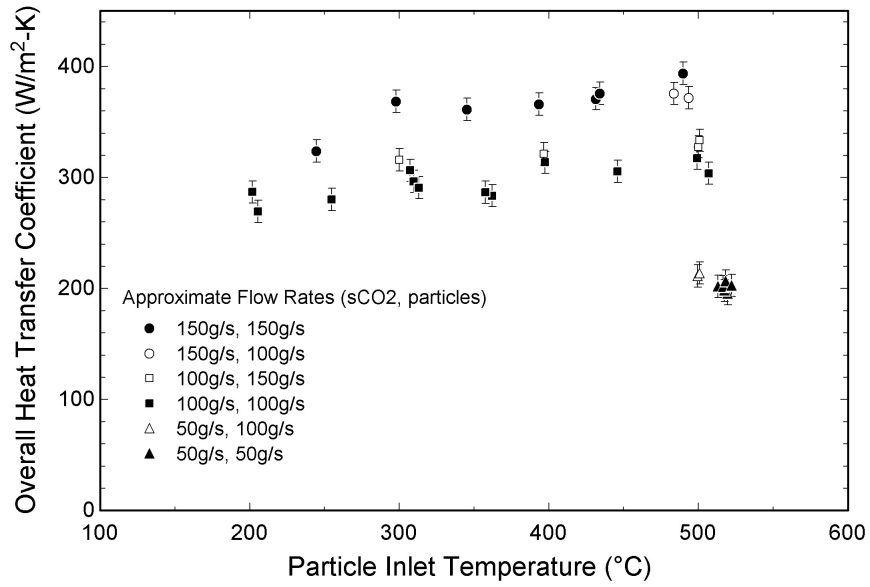


**Figure 4-3 Experimental measurements of the 20 kW<sub>t</sub> heat exchanger overall heat transfer coefficient as a function of the particle inlet temperature**

the value of IN617 (30 MPa) at 800 °C, and the small plate dimensions resulting in shorter flow path lengths. Overall, the measured performance and operation of the 20 kW<sub>t</sub> subscale prototype provides confidence in the modeled results of future designs.

$$\Delta P_{\text{CO}_2} = P_{\text{CO}_2,\text{in}} - P_{\text{CO}_2,\text{out}} \quad (5)$$

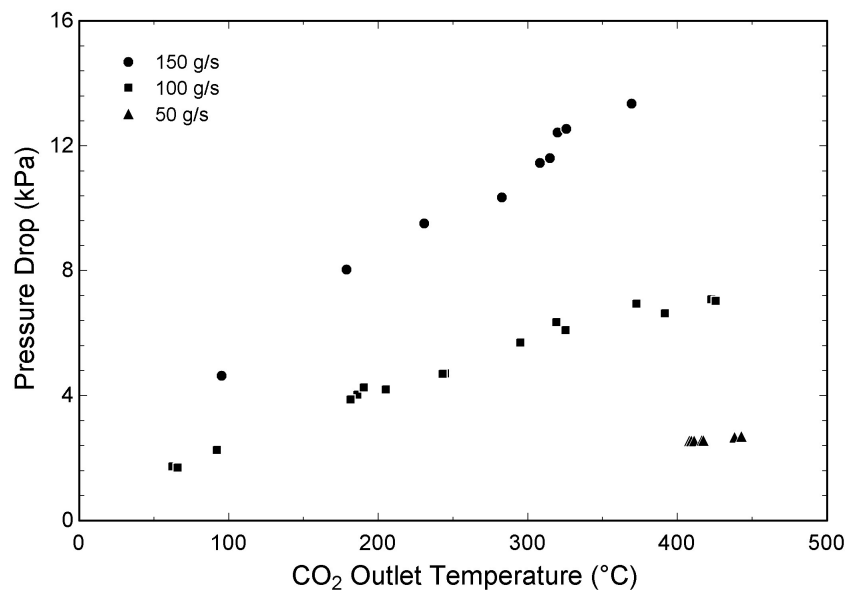


**Figure 4-4 Experimental measurements of the 20 kW<sub>t</sub> heat exchanger pressure drop as a function of operating temperature at the design point flow rate (0.1 kg/s) and 50% above (0.15 kg/s) and below (0.05 kg/s) the design point flow rate**

## 5. CONCLUSION

The design of an integrated test facility for evaluating particle/sCO<sub>2</sub> heat exchanger performance was reported. The facility was used to produce heat exchanger performance data for a novel 20 kW<sub>t</sub> moving packed-bed heat exchanger prototype based on the design developed from the G3P3 project. The prototype design implemented close plate spacing (3 mm) on the particle side, integral porting on the sCO<sub>2</sub> side, and pure counter-flow arrangement in single bank geometry. Overall heat transfer coefficients for the prototype heat exchanger at the design point were measured up to 300 W/m<sup>2</sup>-K and cases using high approach temperature were measured with peak values as high as 400 W/m<sup>2</sup>-K. The heat exchanger pressure drop was measured to be 0.04% at the design point operating conditions, which is consistent with CFD simulations of the microchannel network. The small value is the result of a combination of the heat exchanger scale and operating temperature. The project results provide a significant step forward in the thermal-hydraulic performance of moving packed-bed particle/sCO<sub>2</sub> heat exchangers for next generation particle CSP plants.

### 5.1. Lessons Learned

The following sections describe key lessons learned for both the test facility and prototype heat exchanger design in an itemized format. Additional moving packed-bed particle heat exchanger design and testing lessons learned are available in a prior report.

#### 5.1.1. *Particle and sCO<sub>2</sub> Flow Loops*

- Significant effort is required to construct and commission a test loop that can perform the required operations to reliably measure heat exchanger performance.
- Electrical heat addition with particle recirculation is the preferred approach to perform long-duration heat exchanger testing.
- Particle flow must be conditioned through thermal equilibration prior to making a measurement of bulk averaged temperature.
- Particle conveyance through the use of a screw lift will severely limit particle lifetime through fines generation in commercial systems. Future efforts should try to implement small skip hoists for vertical conveyance and screws for horizontal conveyance.
- Alternative control strategies should be developed for the particle heater such as feed-forward or model-predictive control.
- Integration of a chiller for sCO<sub>2</sub> cooling will result in disturbances in the data due to compressor cycling. Future systems should install a chiller such that fluid temperature remains constant ( $\pm 0.1$  °C).

### **5.1.2. *Particle/sCO<sub>2</sub> Heat Exchanger***

- Close plate spacing and counter-flow configuration significantly improves parallel plate moving packed-bed heat exchanger performance.
- Integral porting of the sCO<sub>2</sub> flow can reduce heat exchanger pressure drop to meet primary heat exchanger performance requirements.
- A particle-side fin array is still a promising approach to improve moving packed-bed heat exchanger performance and should be evaluated in future studies.
- Heat loss can be controlled to produce reliable heat exchanger performance data at a 20 kW<sub>t</sub> scale for valuable model validation studies.
- Significant progress on particle heat exchanger design should target iterative refinement of the heat exchanger through building and testing multiple prototypes.
- Modeling particle heat exchangers using continuum approximations requires numerous assumptions that need to be verified to be accurate within the actual hardware.

## REFERENCES

- [1] Paul Denholm and Mark Mehos. Role of concentrating solar power in integrating solar and wind energy. Technical report, National Renewable Energy Lab, Golden, CO (United States), 2015.
- [2] Mark Mehos, Craig Turchi, Judith Vidal, Michael Wagner, Zhiwen Ma, Clifford Ho, William Kolb, Charles Andraka, and Alan Kruizenga. Concentrating solar power Gen3 demonstration roadmap. Technical report, National Renewable Energy Lab, Golden, CO (United States), 2017.
- [3] Clifford K Ho, Kevin J Albrecht, Lindsey Yue, Brantley Mills, Jeremy Sment, Joshua Christian, and Matthew Carlson. Overview and design basis for the Gen 3 particle pilot plant (G3P3). In *AIP Conference Proceedings*, volume 2303, page 030020. AIP Publishing LLC, 2020.
- [4] PK Falcone, JE Noring, and JM Hruby. Assessment of a solid particle receiver for a high temperature solar central receiver system. Technical report, Sandia National Lab, Livermore, CA (United States), 1985.
- [5] Craig S Turchi, Zhiwen Ma, Ty W Neises, and Michael J Wagner. Thermodynamic study of advanced supercritical carbon dioxide power cycles for concentrating solar power systems. *Journal of Solar Energy Engineering*, 135(4), 2013.
- [6] Kevin J Albrecht, Matthew L Bauer, and Clifford K Ho. Parametric analysis of particle CSP system performance and cost to intrinsic particle properties and operating conditions. In *ASME 2019 13th International Conference on Energy Sustainability collocated with the ASME 2019 Heat Transfer Summer Conference*. American Society of Mechanical Engineers Digital Collection, 2019.
- [7] Kevin J Albrecht, Matthew D Carlson, Hendrik F Laubscher, Robert Crandell, Nicolas DeLovato, and Clifford K Ho. Testing and model validation of a prototype moving packed-bed particle-to-sCO<sub>2</sub> heat exchanger. In *AIP Conference Proceedings*, volume 2303, page 030002. AIP Publishing LLC, 2020.
- [8] Clifford K Ho, Matthew Carlson, Kevin J Albrecht, Zhiwen Ma, Sheldon Jeter, and Clayton M Nguyen. Evaluation of alternative designs for a high temperature particle-to-sCO<sub>2</sub> heat exchanger. *Journal of Solar Energy Engineering*, 141(2), 2019.
- [9] Kevin J Albrecht and Clifford K Ho. Design and operating considerations for a shell-and-plate, moving packed-bed, particle-to-sCO<sub>2</sub> heat exchanger. *Solar Energy*, 178:331–340, 2019.
- [10] Torsten Baumann and Stefan Zunft. Development and performance assessment of a moving bed heat exchanger for solar central receiver power plants. *Energy Procedia*, 69:748–757, 2015.

- [11] Abdelrahman El-Leathy, Hany Al-Ansary, Sheldon Jeter, Eldwin Djajadiwinata, Shaker Alaquel, Matthew Golob, Clayton Nguyen, Rajed Saad, Talha Shafiq, Syed Danish, et al. Preliminary tests of an integrated gas turbine-solar particle heating and energy storage system. In *AIP Conference Proceedings*, volume 2033, page 040013. AIP Publishing LLC, 2018.
- [12] Shaker Alaquel, Abdelrahman El-Leathy, Hany Al-Ansary, Eldwin Djajadiwinata, Nader Saleh, Syed Danish, Rageh Saeed, Abdulelah Alswaiyd, Zeyad Al-Suhaibani, Sheldon Jeter, et al. Experimental investigation of the performance of a shell-and-tube particle-to-air heat exchanger. *Solar Energy*, 204:561–568, 2020.
- [13] Rajgopal Vijaykumar, Matthew L Bauer, Mark Lausten, and Abraham M Shultz. Optimizing the supercritical CO<sub>2</sub> brayton cycle for concentrating solar power application. In *Proceedings of the 6th Int Supercritical CO<sub>2</sub> Power Cycles, Pittsburgh, PA, USA*, pages 27–29, 2018.
- [14] Kevin J Albrecht and Clifford K Ho. High-temperature flow testing and heat transfer for a moving packed-bed particle/sCO<sub>2</sub> heat exchanger. In *AIP Conference Proceedings*, volume 2033, page 040003. AIP Publishing LLC, 2018.
- [15] Matt D Carlson and Clifford K Ho. A particle/sCO<sub>2</sub> heat exchanger testbed and reference cycle cost analysis. In *ASME 2016 10th International Conference on Energy Sustainability collocated with the ASME 2016 Power Conference and the ASME 2016 14th International Conference on Fuel Cell Science, Engineering and Technology*. American Society of Mechanical Engineers Digital Collection, 2016.
- [16] Matthew D Carlson. Guidelines for the design and operation of supercritical carbon dioxide R&D systems. In *AIP Conference Proceedings*, volume 2303, page 130003. AIP Publishing LLC, 2020.
- [17] Kevin J Albrecht, Matthew D Carlson, and Clifford K Ho. Integration, control, and testing of a high-temperature particle-to-sCO<sub>2</sub> heat exchanger. In *AIP Conference Proceedings*, volume 2126, page 030001. AIP Publishing LLC, 2019.

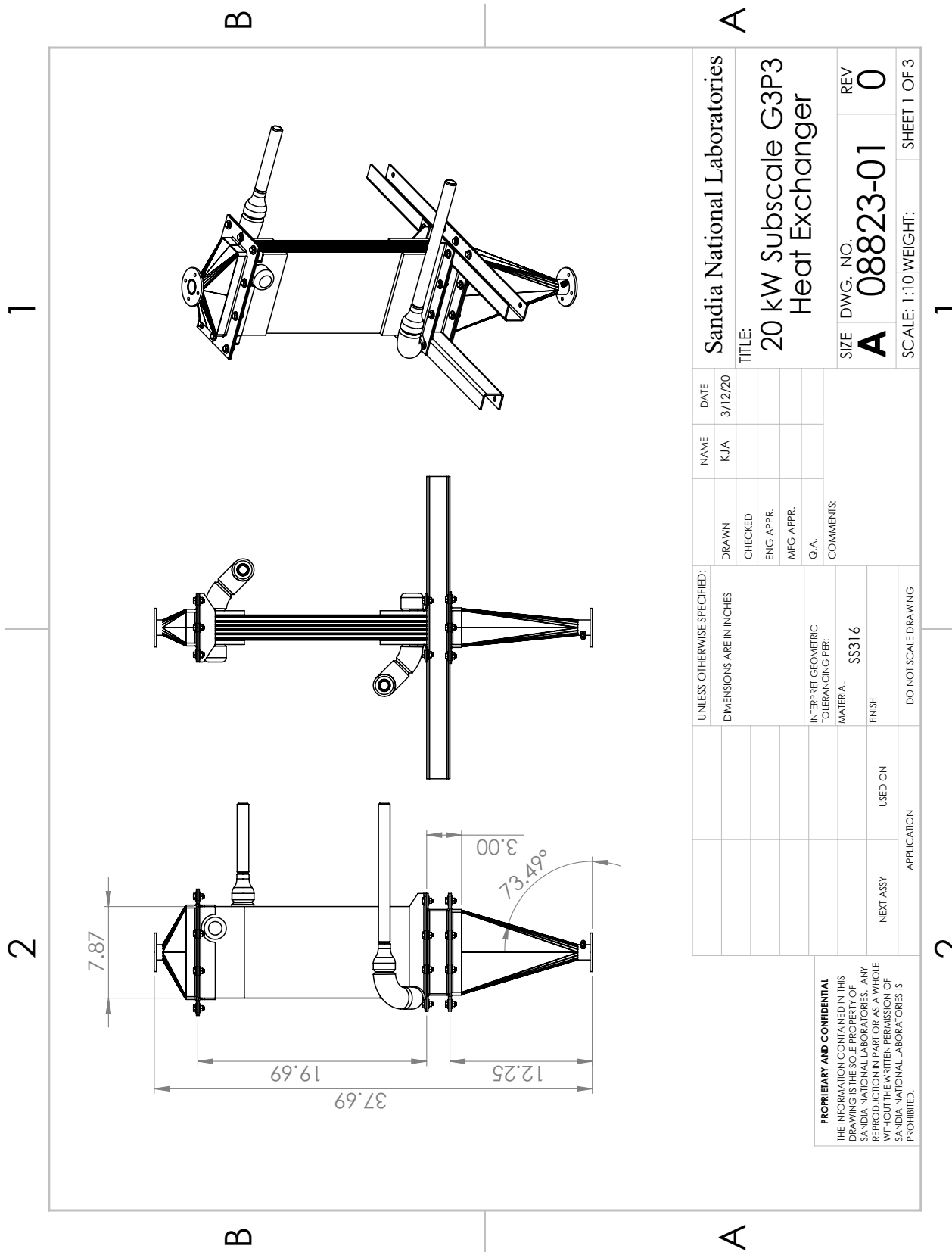


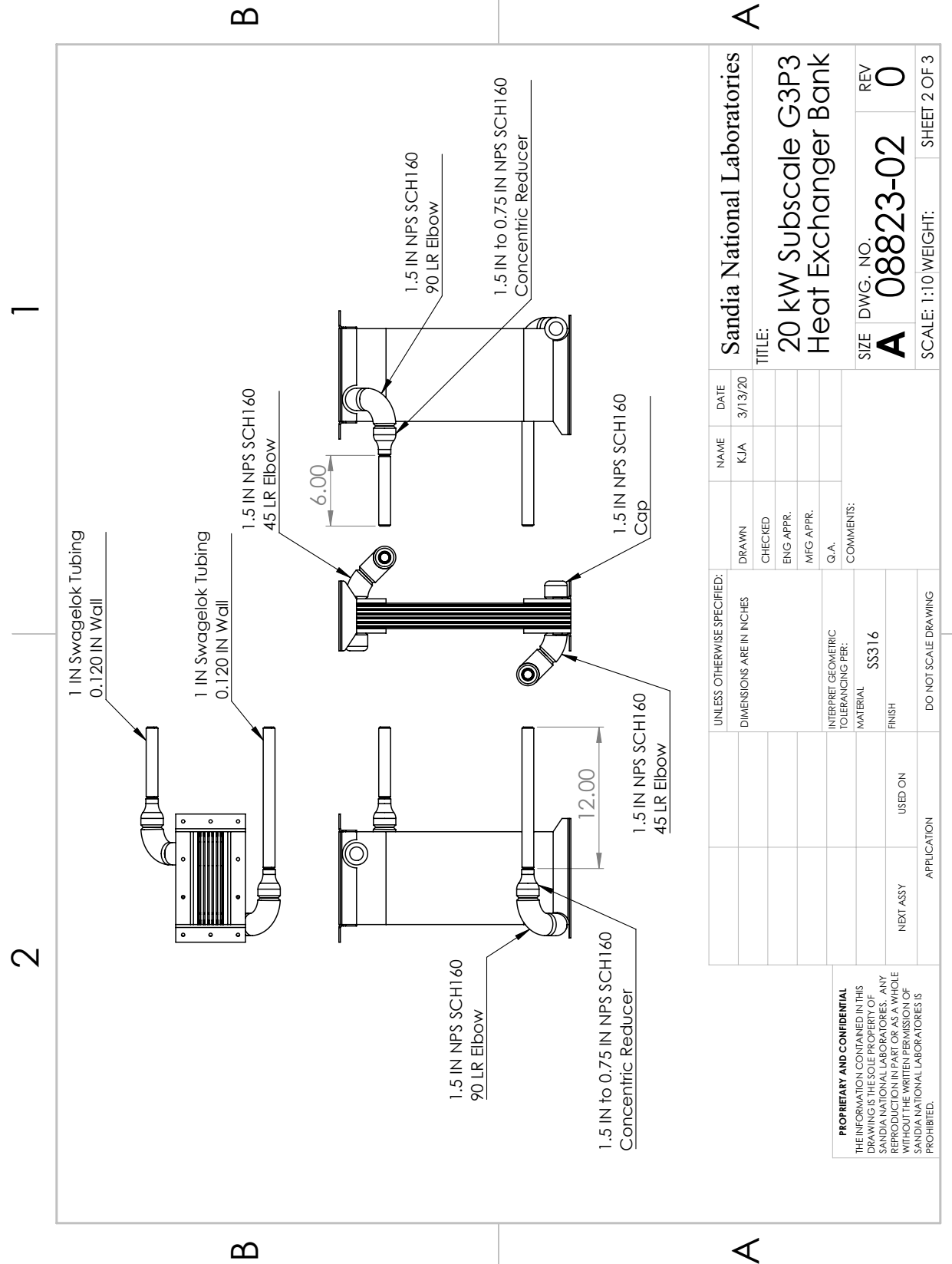
## APPENDIX A. HPROJECT MILESTONES

Milestone Summary Table			
Recipient name:	Sandia National Laboratories	Metric	
Project title:	Particle Heat Transfer Mechanisms	Description	Metric
Milestone Number:	Milestone Title	Assessment Tool	Metric justification
Budget Period 4.1			
1.1	Design of 20 W parallel plate prototype	Size 20 kW moving packed bed heat exchanger with optimized parallel plate arrangement input parameters	Modeled overall heat transfer coefficient subject to uncertainty in $U_{-IK} = 300 \text{ W/m}^2\text{K}$ input for parameters
1.2	Design of 20 W finned prototype	Size 20 kW moving packed bed heat exchanger with optimized particle slide fin array	CFD simulation with prescribed uncertainty in heat transfer coefficient achieves desired performance based on 95% confidence interval
1.3	Modeling pressure drop and flow uniformity	Performs CFD analysis of $\text{CO}_2$ flow in the heat exchanger to evaluate pressure drop and flow uniformity	CFD simulation with prescribed uncertainty in $U_{-IK} = 500 \text{ W/m}^2\text{K}$ under unity in input parameters achieves desired performance based on 95% confidence interval
1.4	Instrumentation and measurement	Develop instrumentation plan based on learning from SellaiaAMP heat exchanger to more accurately diagnose performance issues in the heat exchanger	CFD simulation indicating modeled pressure drop and flow non-uniformity results in 10% reduction in overall heat transfer coefficient
2.1	Procure subscale heat exchanger for testing	Obtain at least one subscale heat exchanger for testing based on most promising modeled performance in milestones 1.1 and 1.2	CFD simulation indicating modeled pressure drop and flow non-uniformity results in 10% reduction in overall heat transfer coefficient
2.2a	Experimental validation	Measure the performance of this subscale prototype $\text{CO}_2$ heat exchanger with $\text{CO}_2$ at 20 Ws and particle inlet temperatures above 500 °C	CFD of experimentally measured values for heat transfer coefficient agree to within 10% with modeled per m <sup>2</sup> for $U_{-IK} = 500 \text{ W/m}^2\text{K}$
2.2b	Measurement of temperature distribution	Use instrumentation to measure particle distribution, inlet temperature distribution, and outlet temperature distribution. Separate particle and $\text{CO}_2$ heat transfer coefficients.	Predictions of temperature distribution in the heat exchanger are important for model validation and the mechanical performance. The local temperature distribution predicted by the model must agree with the experimentally measured values to within 10%.
2.2c	Parametric study on operating conditions	Measure the performance of this subscale particle-to- $\text{CO}_2$ heat exchanger with various inlet temperature, flow rates, and particle types	Experimentally measured values for heat transfer coefficient with variations in operating conditions (flow rate, temperature, particle type) agree with modeled performance to within 10%.
End of Project	Submission of final project report		Robust models that predict performance over a wide variety of operating conditions are critical to design and validate heat exchanger concepts.
Final Deliverable			



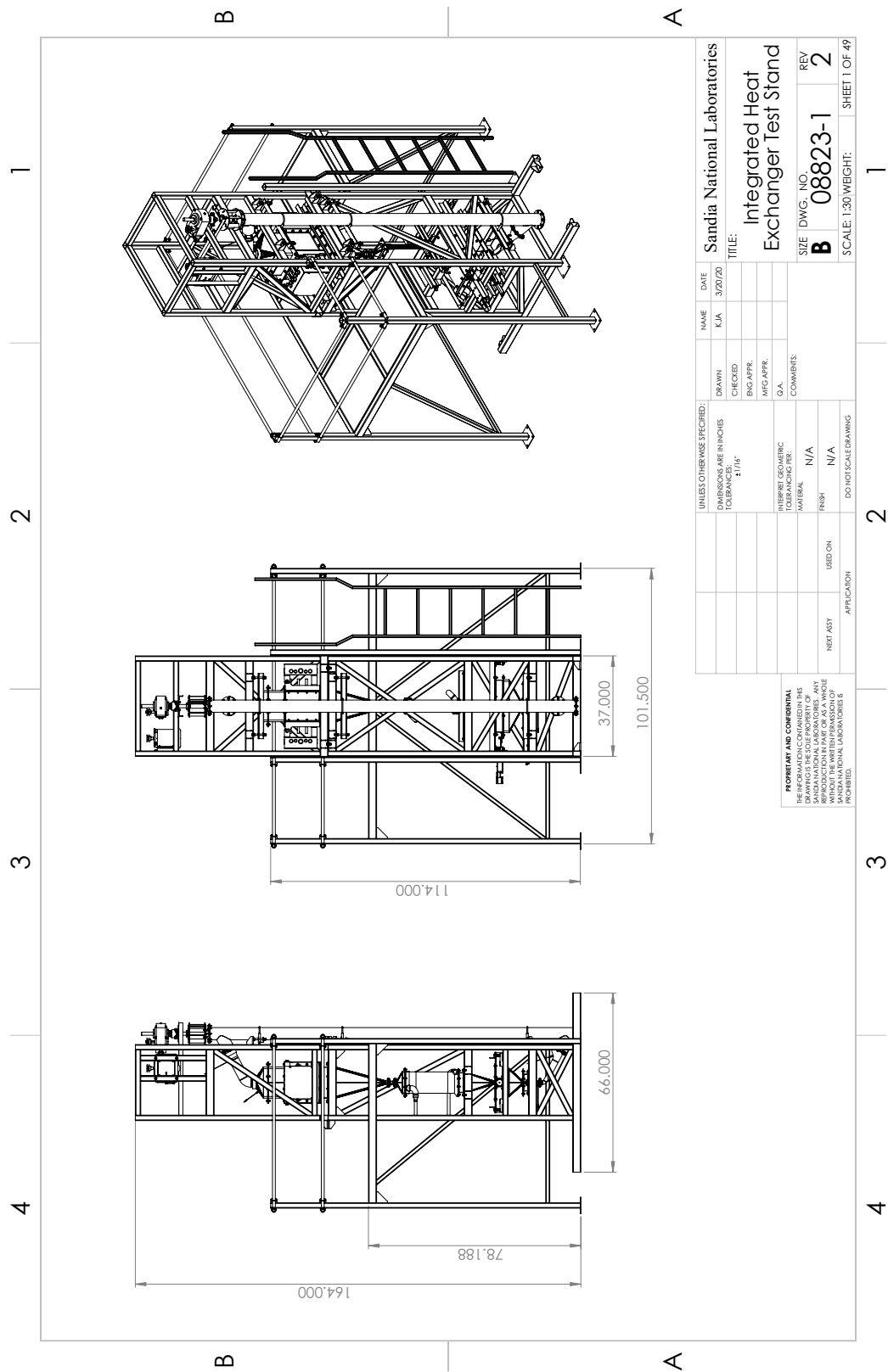
## APPENDIX B. HEAT EXCHANGER GENERAL ARRANGEMENT DRAWINGS

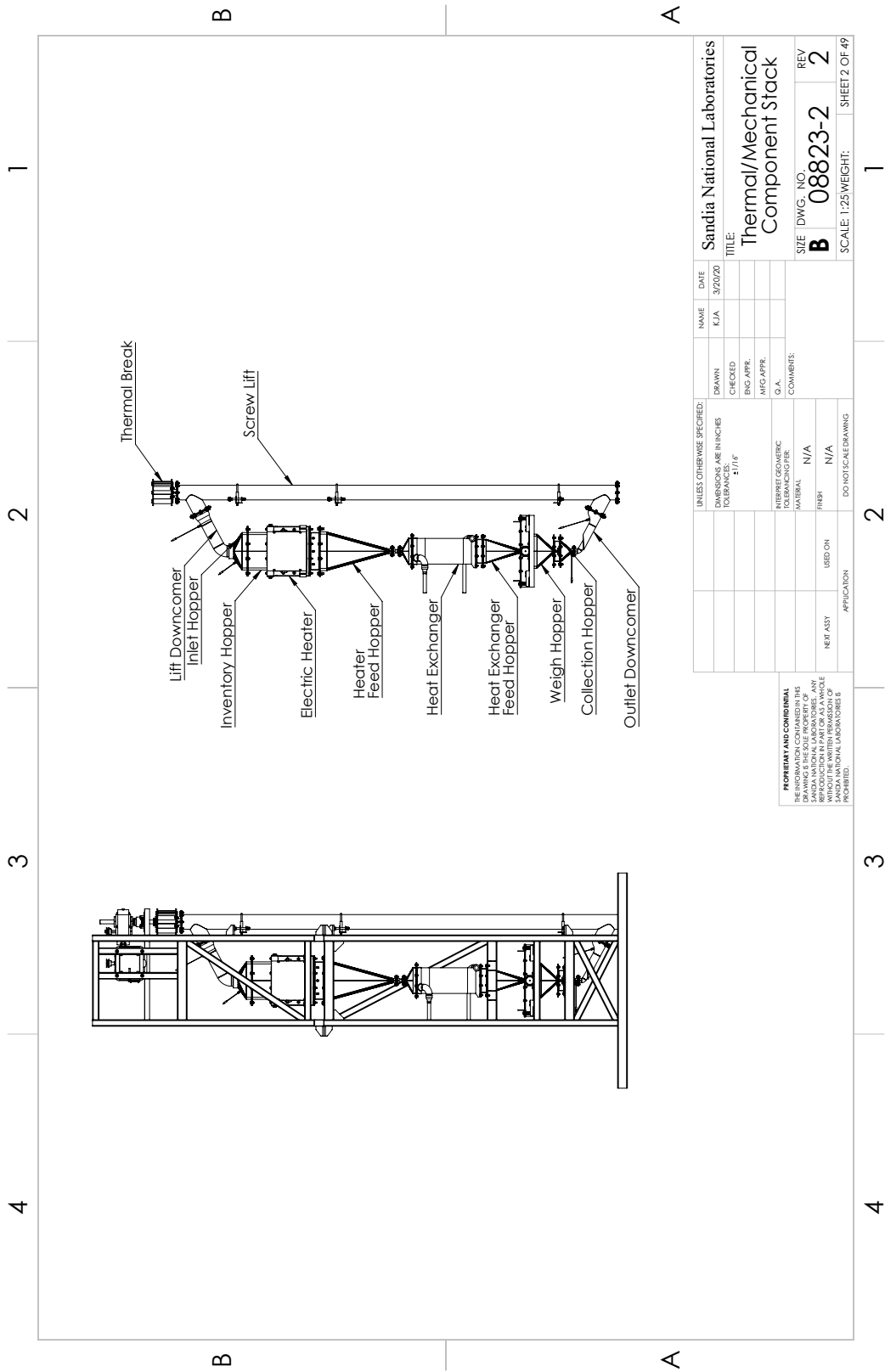


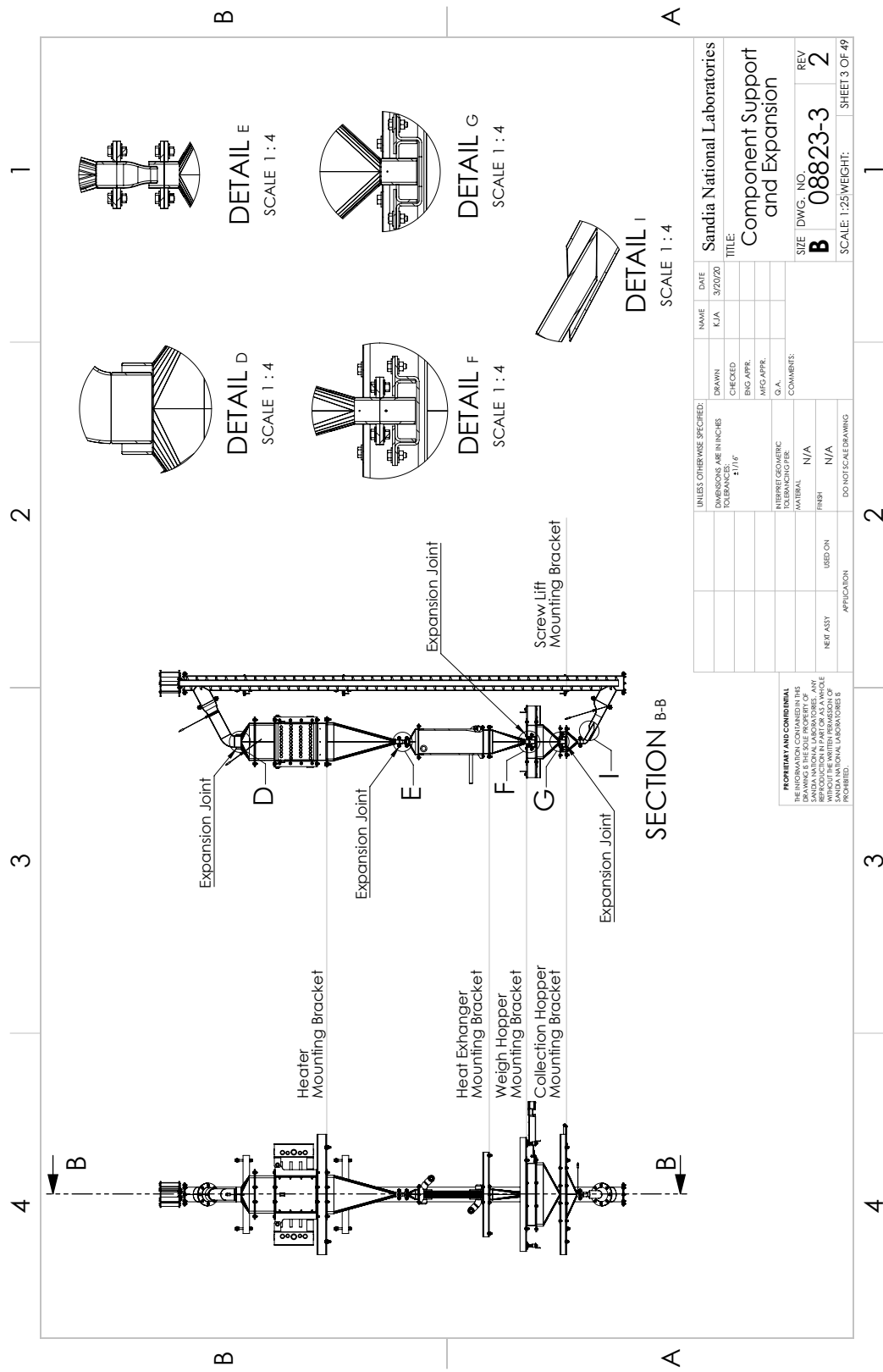


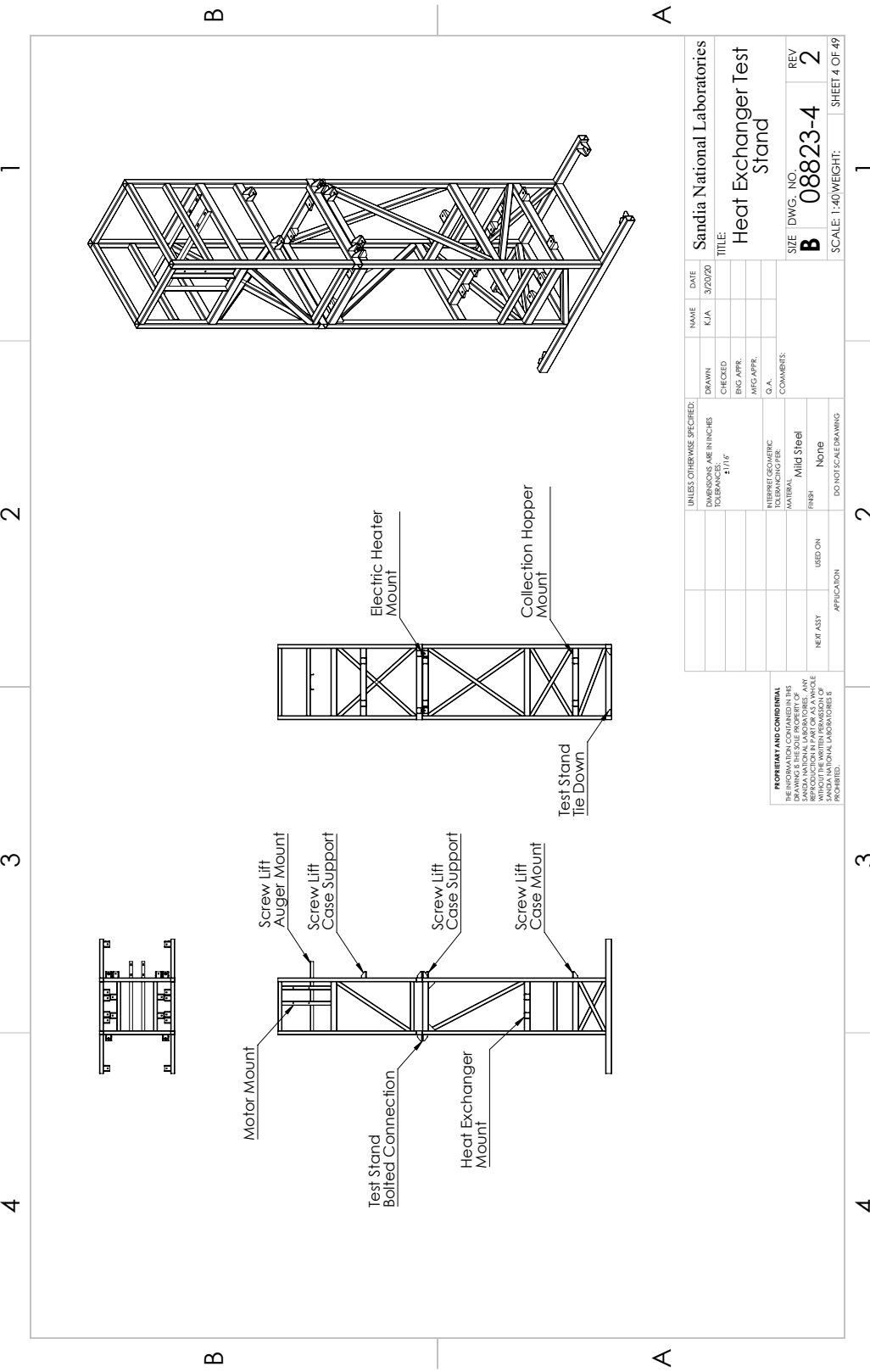


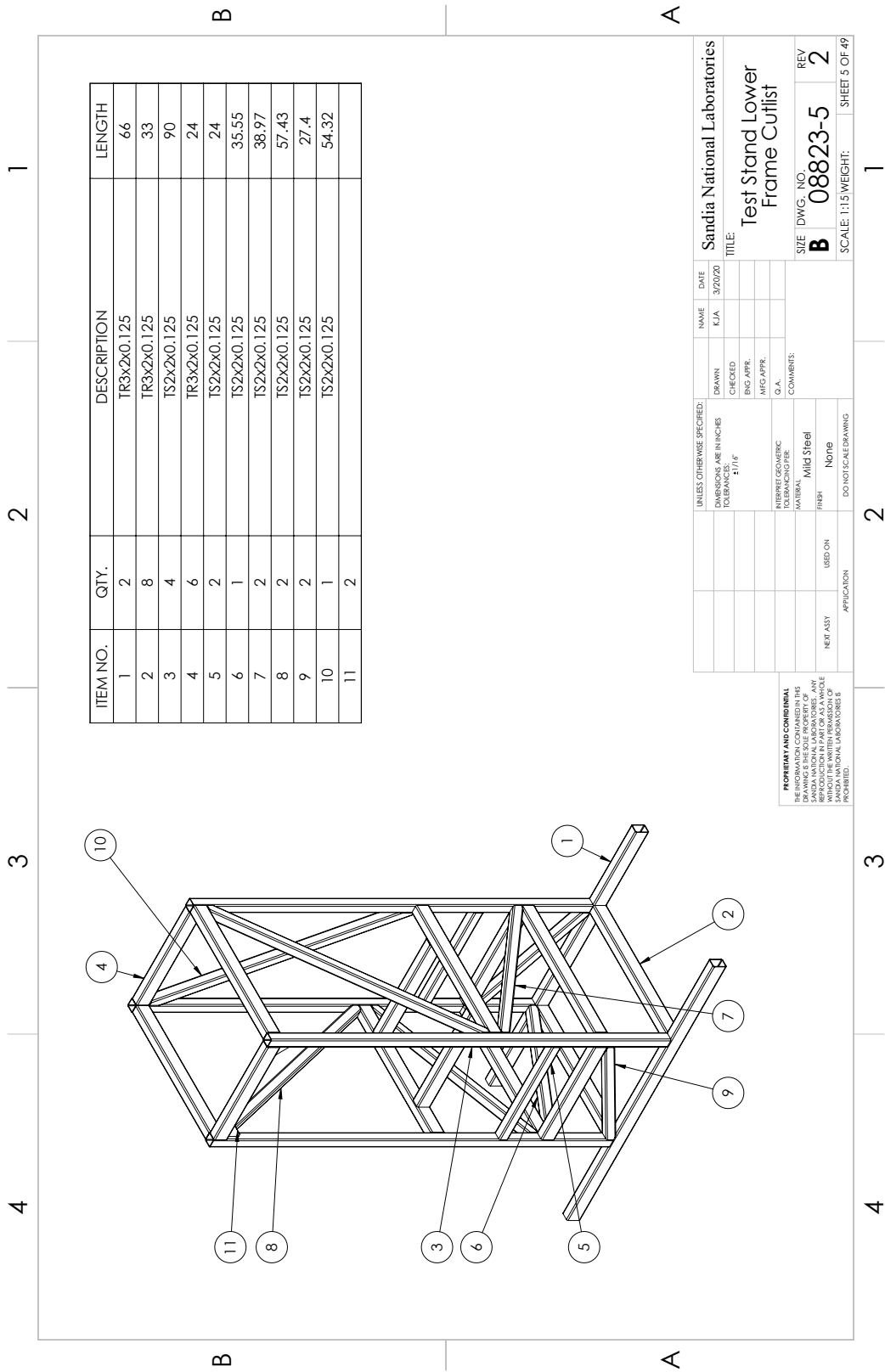
## APPENDIX C. PARTICLE FLOW LOOP DRAWINGS

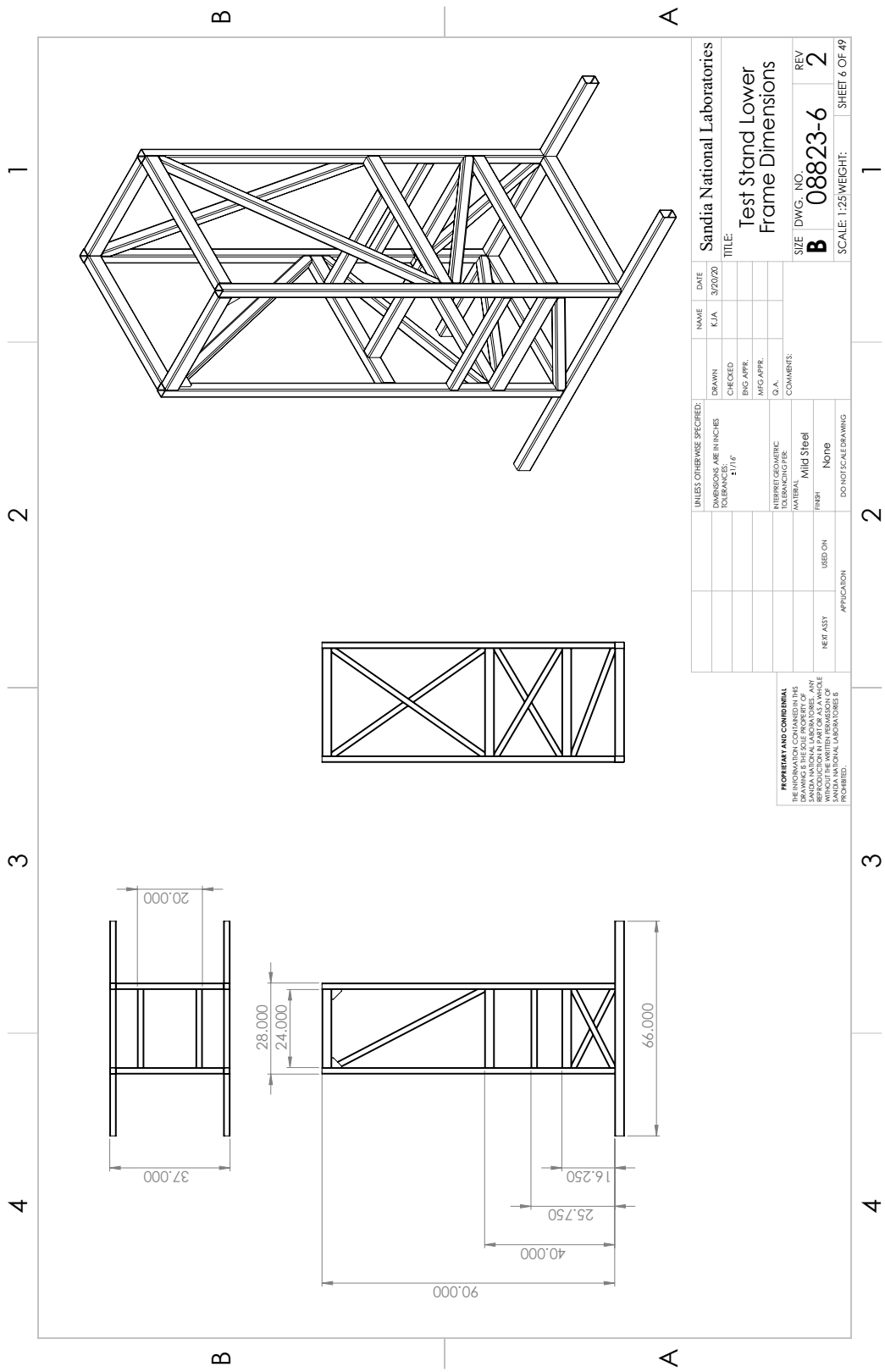


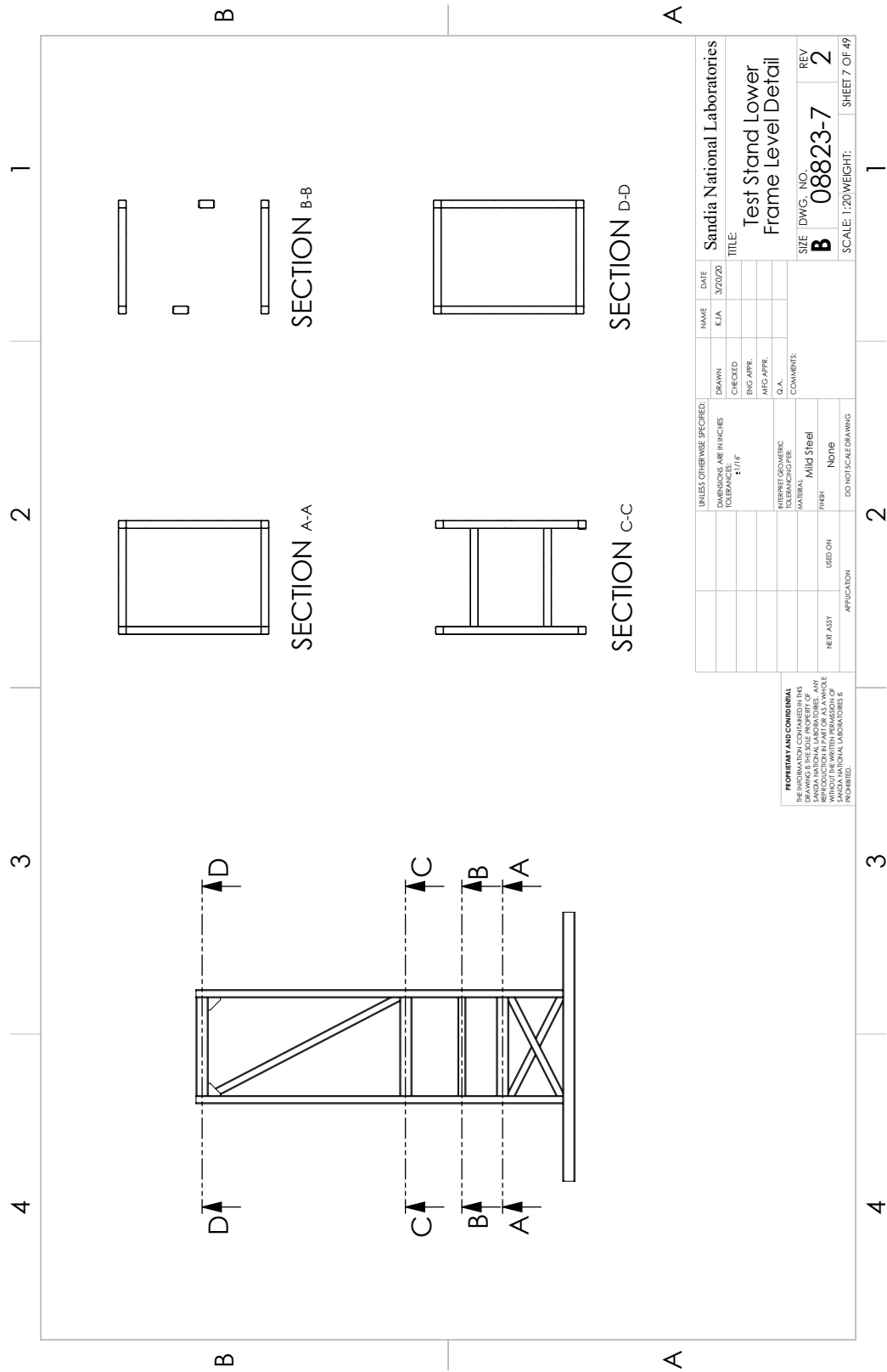




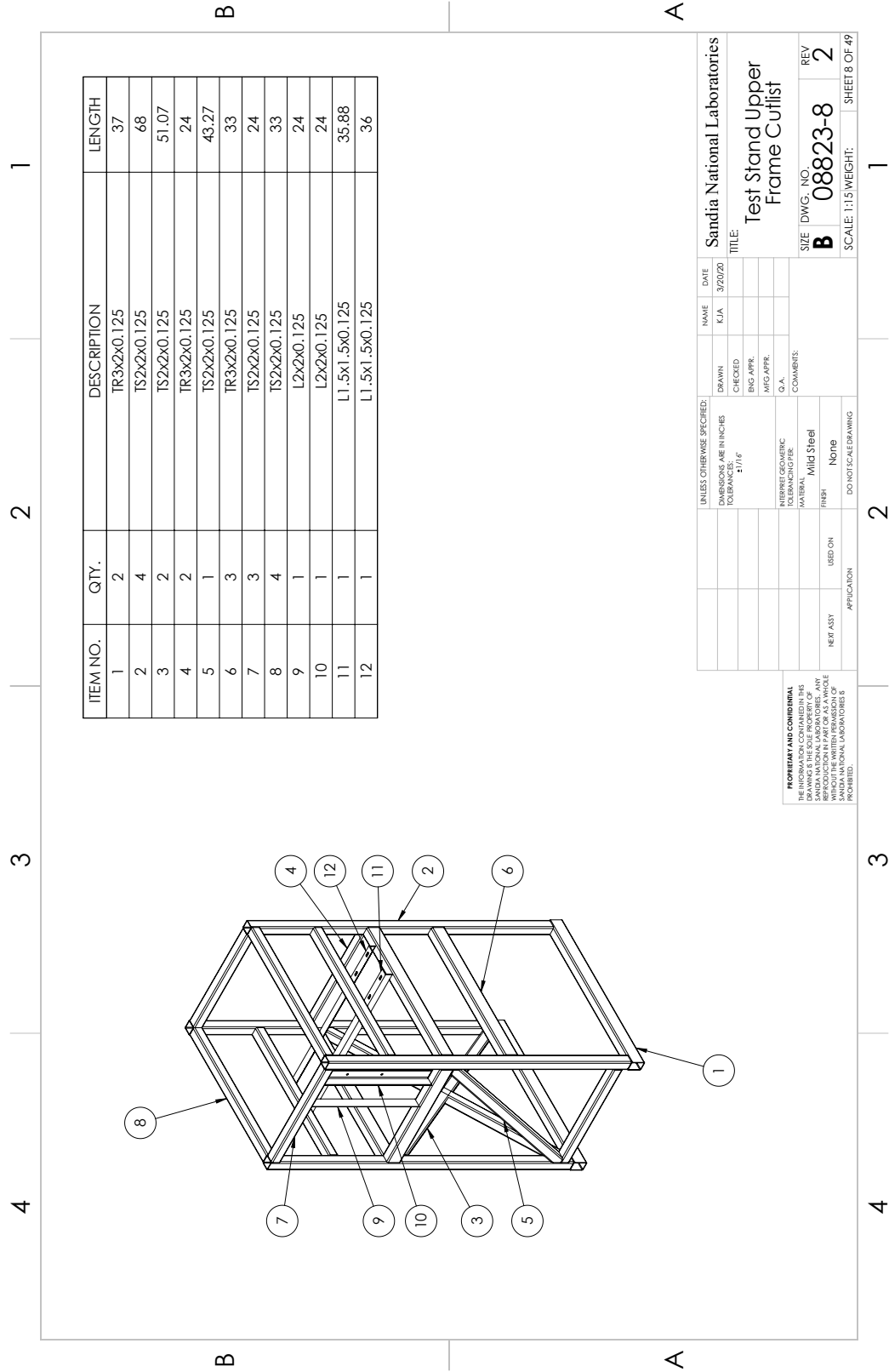


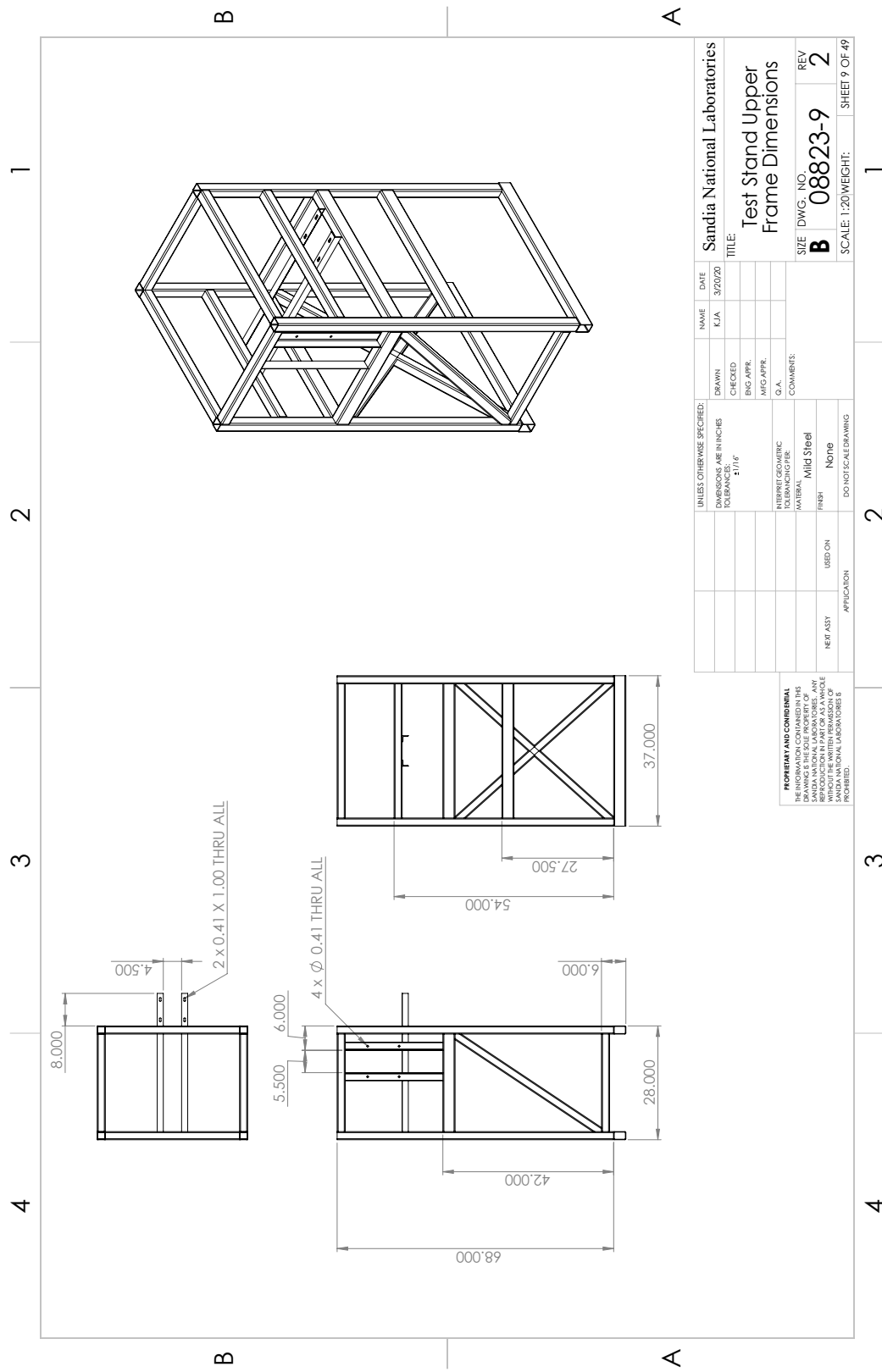


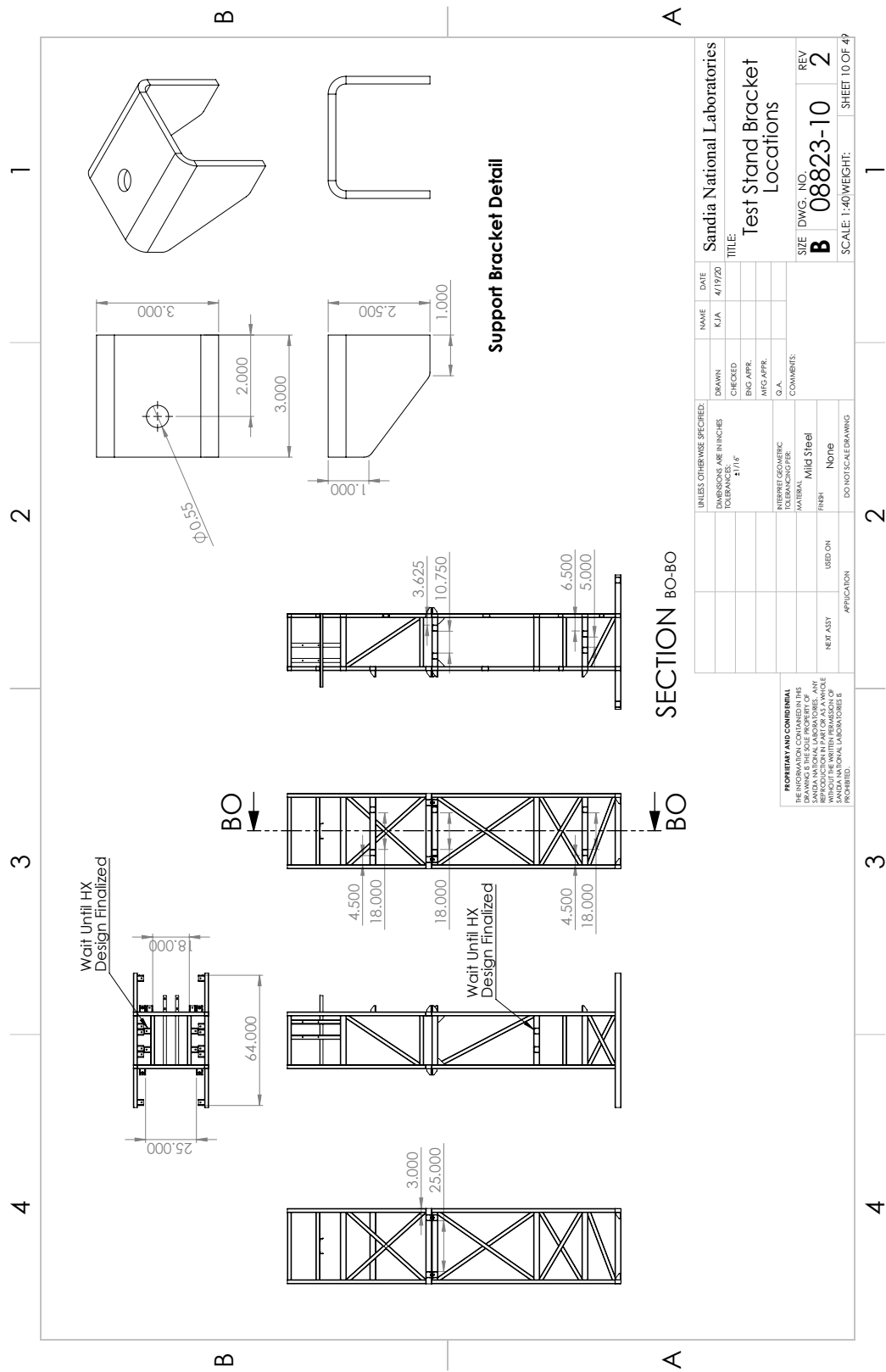


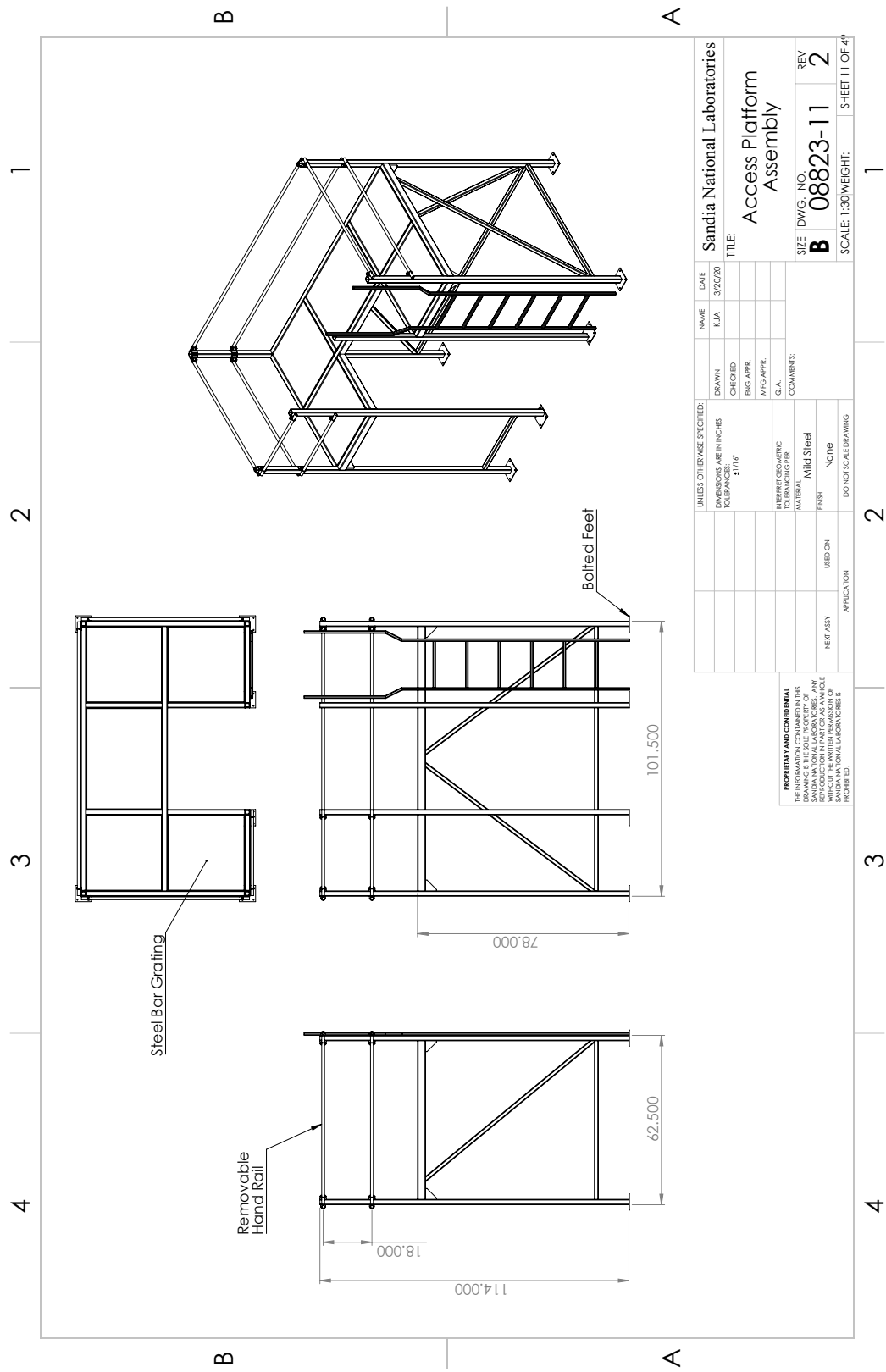


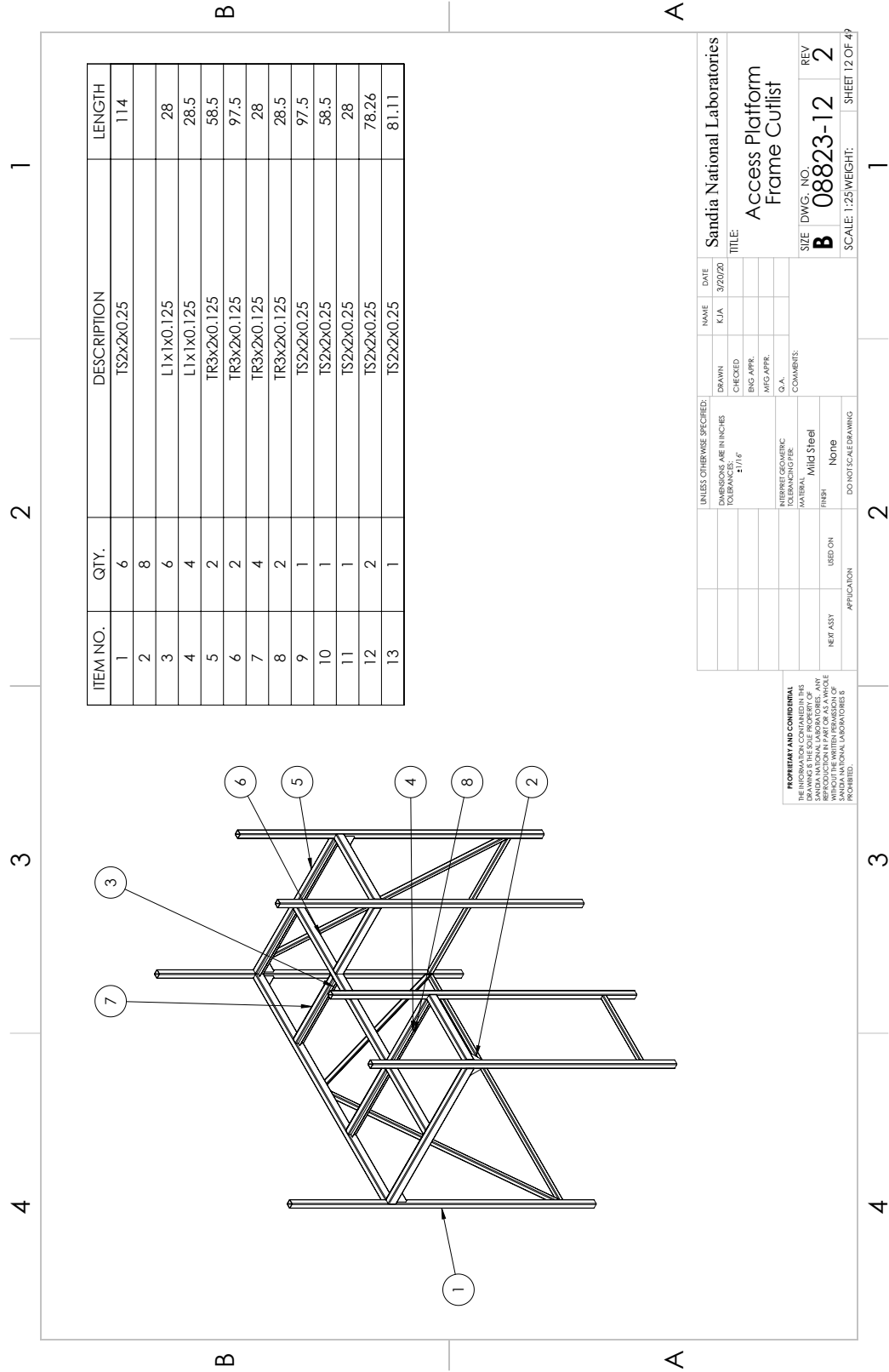
UNLESS OTHERWISE SPECIFIED: DIMENSIONS ARE IN INCHES TOLERANCES: ±1/16		NAME: KIA	DATE: 3/20/20	Sandia National Laboratories
DRAWN: CHECKED: BKG APPR: MFG APPR:				
INVENTOR/CHIEF DESIGNER: TO BRANCHING PIPE:				
O.A.:				
COMMENTS:				
PROPERTY AND CONDITIONS: THE INFORMATION CONTAINED IN THIS DRAWING IS THE SOLE PROPERTY OF SANDIA NATIONAL LABORATORIES. IT IS TO BE KEPT CONFIDENTIAL AND NOT DISCLOSED TO ANY OTHER PERSON OR ORGANIZATION IN PART OR AS A WHOLE WITHOUT THE WRITTEN PERMISSION OF SANDIA NATIONAL LABORATORIES. EXTERNAL REFERENCES ARE PROHIBITED.				
NOT DRAWN TO EXACT SCALE				
MATERIAL: Mild Steel				
FINISH: None				
USED ON: APPLICATION				
DO NOT SCALE DRAWING				
DWG. NO. B 08823-7		REV 2		
SCALE: 1:20 WEIGHT: 1				SHEET 7 OF 49

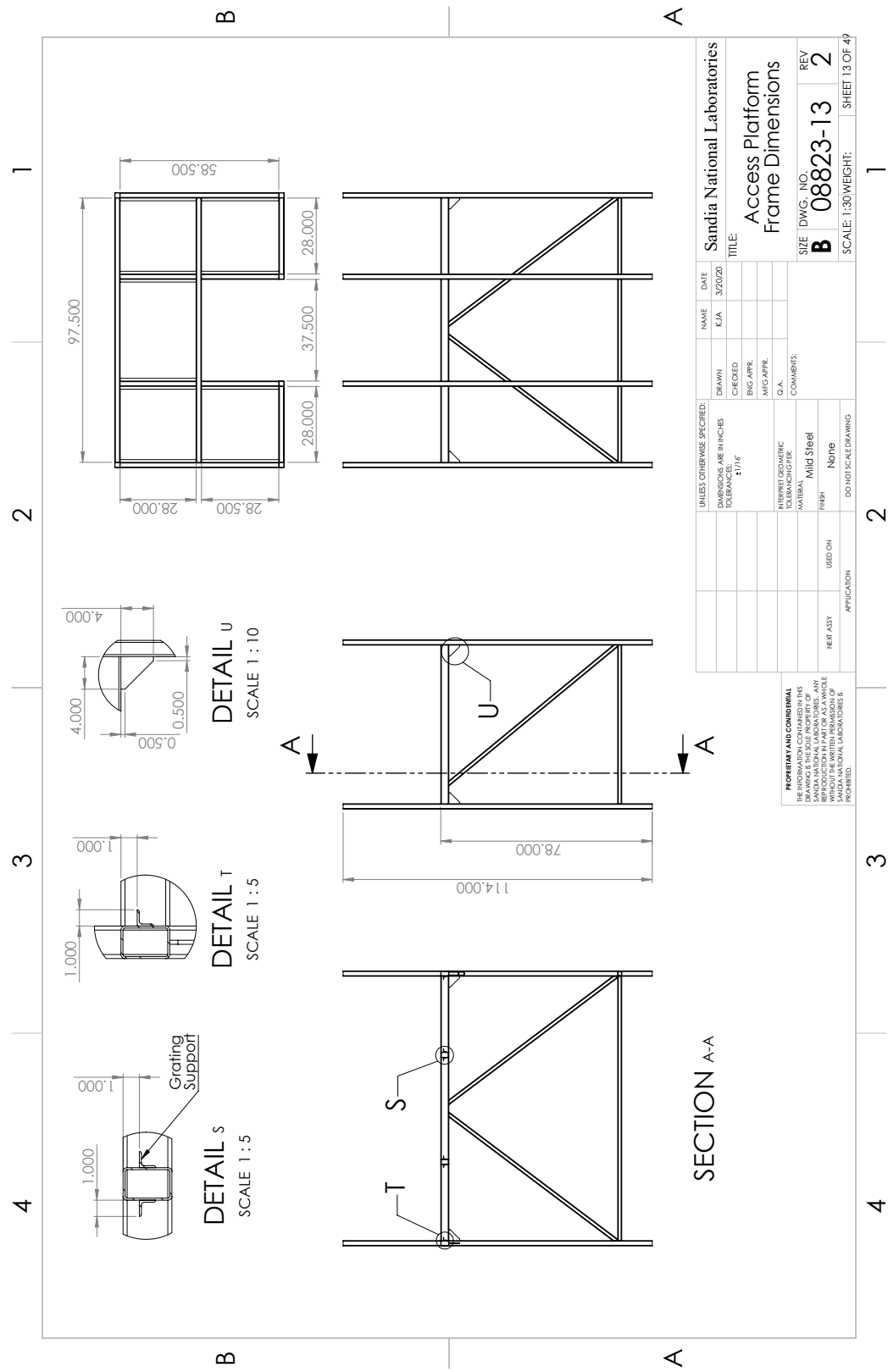


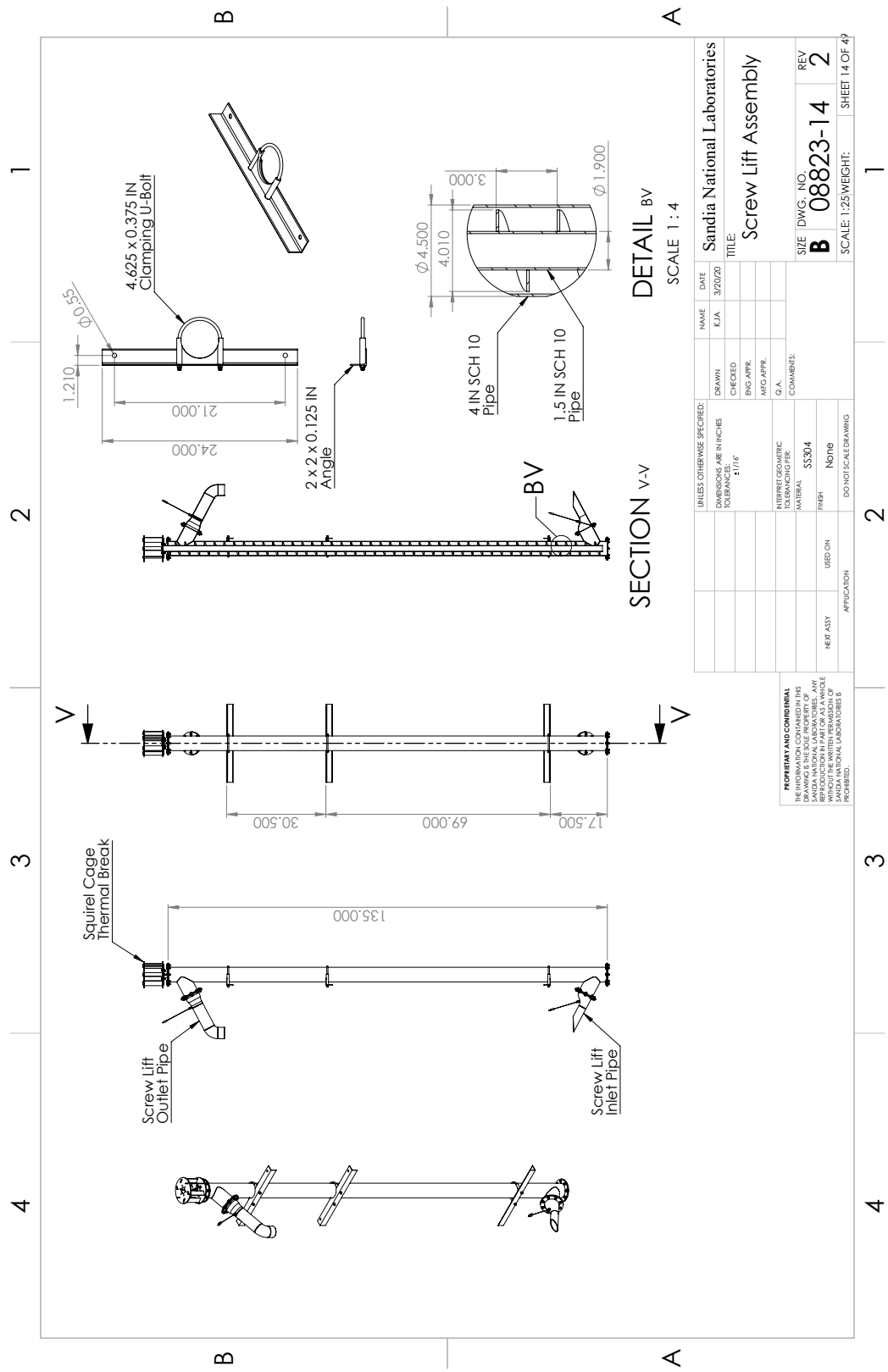


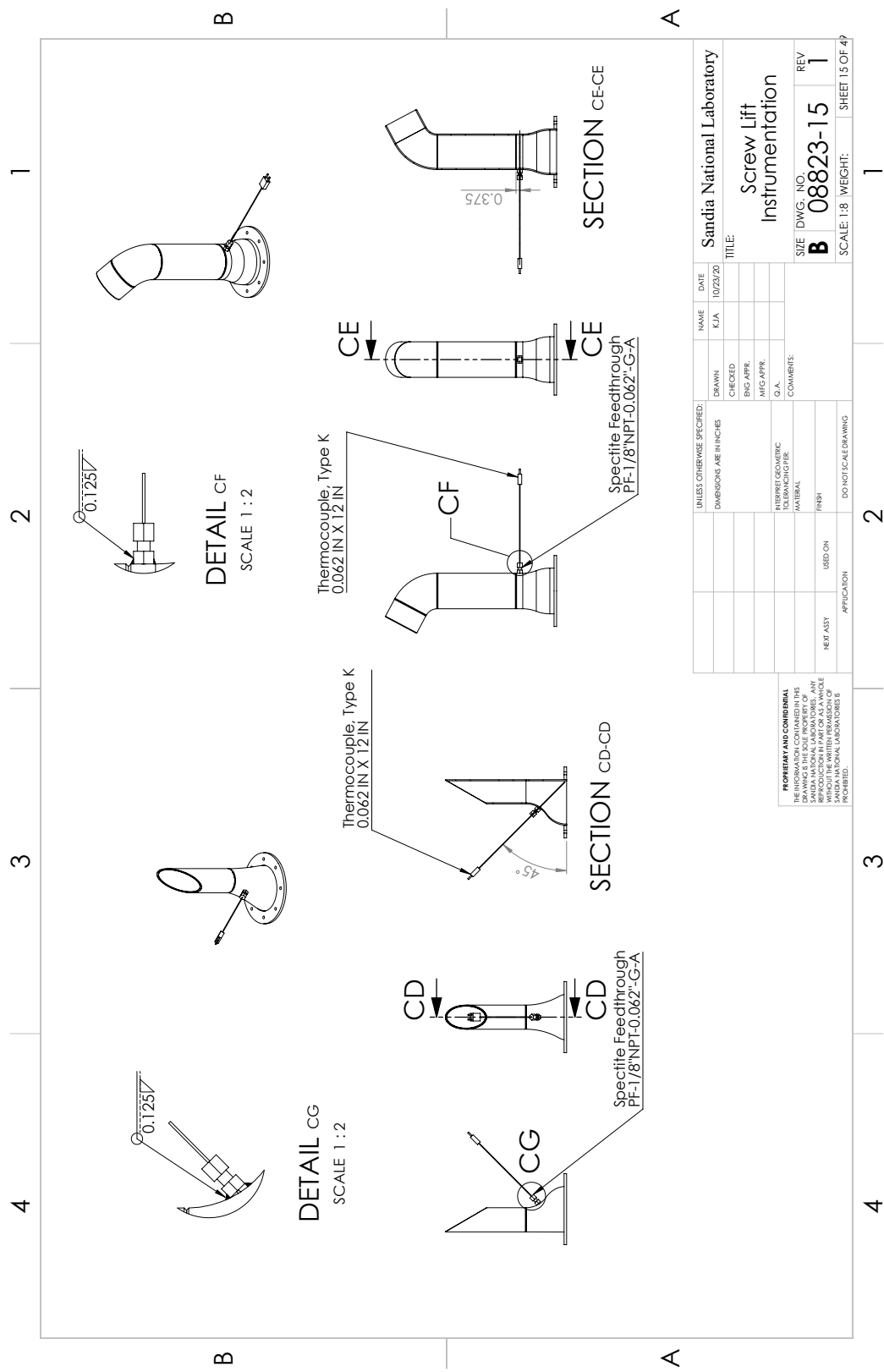


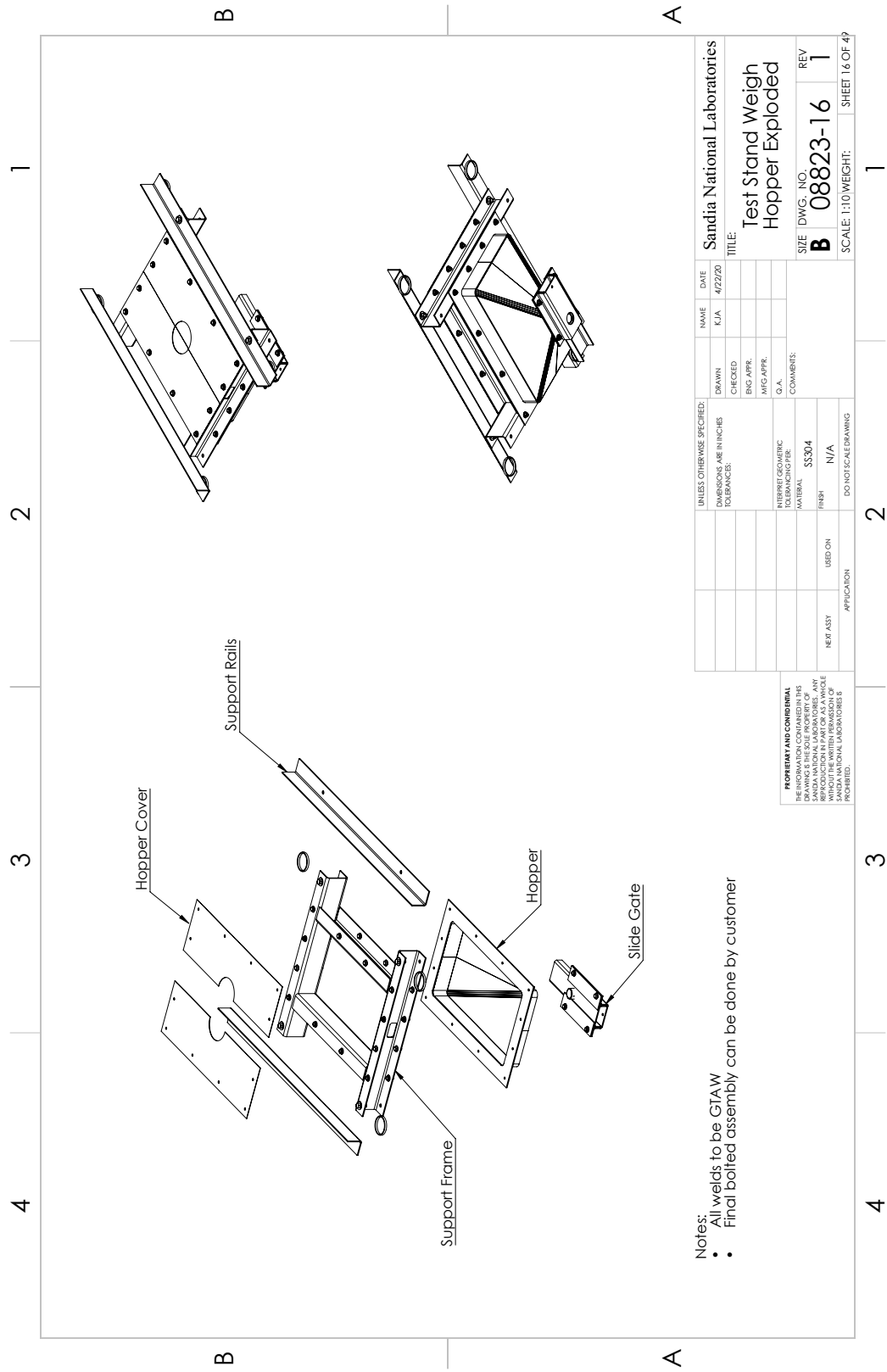


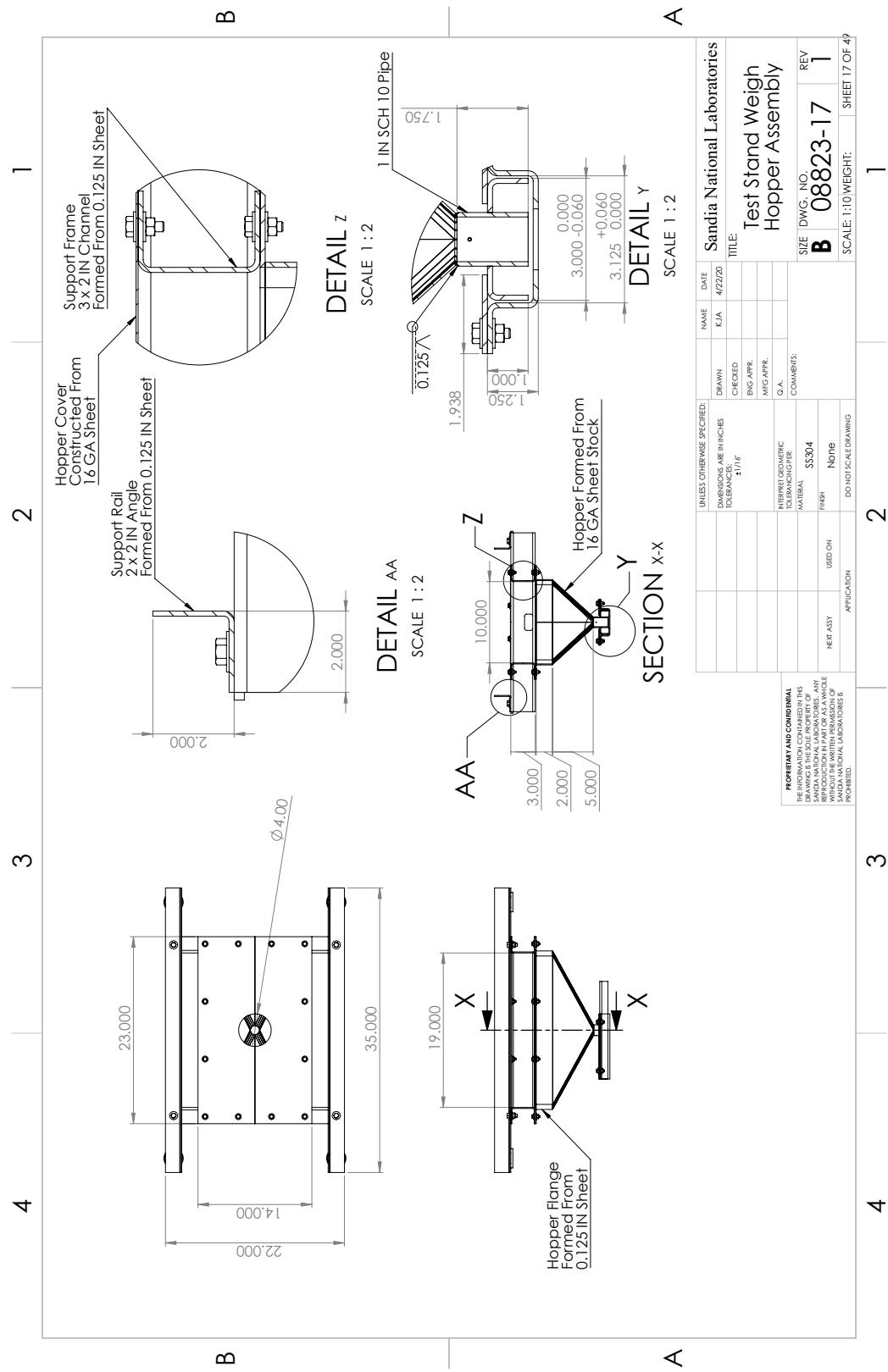


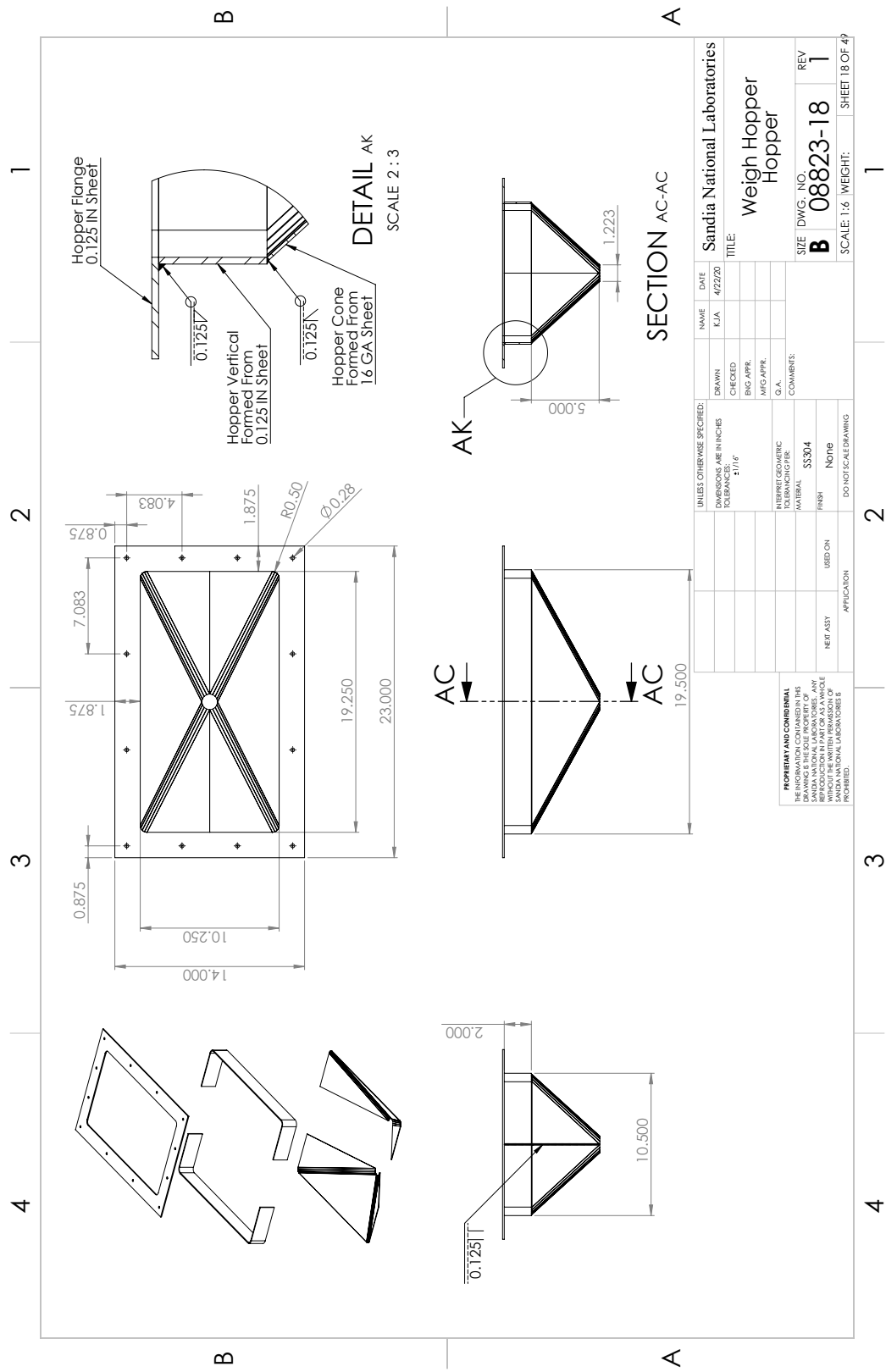


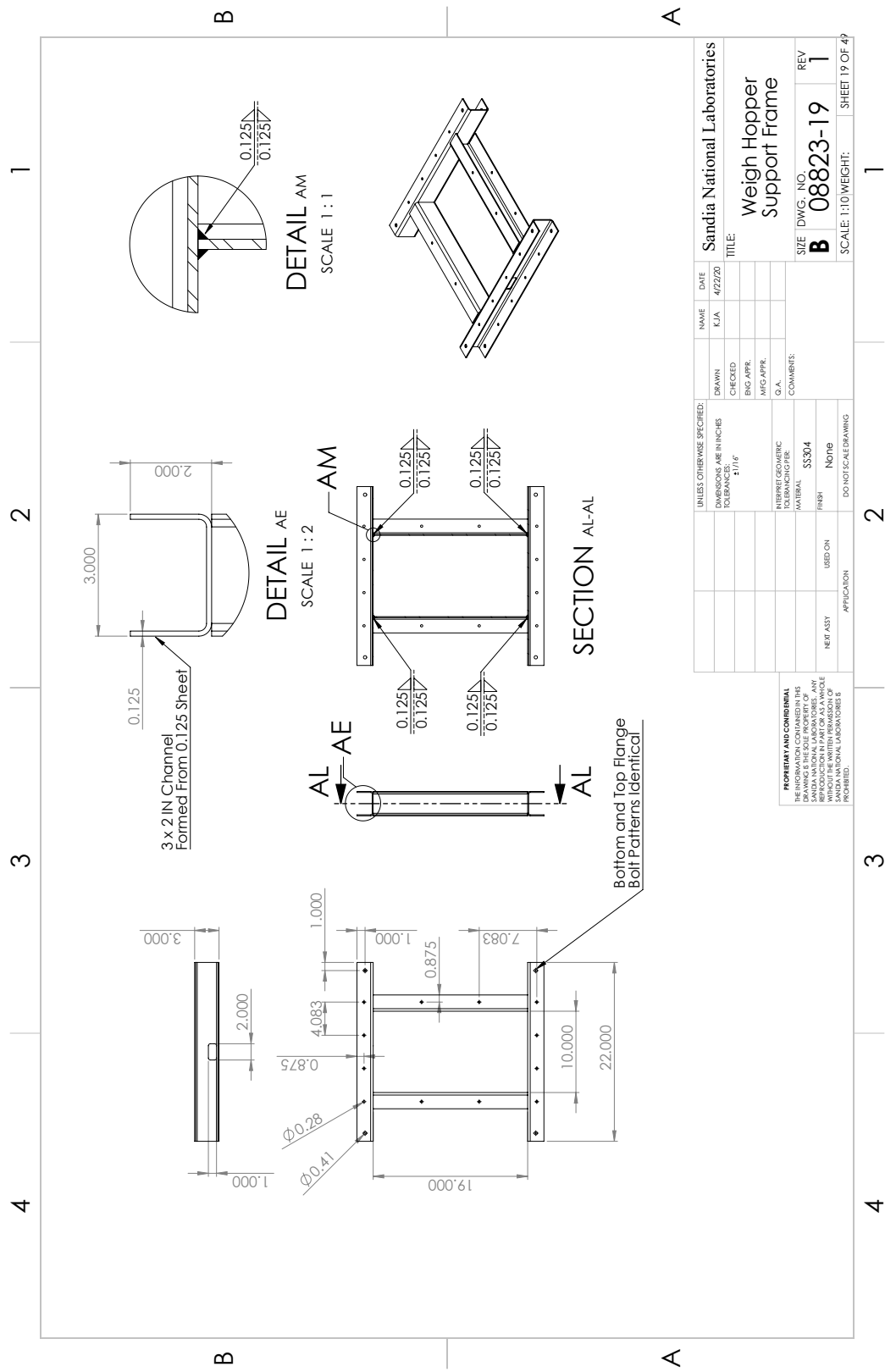


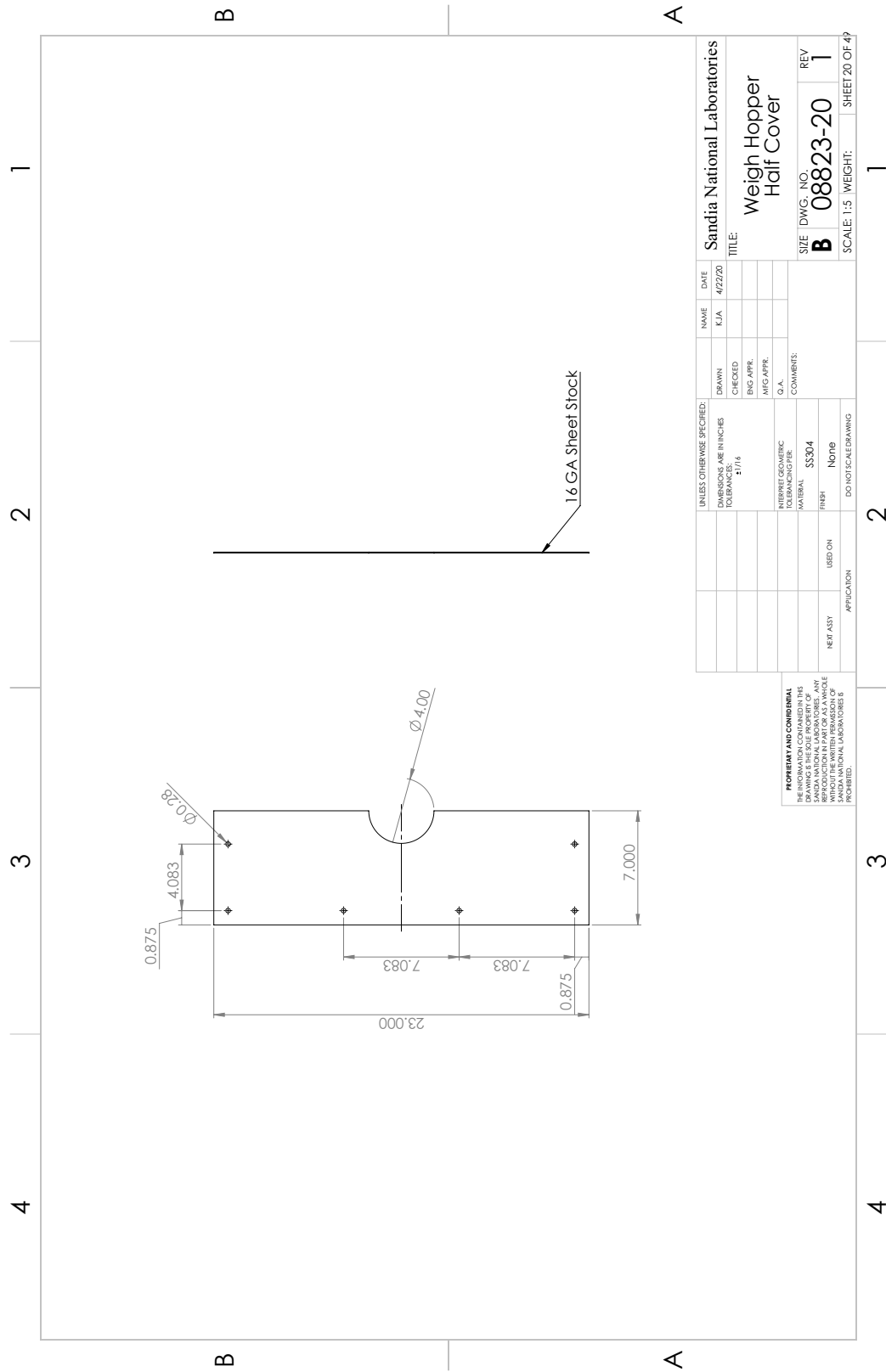


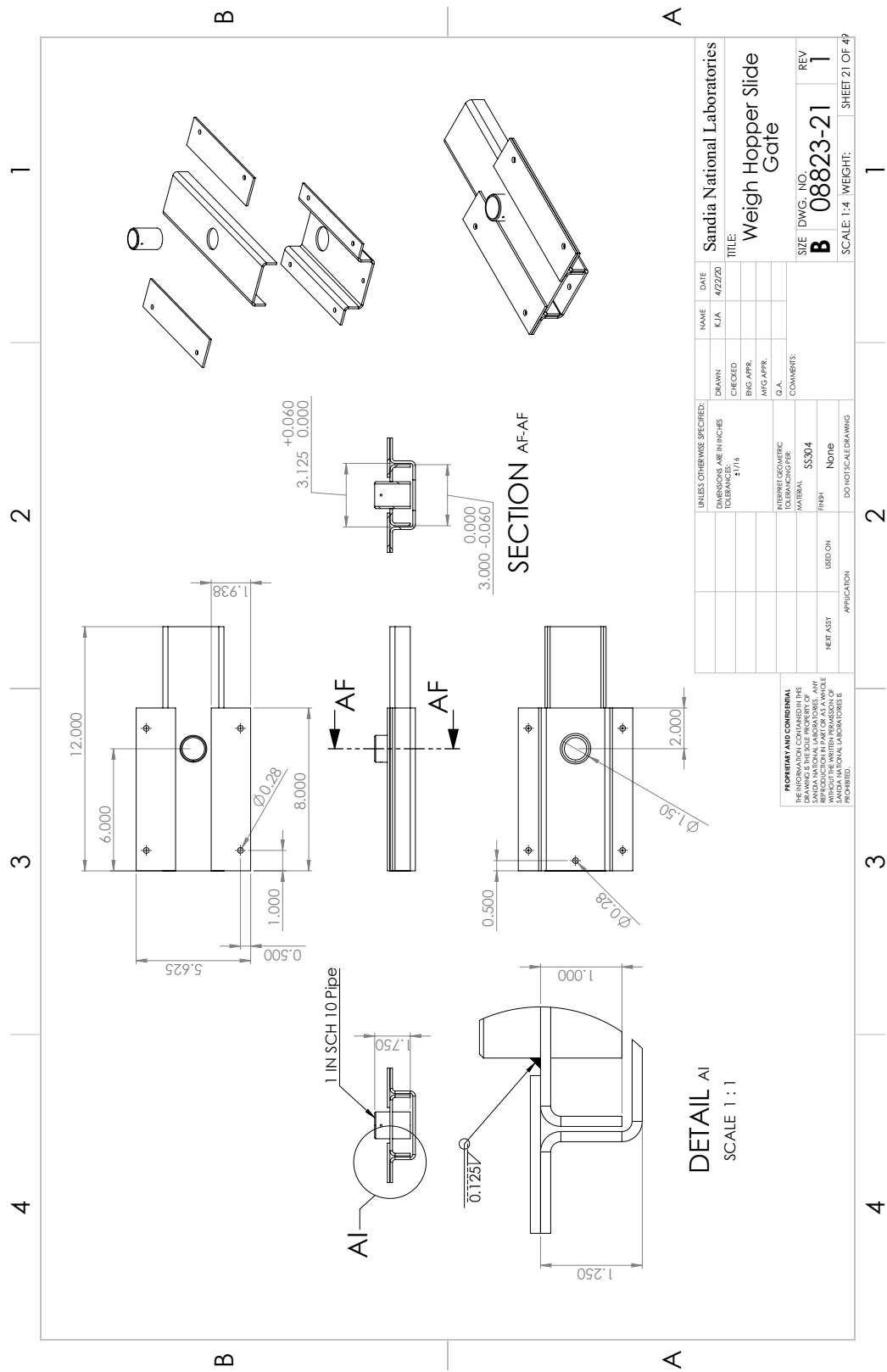


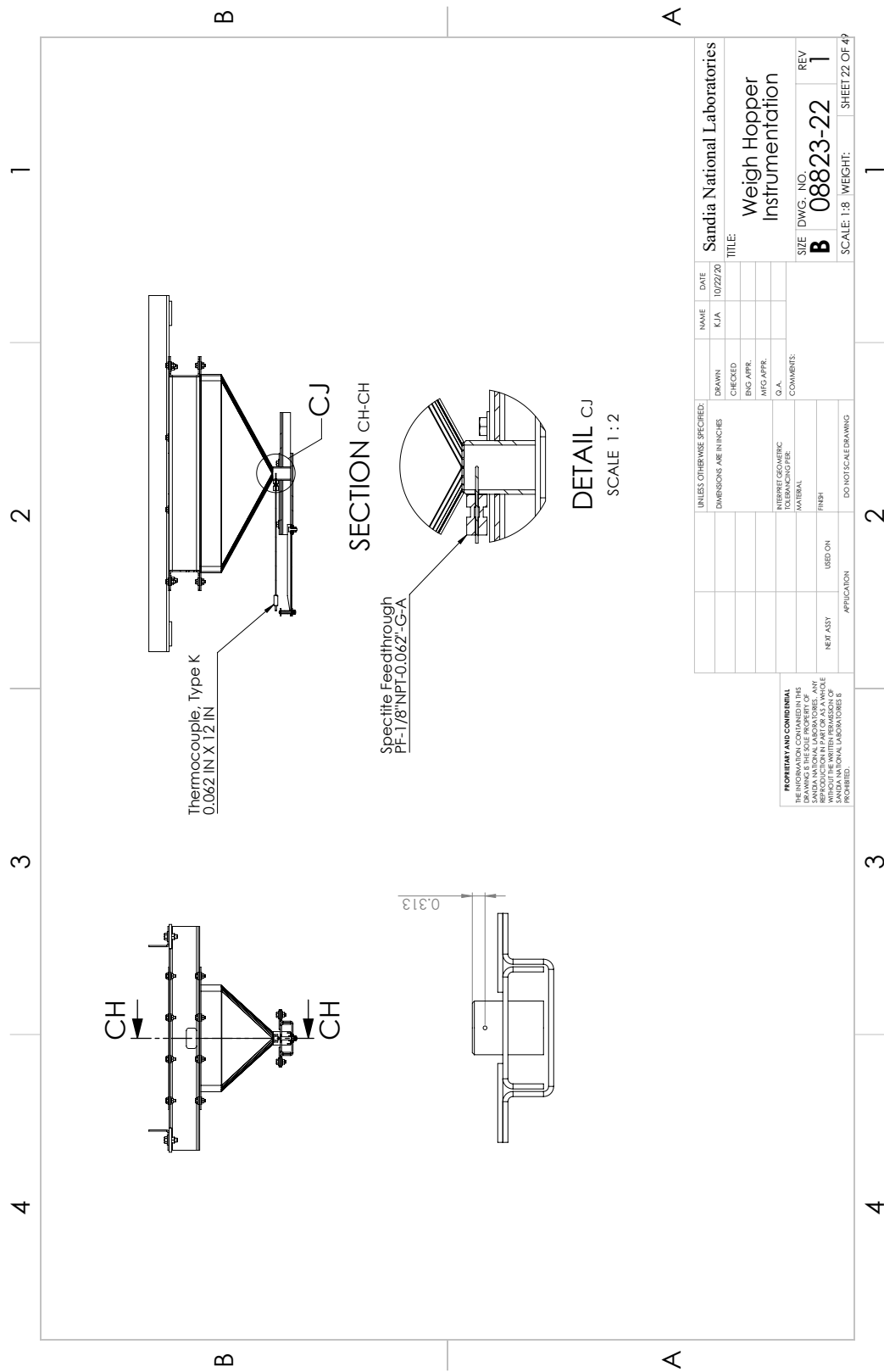


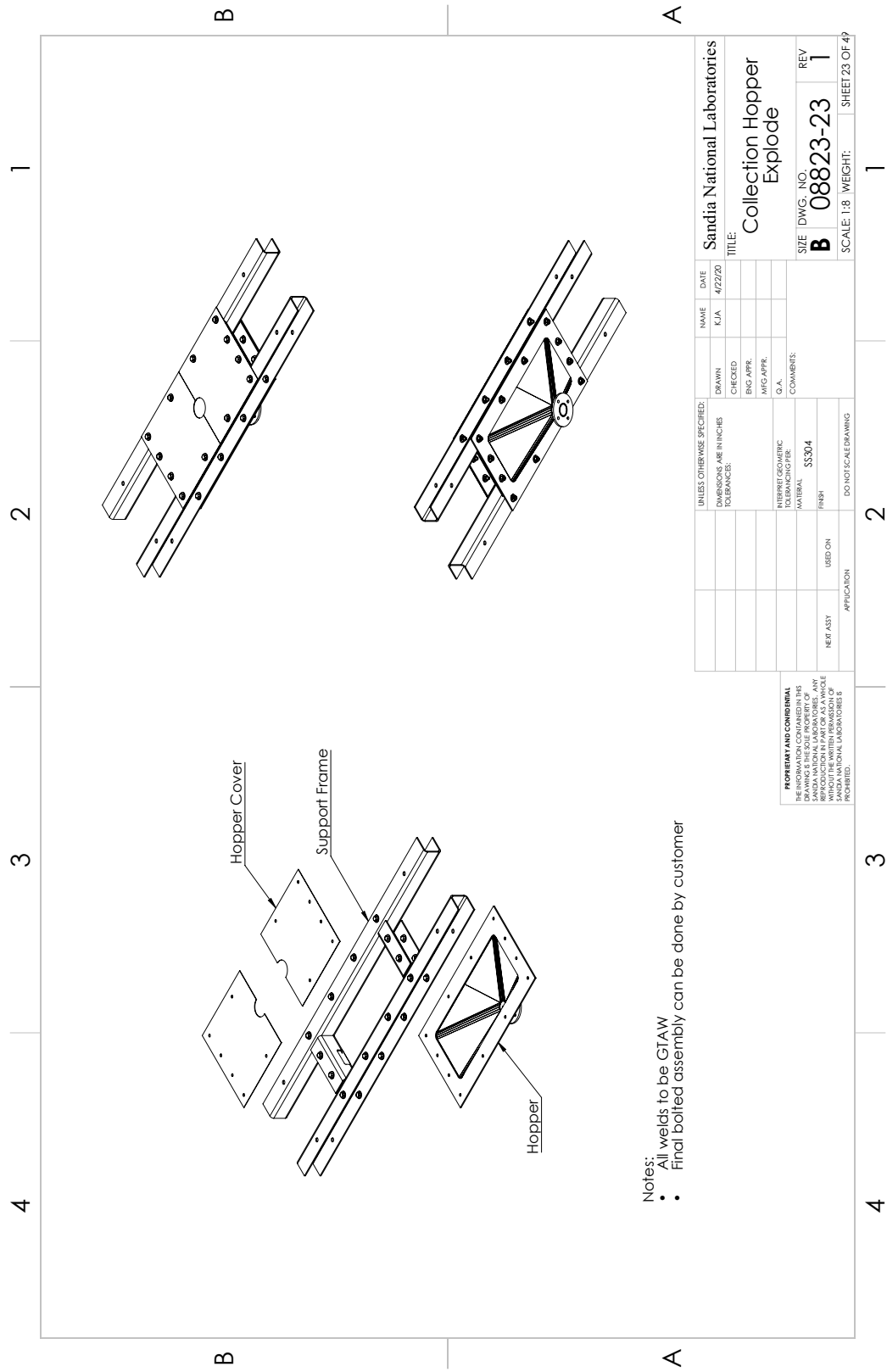


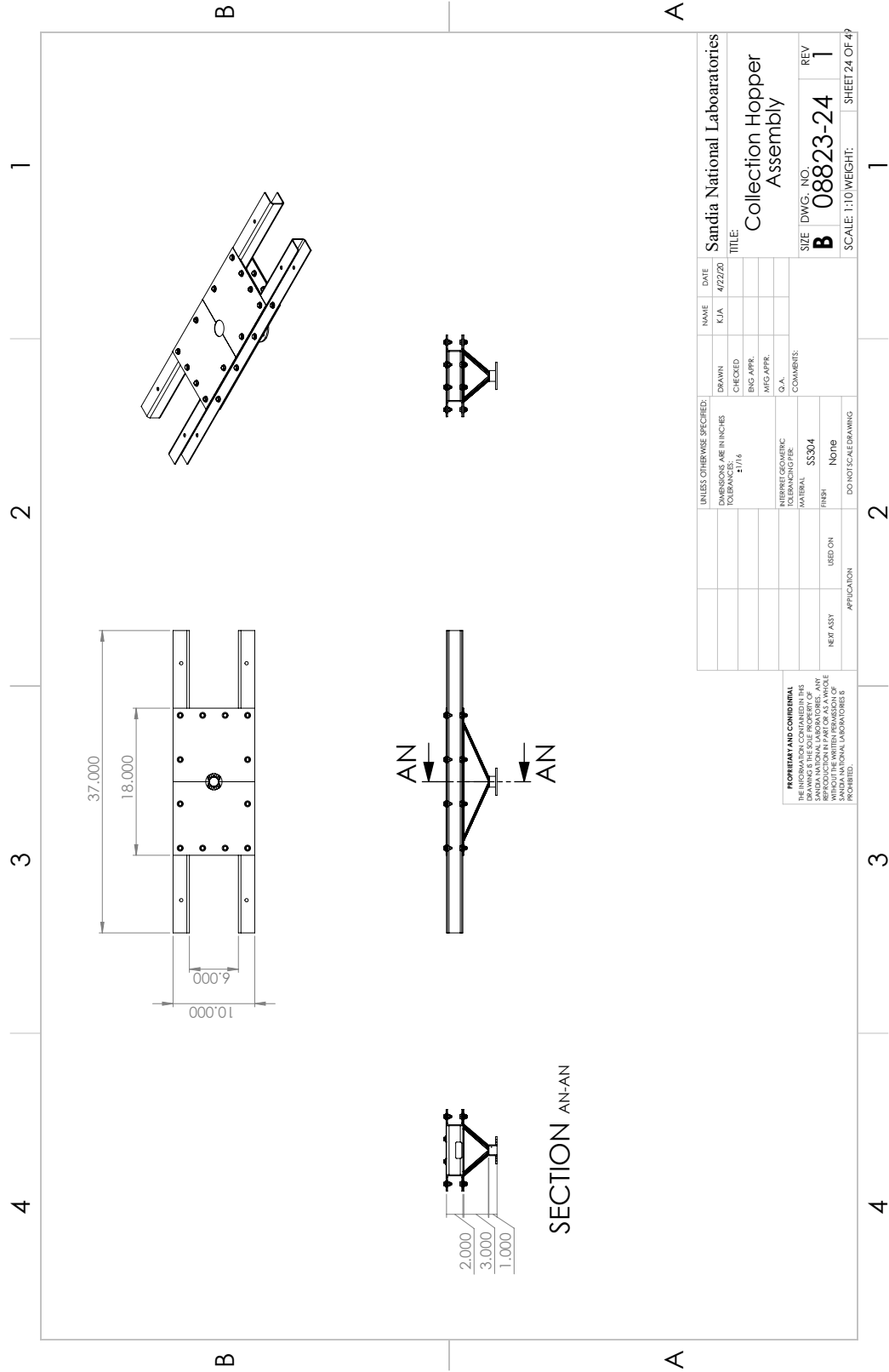


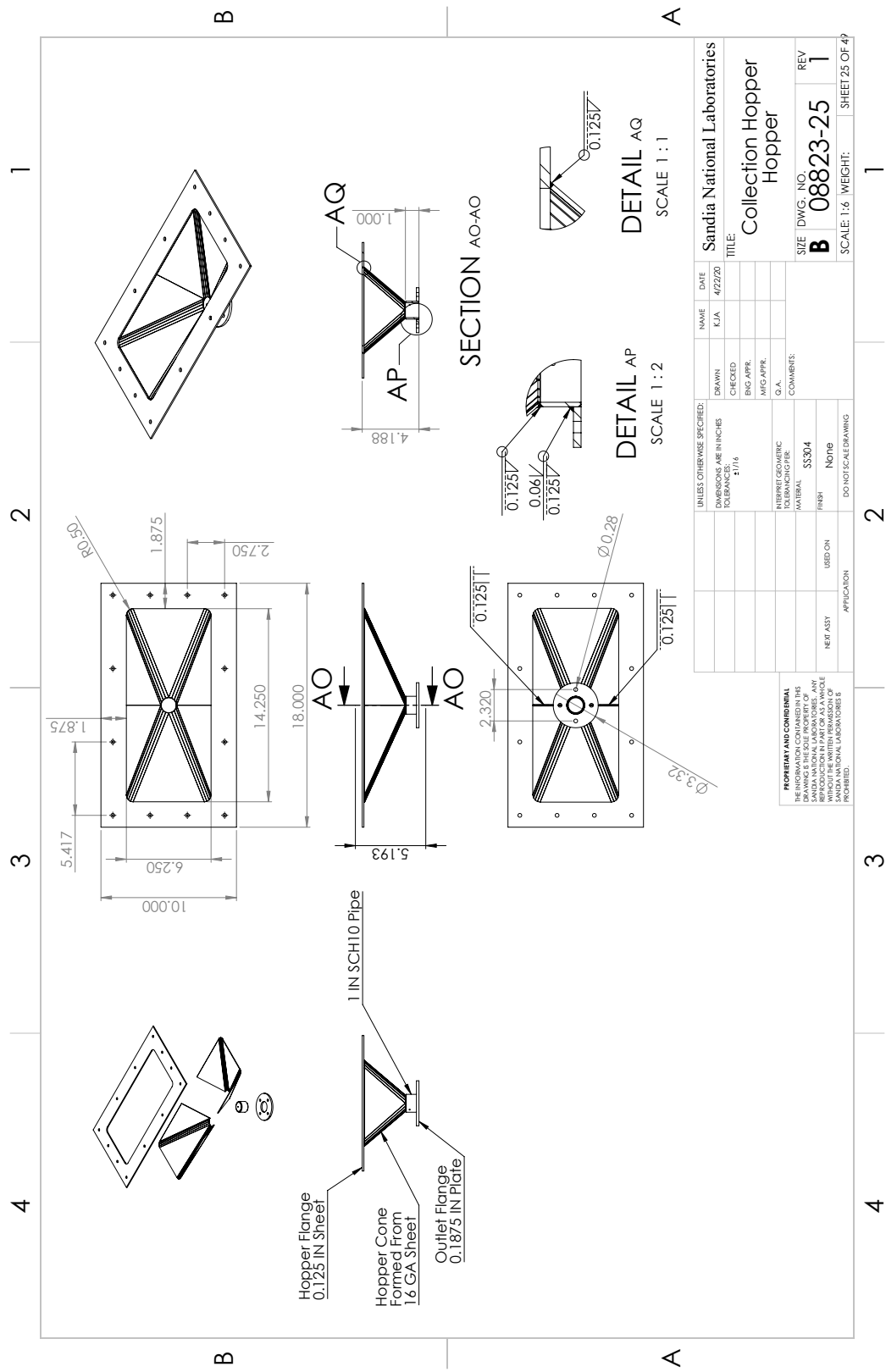


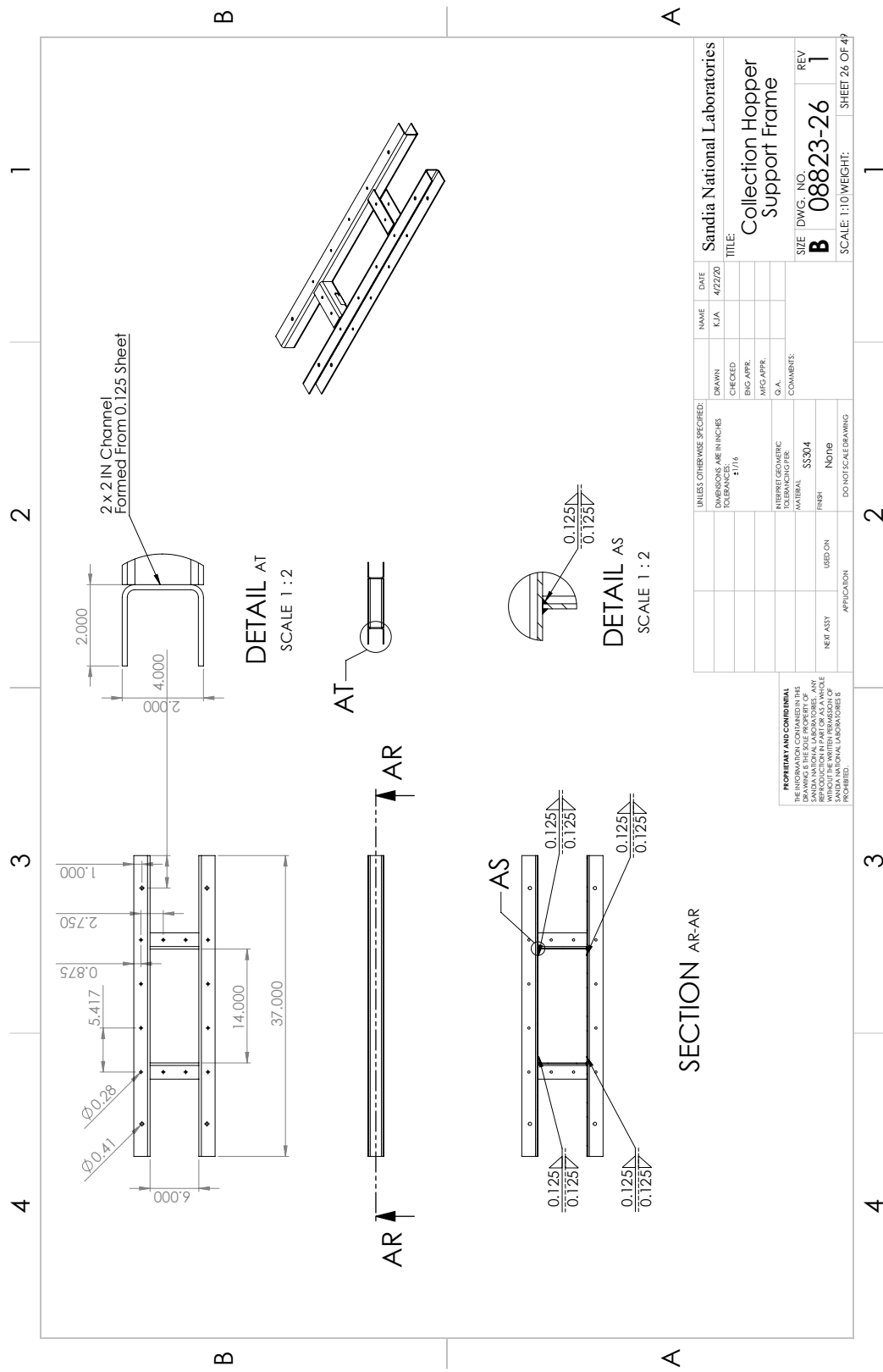


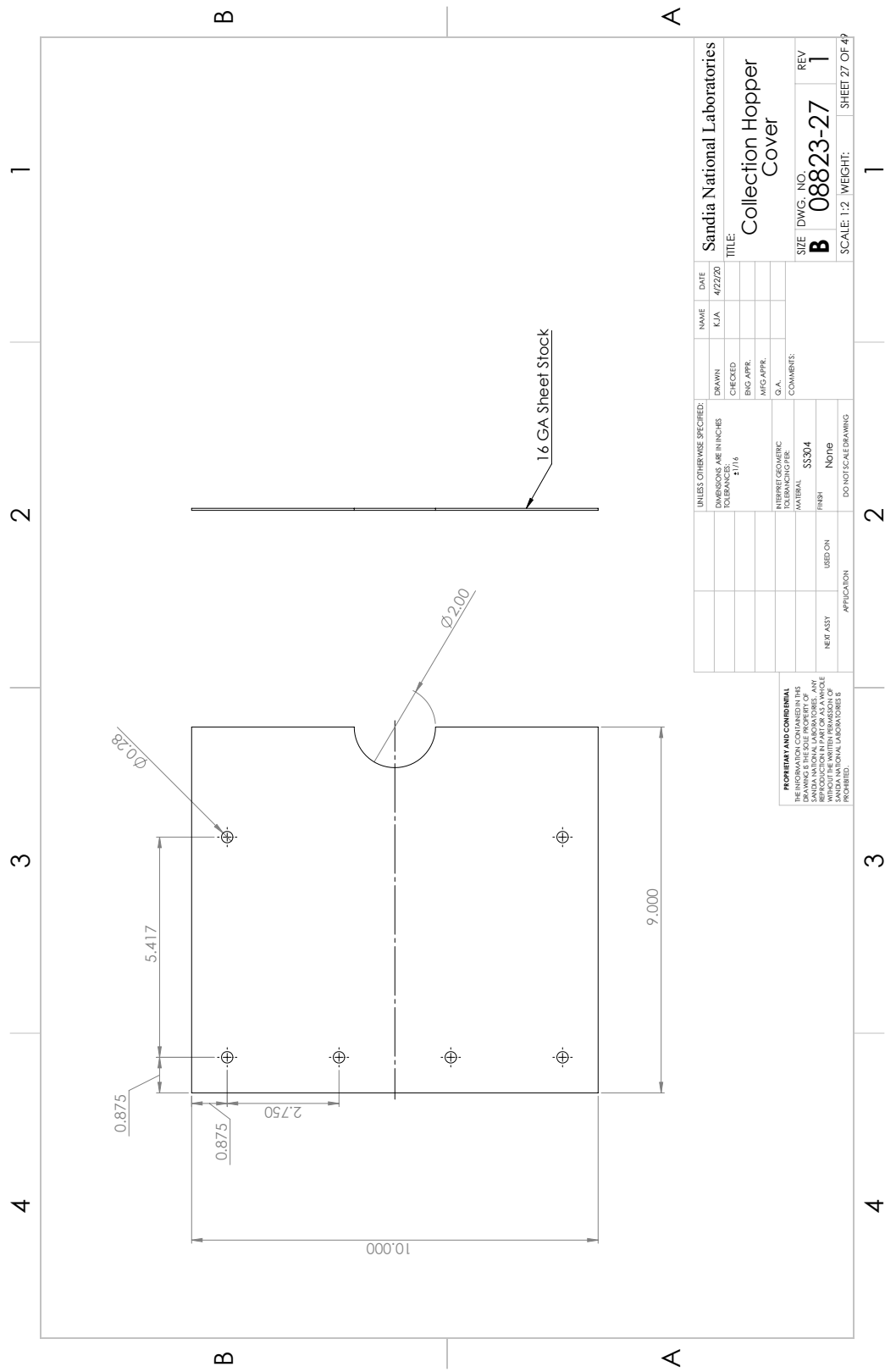


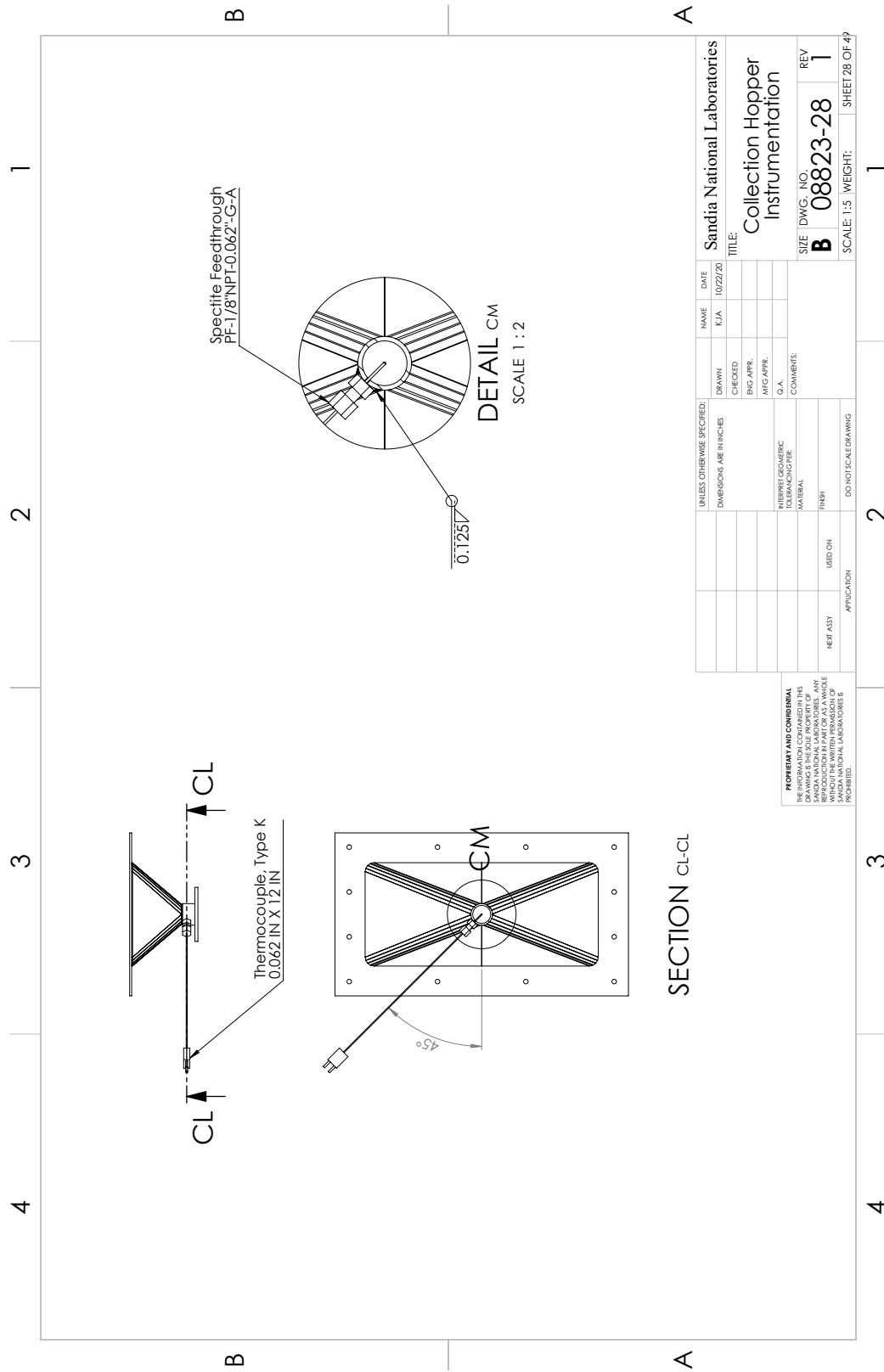


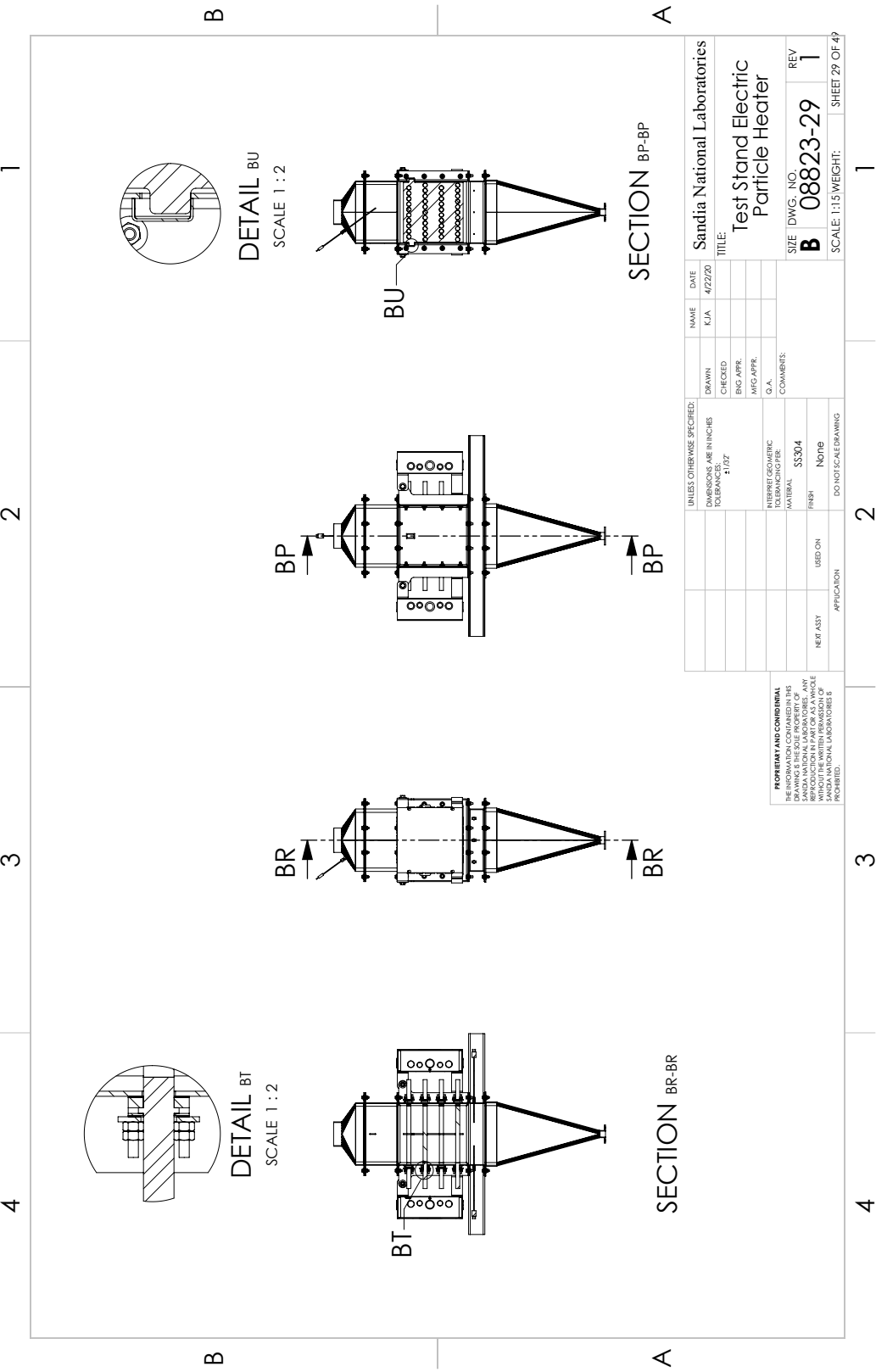


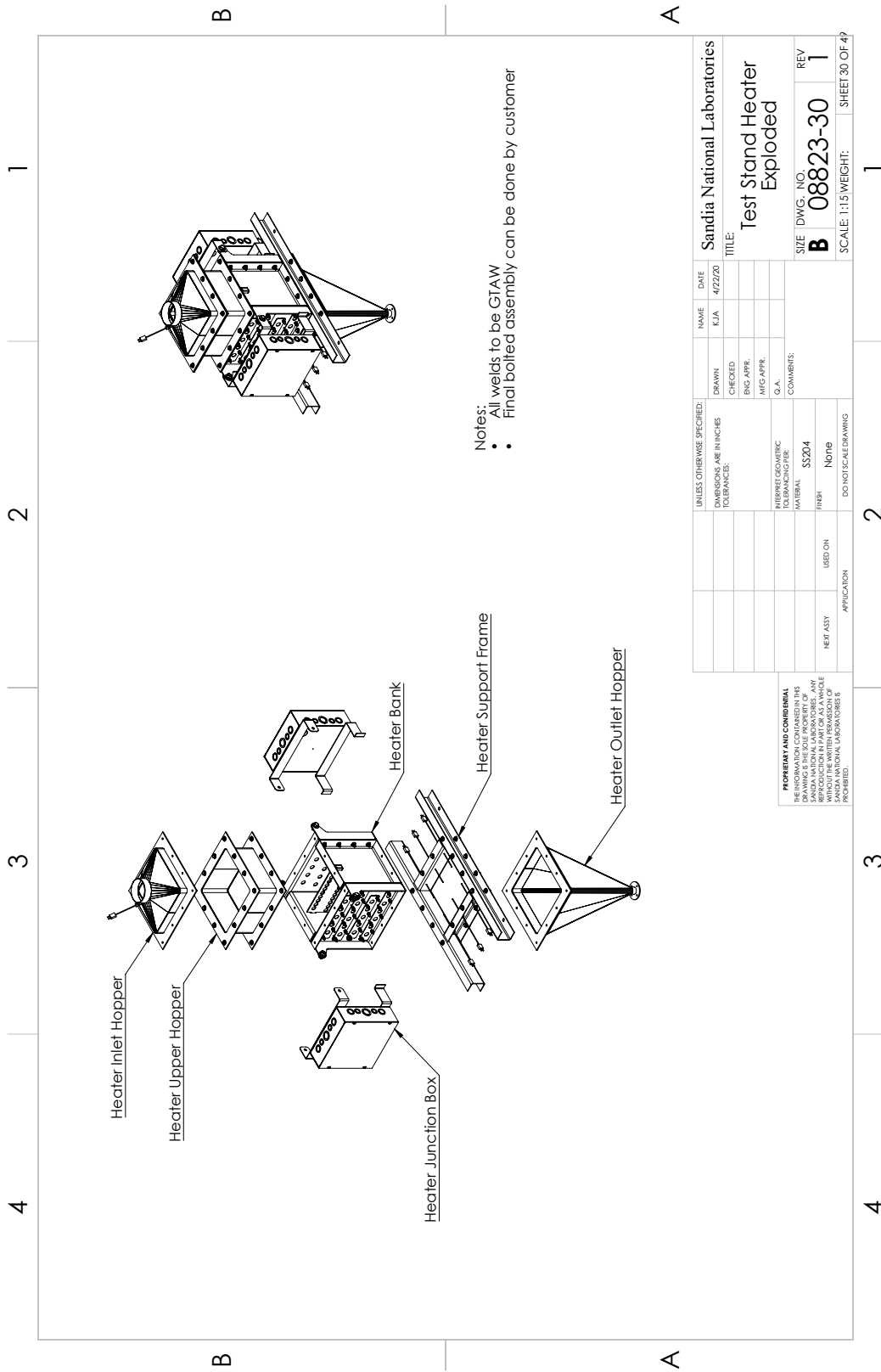


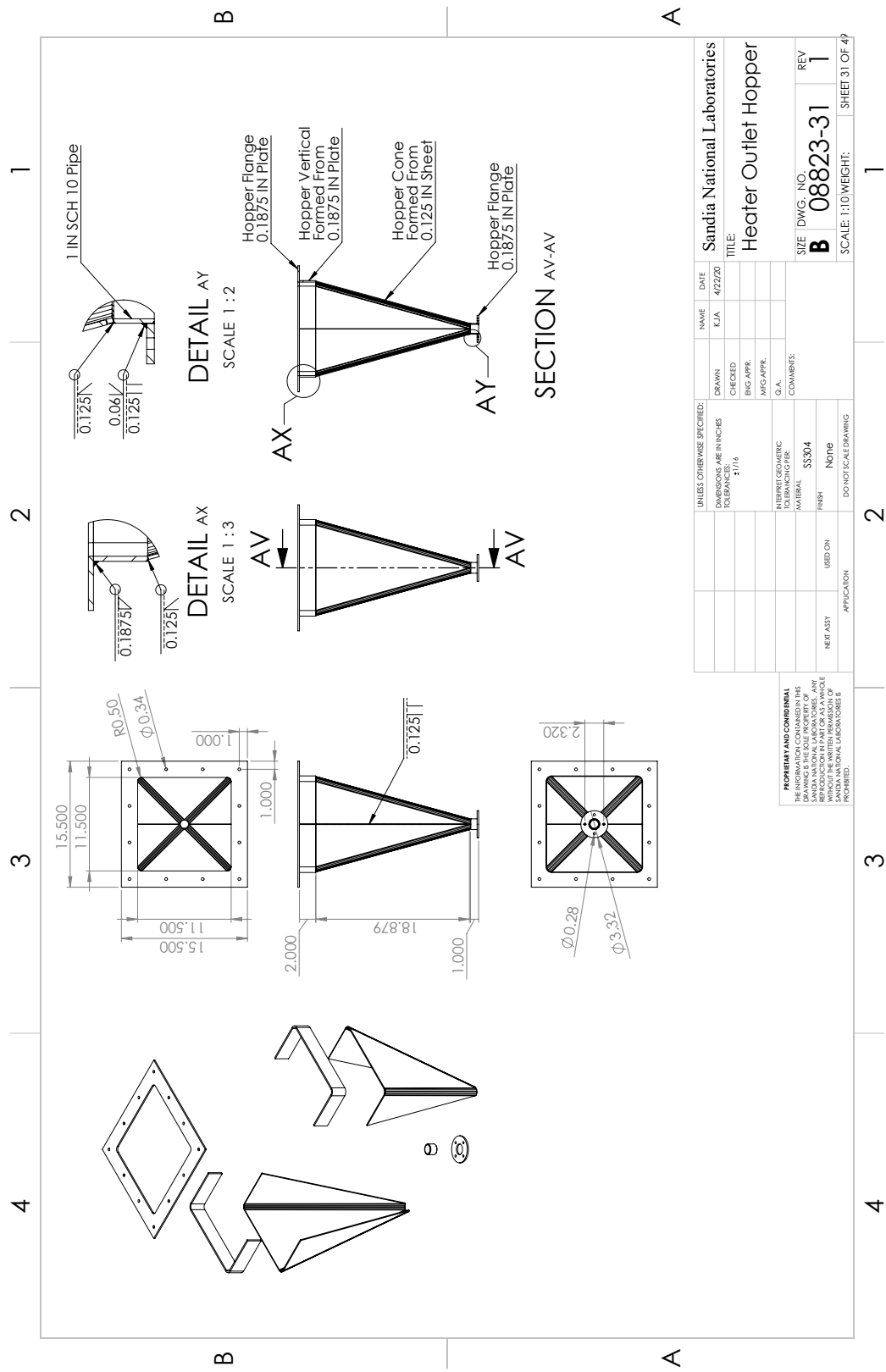


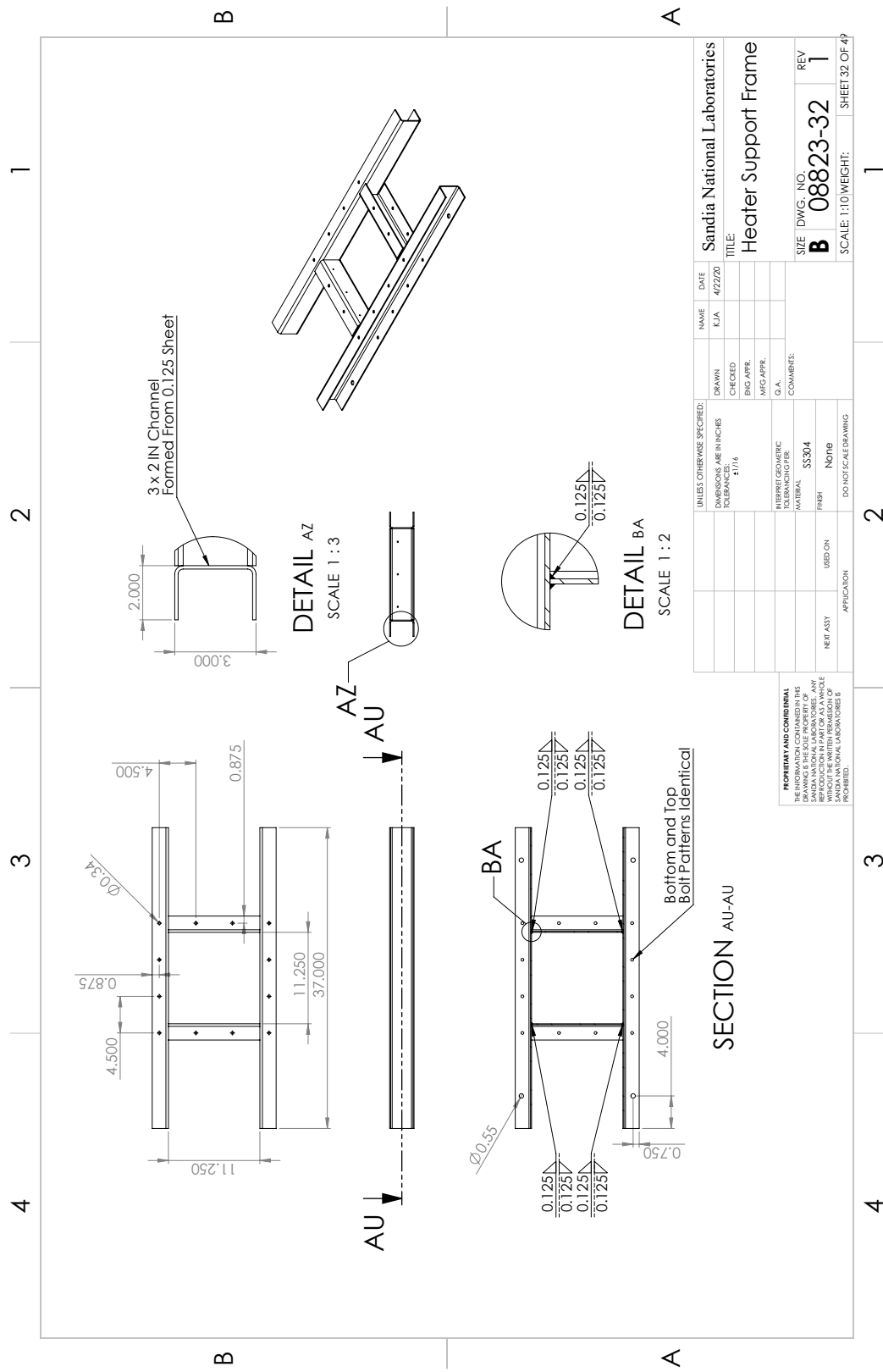


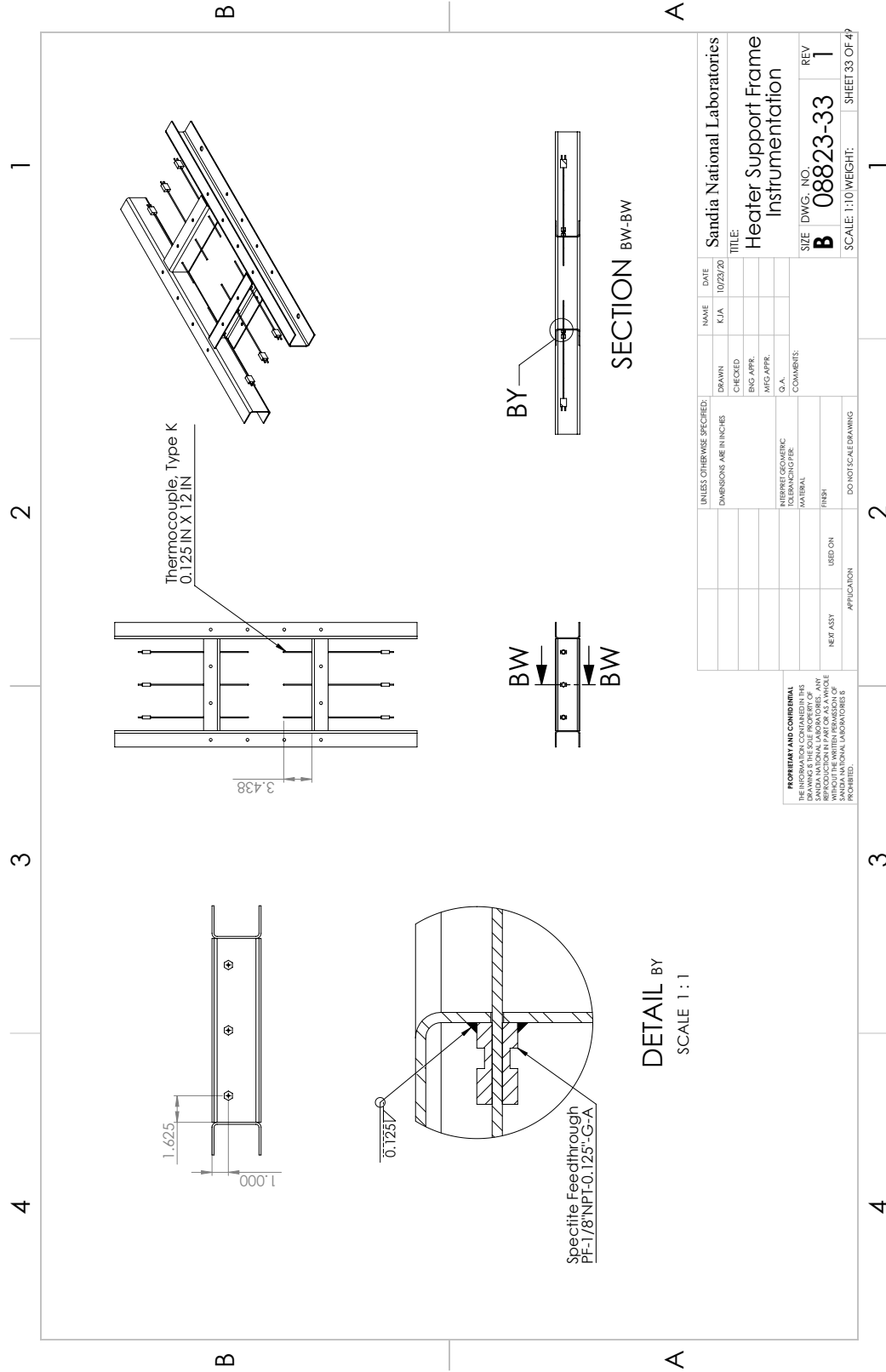


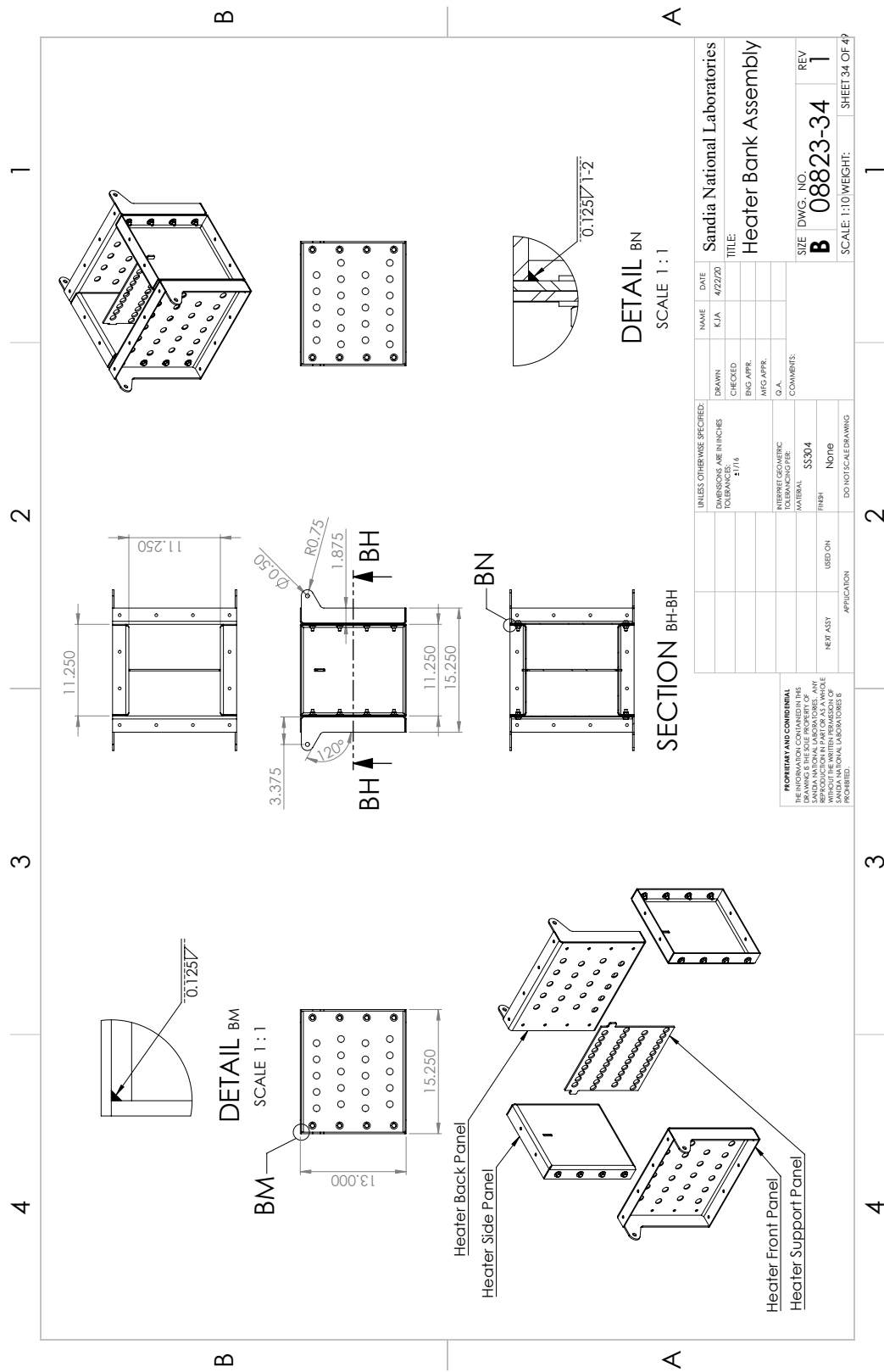


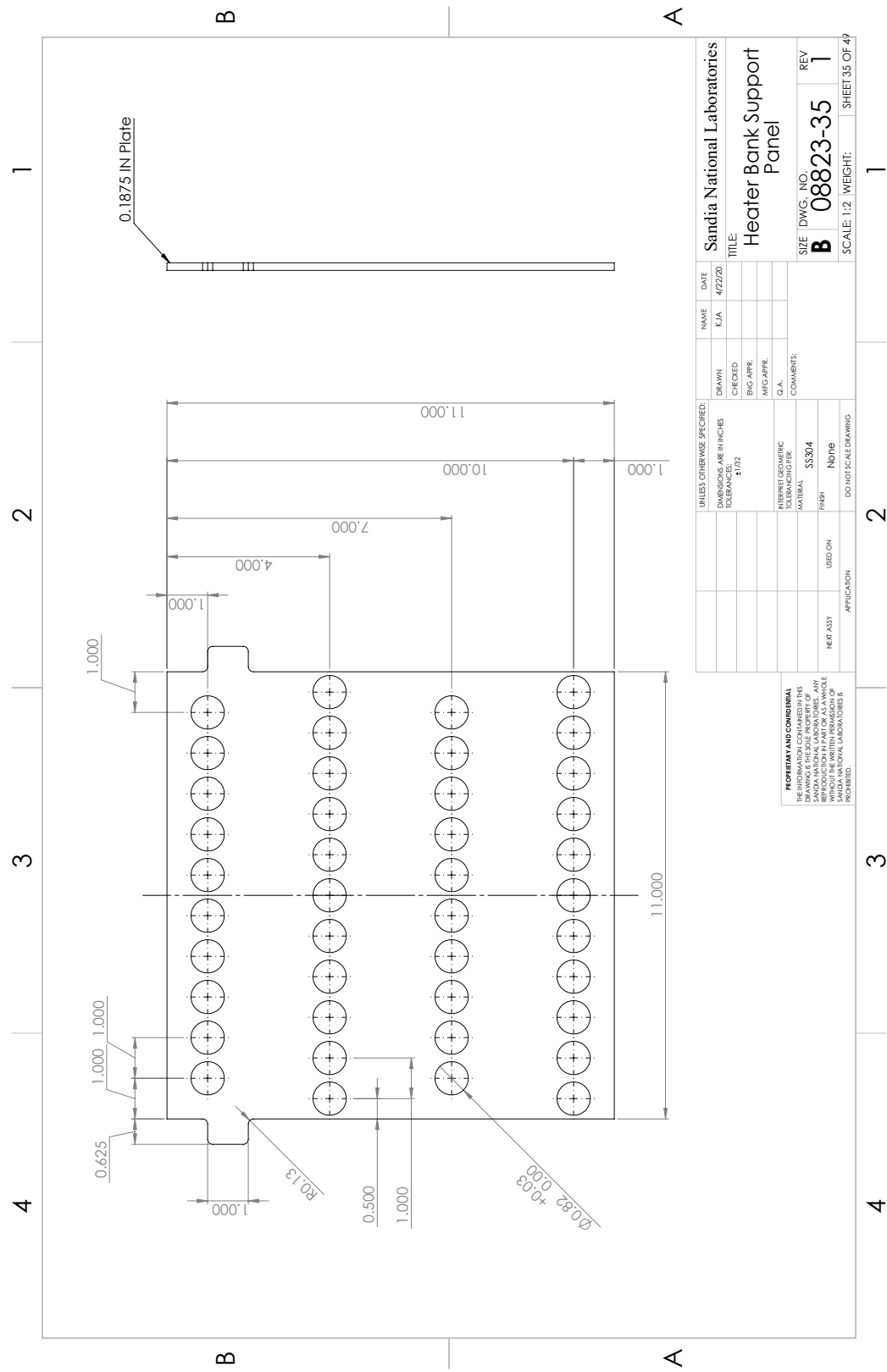


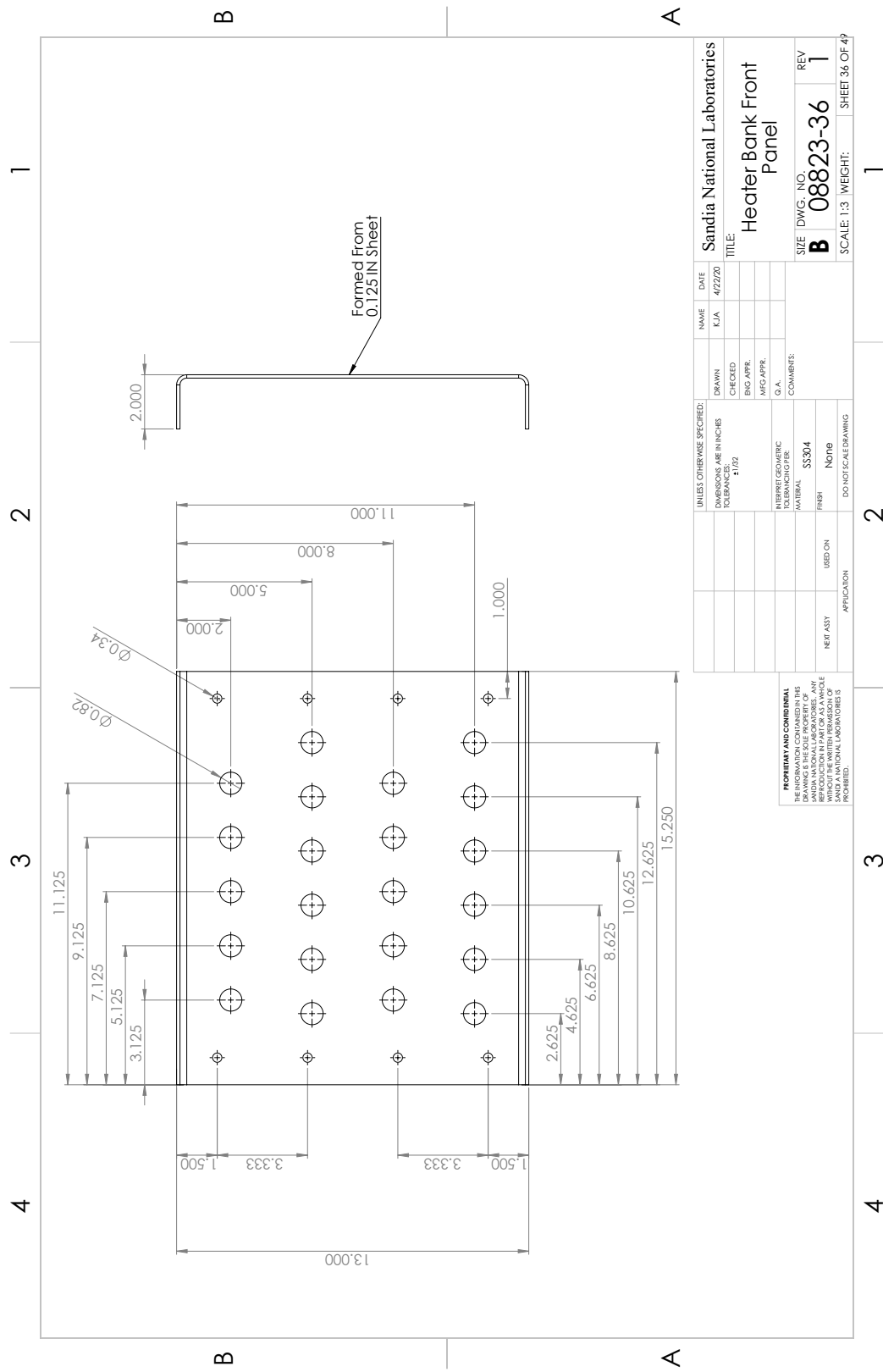


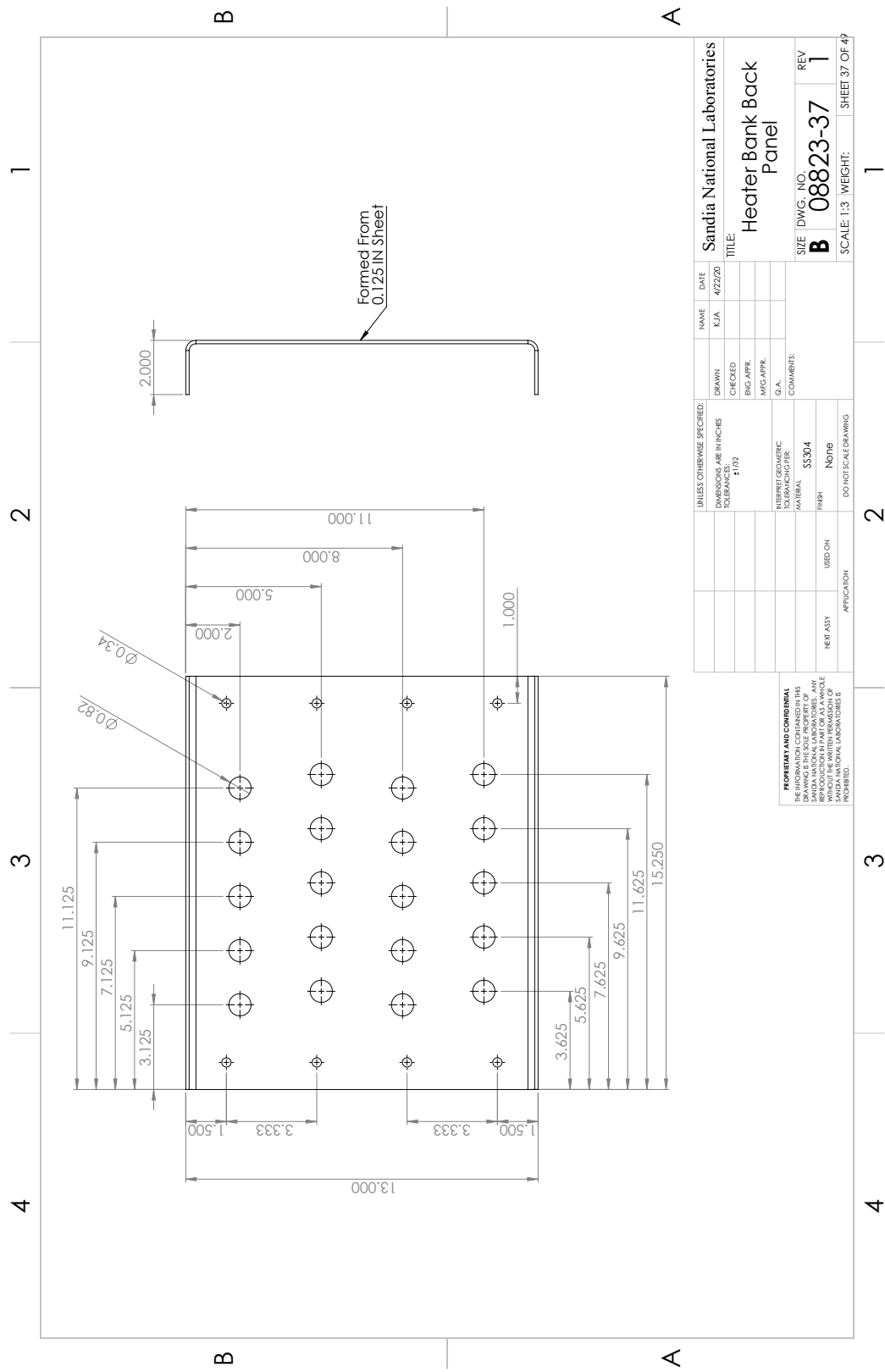


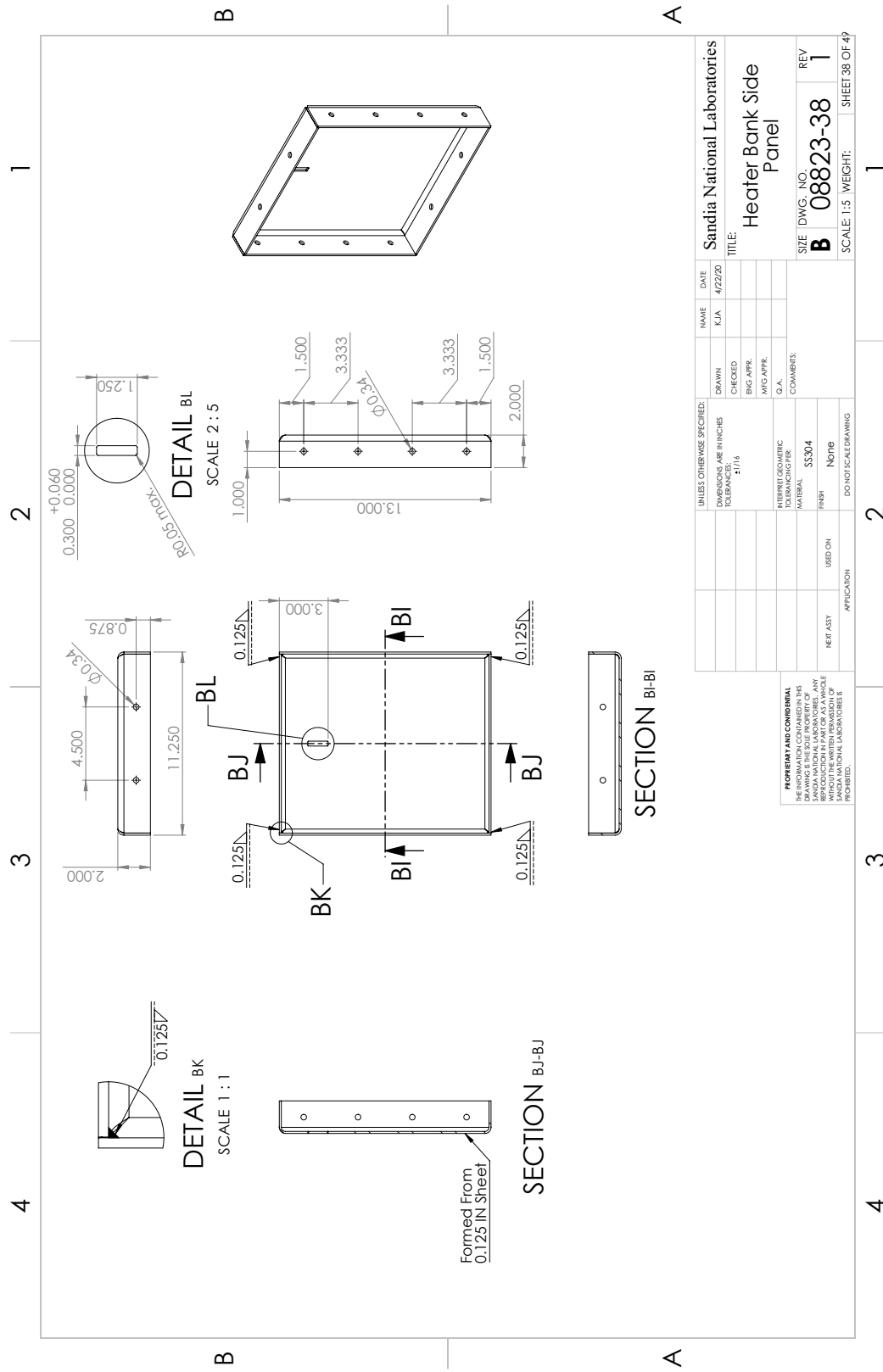


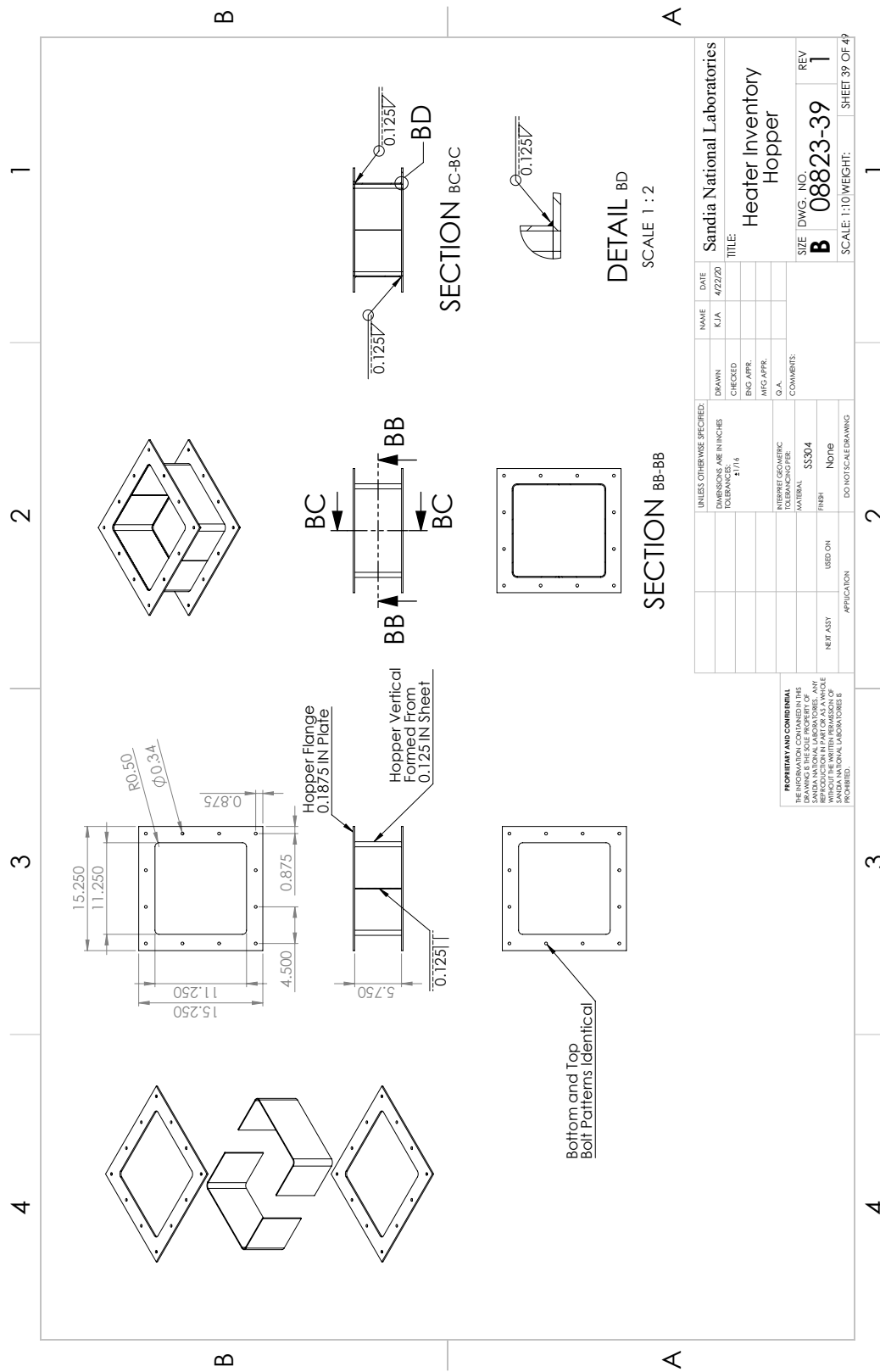


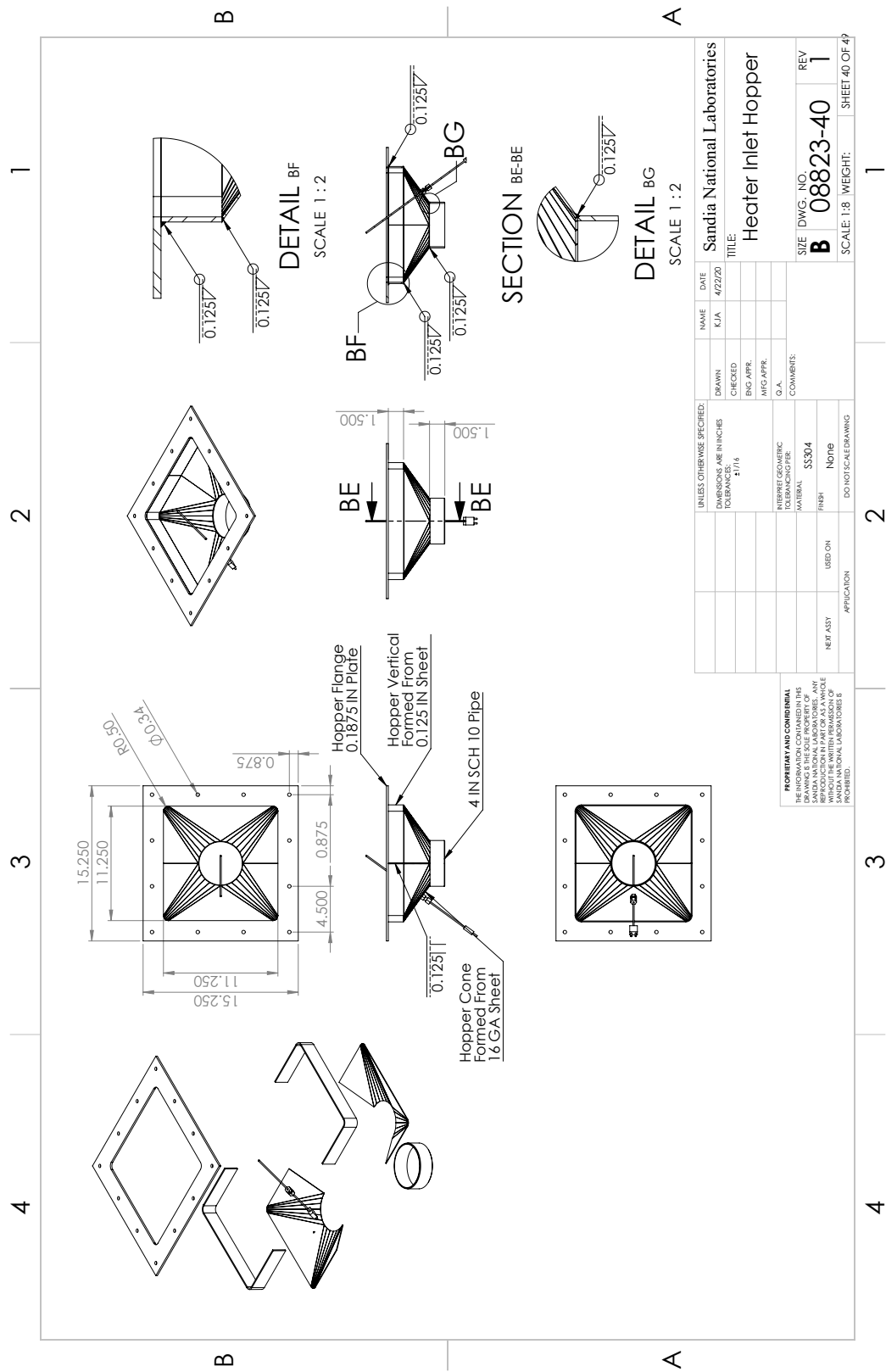


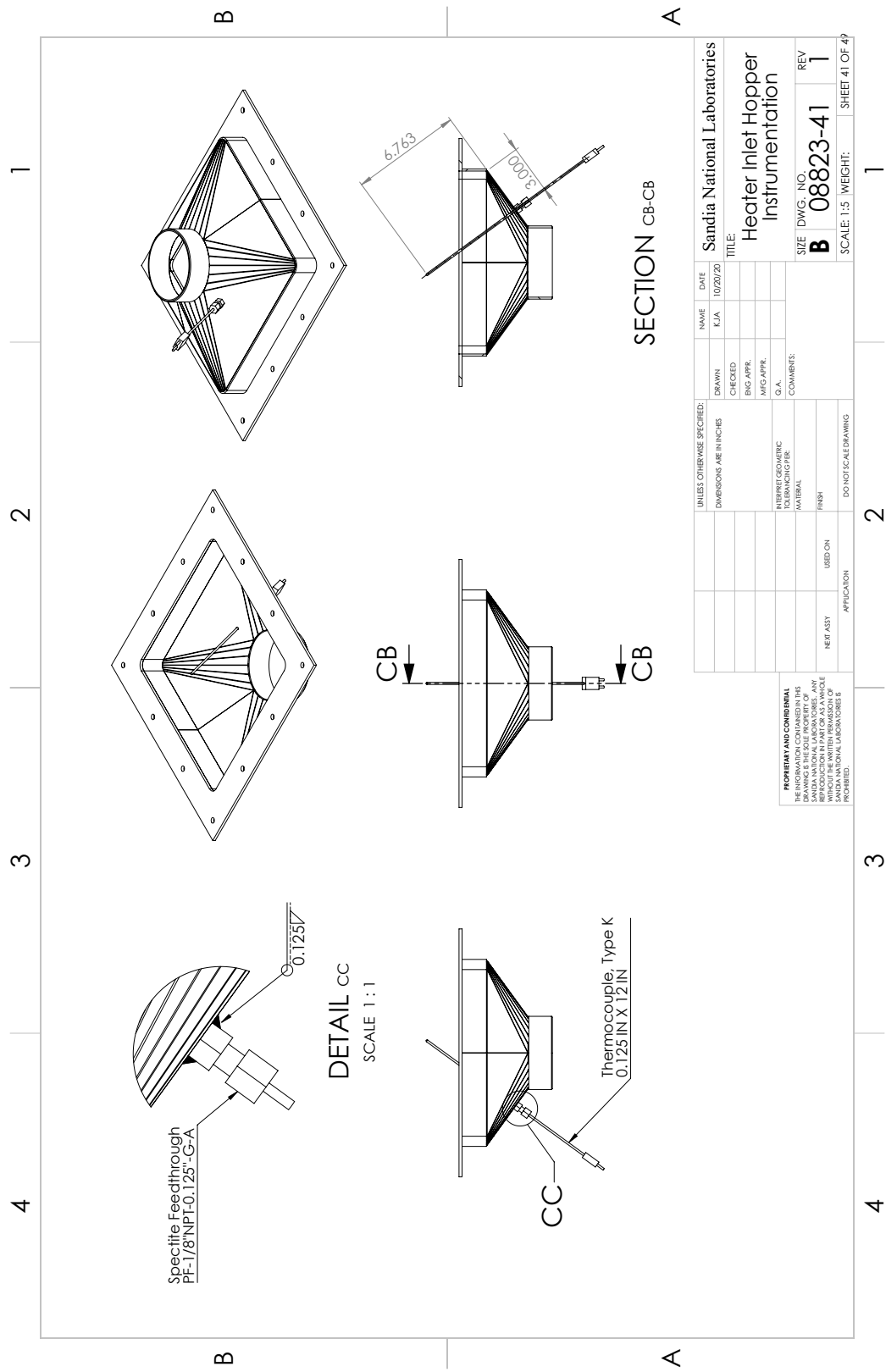












## DISTRIBUTION

### Email—Internal

Name	Org.	Sandia Email Address
Technical Library	1911	sanddocs@sandia.gov

### Email—External

Name	Company Email Address	Company Name
Matthew Bauer	Matthew.Bauer@ee.doe.gov	U.S. Department of Energy, Solar Energy Technology Office





**Sandia  
National  
Laboratories**

Sandia National Laboratories is a multimission laboratory managed and operated by National Technology & Engineering Solutions of Sandia LLC, a wholly owned subsidiary of Honeywell International Inc., for the U.S. Department of Energy's National Nuclear Security Administration under contract DE-NA0003525.